

STRESS CONCENTRATION FACTORS FOR CIRCULAR
NOTCHES

Lawrence Jerome Smith

DUDLEY KNOX LIBRARY
NAVAL POSTGRADUATE SCHOOL
MONTEREY, CALIFORNIA 93940

NAVAL POSTGRADUATE SCHOOL

Monterey, California



THESIS

STRESS CONCENTRATION FACTORS
FOR CIRCULAR NOTCHES

by
Lawrence Jerome Smith

June 1974

Thesis Advisor:

J.E. Brock

Approved for public release; distribution unlimited.

T161560

DUDLEY KNO
NAVAL POSTG
MONTEREY, C

REPORT DOCUMENTATION PAGE		READ INSTRUCTIONS BEFORE COMPLETING FORM
1. REPORT NUMBER	2. GOVT ACCESSION NO.	3. RECIPIENT'S CATALOG NUMBER
4. TITLE (and Subtitle) Stress Concentration Factors for Circular Notches		5. TYPE OF REPORT & PERIOD COVERED Engineer's Thesis; June 1974
7. AUTHOR(s) Lawrence Jerome Smith		6. PERFORMING ORG. REPORT NUMBER
9. PERFORMING ORGANIZATION NAME AND ADDRESS Naval Postgraduate School Monterey, California 93940		8. CONTRACT OR GRANT NUMBER(s)
11. CONTROLLING OFFICE NAME AND ADDRESS Naval Postgraduate School Monterey, California 93940		10. PROGRAM ELEMENT, PROJECT, TASK AREA & WORK UNIT NUMBERS
14. MONITORING AGENCY NAME & ADDRESS (if different from Controlling Office) Naval Postgraduate School Monterey, California 93940		12. REPORT DATE June 1974
		13. NUMBER OF PAGES 166
		15. SECURITY CLASS. (of this report) Unclassified
		15a. DECLASSIFICATION/DOWNGRADING SCHEDULE
16. DISTRIBUTION STATEMENT (of this Report) Approved for public release; distribution unlimited.		
17. DISTRIBUTION STATEMENT (of the abstract entered in Block 20, if different from Report)		
18. SUPPLEMENTARY NOTES		
19. KEY WORDS (Continue on reverse side if necessary and identify by block number) Stress Concentration Finite Element		
20. ABSTRACT (Continue on reverse side if necessary and identify by block number) Existing finite element programs PLISOP and PLIMEG are modified and adapted to the successful determination of stress concentration factors for thin elastic bars containing V-shaped round bottom notches and subjected to tensile or bending loads. Accuracy and reliability are demonstrated. Comparisons are made with previous analytical and experimental determinations. The effects of finite bar thickness are discussed.		

DUBOIS K
NAVAL POS
MONTEREY

DD Form 1473
1 Jan 73
S/N 0102-014-6601

DUDLEY K
NAVAL FOR
MONTEREY

Stress Concentration Factors
for Circular Notches

by

Lawrence Jerome Smith
Lieutenant Commander, United States Navy
B.E., Villanova University, 1960

Submitted in partial fulfillment of the
requirements for the degrees of

MECHANICAL ENGINEER

and

MASTER OF SCIENCE IN MECHANICAL ENGINEERING

from the

NAVAL POSTGRADUATE SCHOOL

June 1974

70-1000
8-5700

ABSTRACT

Existing finite element programs PLISOP and PLIMEG are modified and adapted to the successful determination of stress concentration factors for thin elastic bars containing V-shaped round bottom notches and subjected to tensile or bending loads. Accuracy and reliability are demonstrated. Comparisons are made with previous analytical and experimental determinations. The effects of finite bar thickness are discussed.

TABLE OF CONTENTS

I.	INTRODUCTION -----	9
II.	BASIC METHODS OF OBTAINING SCF'S -----	11
	A. CLASSICAL ANALYSIS -----	11
	1. Neuber's Notch Analysis -----	11
	2. Limitations of Neuber's Analysis -----	14
	3. Availability of Neuber's Solution -----	14
	B. EXPERIMENTAL INVESTIGATION -----	15
	1. Strain Gage Measurements -----	15
	2. Limitations of Strain Gage Measurements -	16
	3. Photoelastic Evaluations -----	16
	4. Limitations of Photoelastic Evaluation --	19
	C. NUMERICAL TREATMENT OF ELASTIC FIELD EQUATIONS -----	20
III.	DETAILED PROBLEM SPECIFICATION -----	22
	A. GENERAL -----	22
	B. FOUR PROBLEMS -----	22
	C. ONE STRUCTURE -----	26
	D. FOUR SETS OF BOUNDARY CONDITIONS -----	27
IV.	SOFTWARE SELECTION -----	31
	A. BASIC PROGRAM SELECTION -----	31
	B. MESH GENERATION -----	32
	C. MODIFICATIONS TO PLIMEG -----	34
	1. Stress Gradient Considered -----	34
	2. Curved Boundary Node Relocation -----	36
	3. Boundary Condition Calculations -----	40

	D. SUBROUTINE PROBLM -----	40
	E. SUBROUTINE ANS -----	42
V.	PROGRAM OPERATION -----	46
	A. INPUT -----	46
	B. OUTPUT -----	46
VI.	PROGRAM OUTPUT ANALYSIS -----	49
	A. EQUILIBRIUM -----	49
	B. MAXIMUM STRESS LOCATION -----	49
	C. CONVERGENCE -----	49
	D. CORRELATIONS -----	54
VII.	DISCUSSION OF RESULTS -----	55
	A. RESULTS PRESENTED -----	55
	B. EFFECT OF NOTCH DEPTH -----	56
	C. EFFECT OF ANGLE θ -----	58
	D. SINGLE NOTCH GEOMETRY -----	62
VIII.	CONCLUSIONS AND RECOMMENDATIONS -----	65
	A. CONCLUSIONS -----	65
	B. RECOMMENDATIONS -----	66
APPENDIX A.	CURVES OF RESULTS -----	67
APPENDIX B.	NEUBER'S NOTCH ANALYSIS -----	73
APPENDIX C.	THREE-DIMENSIONAL EFFECT -----	78
	1. PREAMBLE -----	78
	2. A SPECIFIC PROBLEM -----	79
	3. PROCEDURES TO SOLVE THE PROBLEM -----	81
	4. NUMERICAL DIFFERENTIATION FROM 2D FEM --	90
	5. DIRECT COMPARISON FROM 3D FEM -----	91
	6. CONCLUSION -----	93

APPENDIX D.	SUGGESTIONS FOR PRODUCING ADDITIONAL NUMERICAL RESULTS -----	95
APPENDIX E.	PROGRAM USER'S MANUAL -----	97
	1. TO EXECUTE THE PROGRAM -----	97
	2. TO CHANGE BOUNDARY CONDITIONS -----	104
	3. TO CHANGE THE SHAPE OF THE NOTCH -----	105
	4. TO CHANGE DIMENSIONING -----	108
	5. TO MAKE A MAJOR MODIFICATION -----	109
APPENDIX F.	COMPUTER PROGRAM LISTING -----	113
BIBLIOGRAPHY	-----	164
INITIAL DISTRIBUTION LIST	-----	166

ACKNOWLEDGEMENT

The invaluable advice and counsel of Professor John E. Brock is gratefully acknowledged. A special thank you, also, to the computer operating personnel, especially those on the swing shift.

The work was made easier by the encouragement and sacrifices of my wife, Polly, and the understanding of our boys, Kevin and Kurt.

I. INTRODUCTION

Stress intensifiers, in the form of holes, grooves, keyways, threads, etc., result in local modification of simple stress patterns and give rise to stress concentrations. The designer or analyst is interested in determining the locally maximum, governing or limiting value of stress, designated by the symbol σ_{\max} , which is calculated as the product of a nominal stress, σ_{nom} , and a stress concentration factor, designated by the abbreviation SCF, thus:

$$\sigma_{\max} = \text{SCF} \times \sigma_{\text{nom}}$$

An elementary formula is used to compute σ_{nom} , the terms of which must be precisely defined; this accounts for the gross geometry of the member and the loading which is applied. The SCF is intended to provide a corrective multiplying factor; its value depends on the details of local geometry and, usually, on the particular type of loading that is applied.

The designer employs available tabulations of SCF's, together with the appropriate and easily calculated σ_{nom} , employing the formula given above, to estimate the maximum stress which he compares with an allowable value; the latter being established by experience, by code, or by contract.

The task of the person who supplies values of SCF is to determine values of σ_{\max} and of σ_{nom} and their quotients, the

SCF's. To make the values of SCF most widely useful, the stress analyst selects an appropriate set of parameters to describe the geometry of a class of stress intensification problems. A number of individual problems are undertaken, taking care to vary the parameters so as to cover the useful range of each and thus to permit making reasonable interpolations for intermediate values.

The SCF's obtained in this manner are usually presented in the form of parametric curves drawn through the actual data points established. The designer then must interpolate between the curves to match the actual parameters of his problem.

The particular classes of problems selected for this study, because of their prominence and importance, are characterized by a thin, flat bar under tension and/or bending. We consider two forms of stress intensifiers:

1. Two notches on opposite edges of the bar, located symmetrically about the long axis of the bar and shaped symmetrically with respect to a plane normal to the long axis of the bar.
2. A notch on only one edge of the bar.

In general, the notches are circular at the bottom. Details of the notches, with sketches, are presented in Section III. Much of what follows, however, is applicable to other geometries.

We confine attention to the two-dimensional case, i.e., the case of plane stress. Realizing that a condition of plane stress is never actually found in a real world application, the effect of three dimensionality on SCF's was also investigated, see Appendix C.

II. BASIC METHODS OF OBTAINING SCF'S

A. CLASSICAL ANALYSIS

Neuber [11] has made the most extensive analytical investigation of SCF's. His book contains treatments of a number of geometries and loadings and his methods include a few cases of exact analytical solutions together with a number of ingenious approximations and interpolations. The best known of Neuber's analyses is that of the deep hyperbolic notch.

1. Neuber's Notch Analysis

Using curvilinear coordinates and complex stress functions, Neuber presented a solution for axial tensile loading (without bending) of a geometry consisting of symmetrically located, hyperbolic shaped notches in an infinite sheet of unit thickness (Fig. 1).

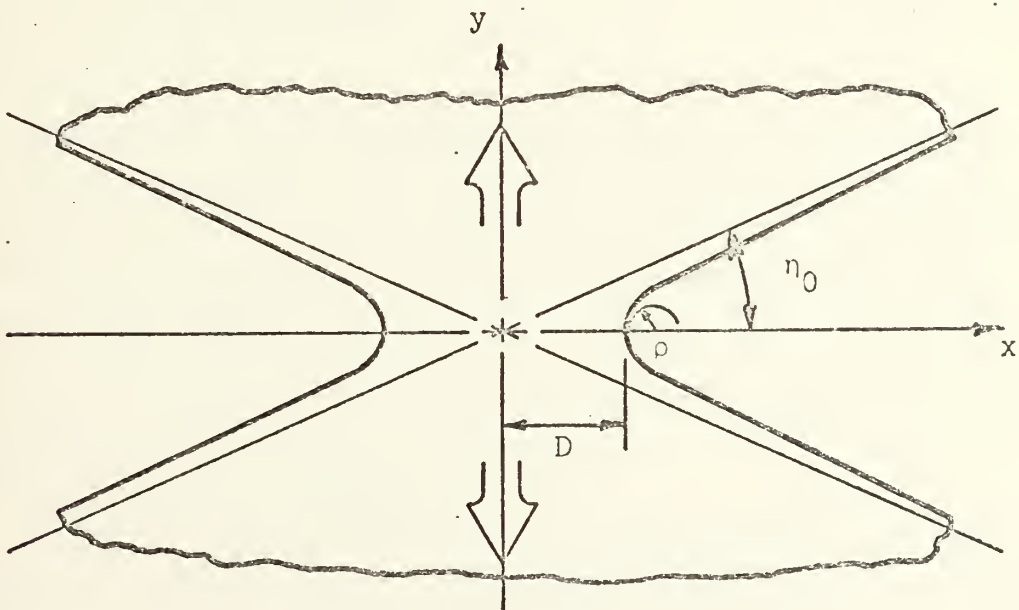


Fig. 1. Symmetric hyperbolic notches in an infinite sheet.

He arrived at the following solution for the stress concentration factor for this notch:

$$SCF = \frac{4 \cot \eta_0}{\pi - 2\eta_0 + \sin(2\eta_0)}$$

where η_0 is a parameter defining the particular notch geometry, namely, the angle between asymptote and notch centerline. The nominal stress is given by the axial force divided by the minimum width of the sheet at the notch. The hyperbolic boundary is described by the equation:

$$\frac{x^2}{a^2 \cos^2 \eta_0} - \frac{y^2}{a^2 \sin^2 \eta_0} = 1$$

The half width at the bottom of the notch is D . The minimum radius of curvature is

$$\rho = D \tan^2(\eta_0) \quad .$$

The width of the sheet approaches infinity on each side, unlike cases of practical interest in which the notch is an indentation in a bar of finite width. Accordingly, for Neuber's deep hyperbolic notch, it is not possible to specify a gross width or the ratio of gross width to net width as is usually done for practical cases.

Neuber further presents an approximation for shallow notches in a bar of finite width with notch depth specified.

The analysis involves employing a solution for an elliptic hole in a bar. Somewhat arbitrarily the bar is cut through the center of the hole parallel to the edges of the bar and reassembled to form the notched bar (Fig. 2).

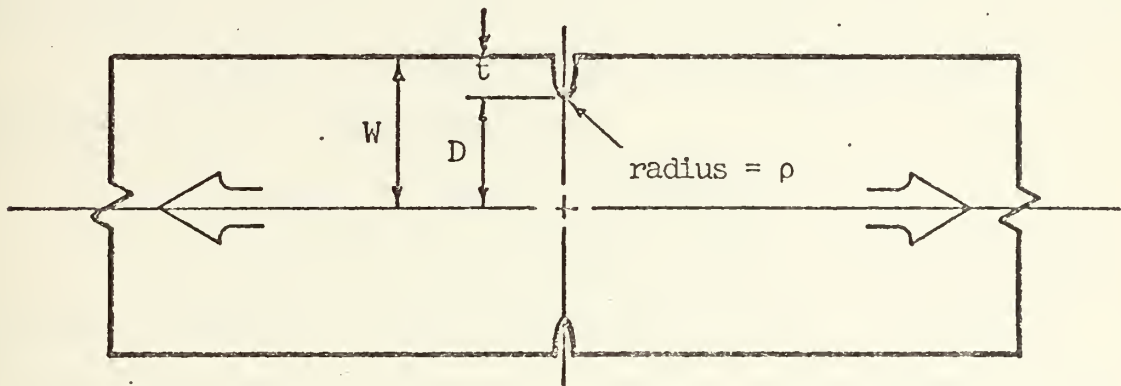


Fig. 2. Neuber's shallow notch approximation

The boundaries of the notched bar are not unloaded as they should be and there are unaccounted for dislocations along the axial center line.

Taking the half width of the bar as W and using D , ρ , and σ_{nom} as defined for the hyperbolic notch analysis, Neuber arrived at the following approximation for stress concentration factor for the shallow notch:

$$\text{SCF} = 1 + 2[(W - D)/\rho]^{\frac{1}{2}}$$

Noting that nominal stress was defined the same way in both cases, i.e., on the basis of net area, Neuber devised

a nomographic scheme to obtain SCF for a wide range of the parameters:

ρ = minimum radius of curvature

D = half width of the bar at the notch (net half width)

W = half width of the undisturbed bar (gross half width)

The nominal stress is $\sigma_{nom} = (\text{axial force per unit thickness})/2D$.

A summary of Neuber's solution for the hyperbolic notch is shown in Appendix B.

2. Limitations of Neuber's Analysis

The hyperbolic notch analyzed has a definite shape, namely a hyperbola having the asymptotes $y = \pm x \tan \eta_0$. The values presented by Neuber are based on two extremes and an interpolation between them. It must be recognized that other geometries only approximate these notch shapes and therefore the data must be judiciously applied.

The reasoning used to arrive at this solution is ingenious but experimental evidence described later indicates a systematic difference between Neuber's analysis and the behavior of actual test sections.

3. Availability of Neuber's Solution

A designer may use Neuber's equations and perform the indicated interpolation to determine a particular SCF based on the parameters of interest. However, much of that work has already been done.

The most extensive, readily available tabulation of SCF for this case is presented by Peterson[12]. He presents a family of curves using dimensionless ratios of the

parameters as arguments. Other authors, such as Fairies [6] present the same data over a narrower range of parameters.

B. EXPERIMENTAL INVESTIGATION

Values of maximum stress may be determined by experimental stress analysis including strain gage measurements and photo-elastic evaluations.

1. Strain Gage Measurements

Kikukawa [9] used resistance strain gages to study the stress in a bar with two symmetrically located U-shaped notches subjected to an axial tensile load.

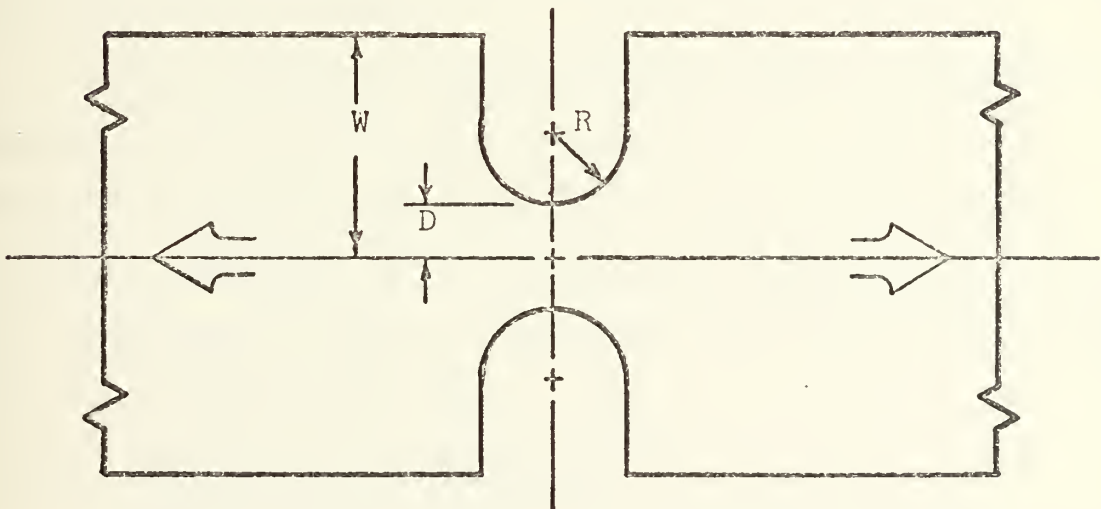


Fig. 3. Symmetric U-shaped notches

The geometry of the test section (Fig. 3) is specified by:

R = radius at the bottom of the notch

D = net half width

W = gross half width

Only the gross width of the bar was varied during the tests.

2. Limitations of Strain Gage Measurements

In using strain gages, difficulty arises from the highly localized character of the stress distribution at the place in question. A very small gage length is necessary to obtain satisfactory results. Accordingly, the physical size of available strain gages limits their usefulness to the investigation of relatively large notches. Furthermore, models must be very carefully machined to obtain dimensions within satisfactory tolerances. Good adhesion of the gage to the model and correct placement and orientation on the specimen are difficult to obtain.

Data scatter dictates that some sort of smoothing process must be used before the results are useful to a designer. Large expenditures of time and other valuable resources are required to obtain even a few benchmarks which can reasonably be used to infer SCF's over some useful range of the parameters employed.

3. Photoelastic Evaluations

Flynn and Roll [7] used photoelastic techniques to study the stress in a bar subjected to an axial tensile load for both U-shaped and hyperbolic-shaped symmetrically located notches. The geometry of the U-notched test section (Fig. 3) is specified by:

R = radius at the bottom of the notch

D = net half width

W = gross half width

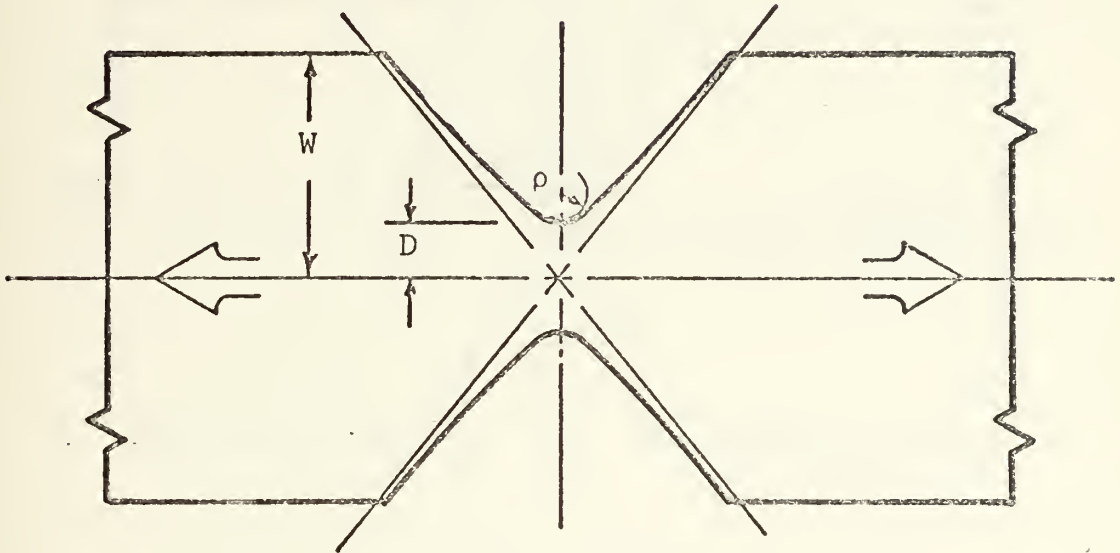


Fig. 4. Symmetric hyperbolic notches

The geometry of the hyperbolic-notched test section (Fig. 4) is specified by:

ρ = minimum radius of curvature

D = net half width

W = gross half width

The gross width of the bar was the only parameter which was varied in these tests, also.

Appl and Koerner [2] used photoelastic techniques to study the stress in a notched bar subjected to an axial load. The notches were symmetrically located, V-shaped with various angles and had round bottoms.

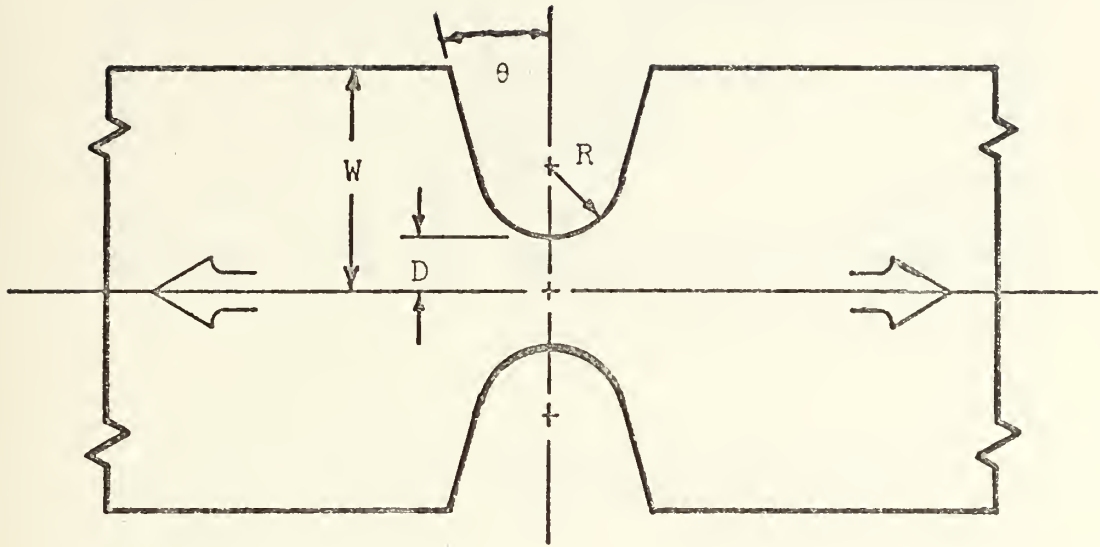


Fig. 5. Symmetric V-shaped notches

The geometry of the test section (Fig. 5) is specified by:

R = radius at the bottom of the notch

D = net half width

W = gross half width

θ = half included angle

They present SCF's for several notch angles using the ratio D/W as a parameter.

Cole and Brown [5] used photoelastic techniques to study the stress in a bar with a U-shaped notch on only one side of the bar. An axial load was applied such that its line of application was through the center of the net cross section.

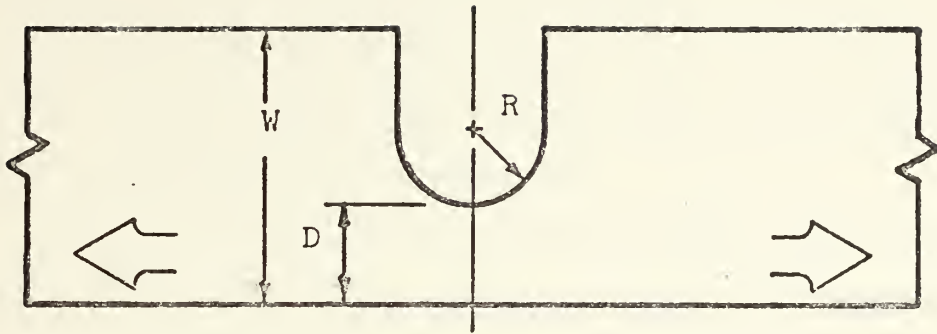


Fig. 6. U-shaped notches, one side only

The geometry of the test section (Fig. 6) is specified by:

R = radius at the bottom of the notch

D = net width

W = gross width

They present SCF's for several combinations of the parameters.

4. Limitations of Photoelastic Evaluation

Models, no matter how thin, do have a third dimension.

These experimenters have chosen thin models purposely so that their results could be reported as plane stress values.

Appendix C discusses the effect of the third dimension, showing that the stress at the base of the notch actually varies through the thickness. Photoelastic evaluation reveals the stress

averaged through the model thickness. The difference between the averaged and true maximum is small, but the three dimensional effect should be recognized.

Errors due to several edge effects including those caused by residual machining stresses and time dependent material changes must be recognized.

The same limitations regarding model preparation, data scatter and resource expenditure that were mentioned as limitations to strain gage measurements apply also to photoelastic evaluations.

C. NUMERICAL TREATMENT OF ELASTIC FIELD EQUATIONS

Several numerical techniques, notably the Finite Difference method, are available and have been used to solve partial differential equations. However, useful results to the elastic field equations are difficult to obtain, especially if the geometry of the problem is not very simple.

Recently a new numerical method called the Finite Element Method (FEM) has been extensively developed and used. In many ways it is similar to earlier numerical methods in that the partial differential equations are replaced by a finite system of algebraic equations. There is, however, a big difference in the detail of this replacement and this difference in detail permits the user to deal with complex geometric shapes.

The method has been well proved by the solution of problems which have classically known solutions. Thus it

seems to provide a new and powerful way to determine stress concentration factors.

Considering all of the above, the Finite Element Method (FEM) was chosen for use in this study.

III. DETAILED PROBLEM SPECIFICATION

A. GENERAL

Before proceeding with FEM program selection, it will be convenient to have the problem specified in full detail. This is done so that further reference to computer program selection and modification can be with the requirements of this problem specifically established.

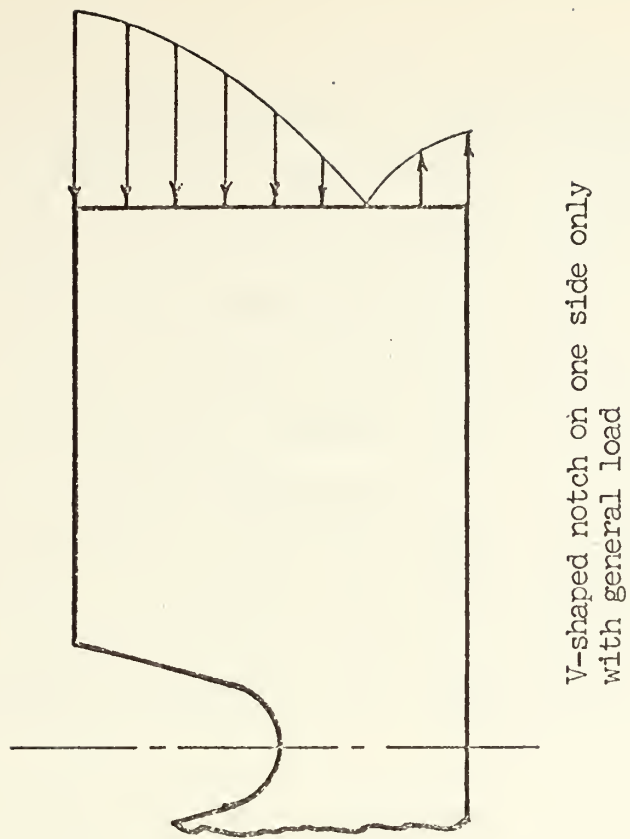
In Section I we limited the study to a family of thin, flat bars with general end loading. The stress intensifiers were limited to two forms: a single notch and two symmetrically located notches. Now specifically we deal with that general loading and a detailed description of notch shape. A single notch shape is considered: the bottom of the notch is circular, characterized by its radius, and the sides are V-shaped. The included angle of the V may be between 0° (U-shaped notch) and 180° (unnotched bar).

This problem family was chosen because of its practical importance and because it includes much of the available experimental data.

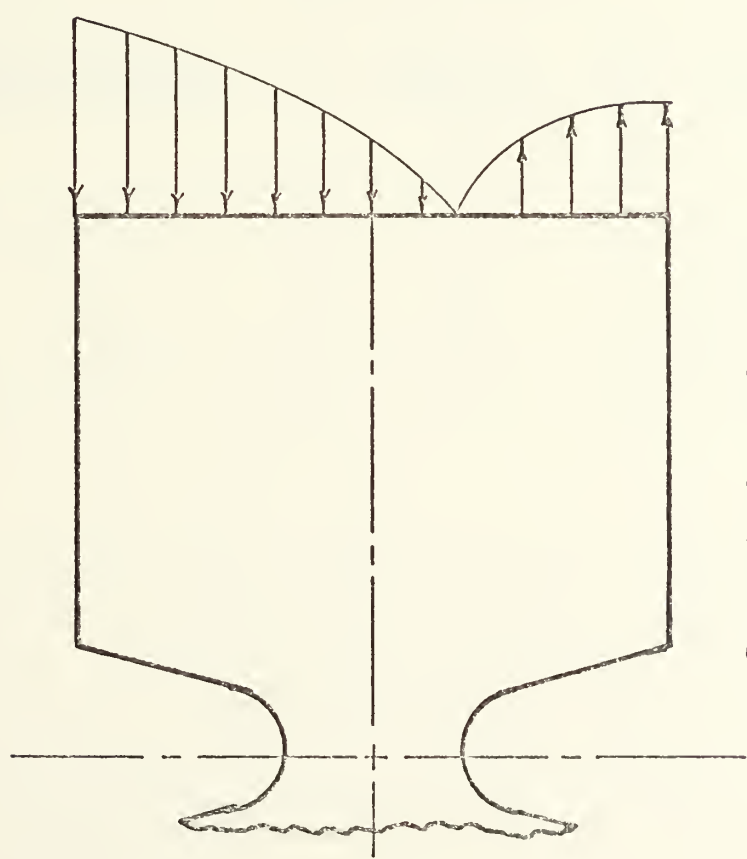
B. FOUR PROBLEMS

Division of the problem family into two general classes based on the number of notches has already been indicated. The two classes are shown in Fig. 7.

We speak of general loading at the ends of the bar containing the stress intensifier. However, by virtue of the



V-shaped notch on one side only
with general load



Symmetric V-shaped notches
with general load

Fig. 7. Two Problem Classes

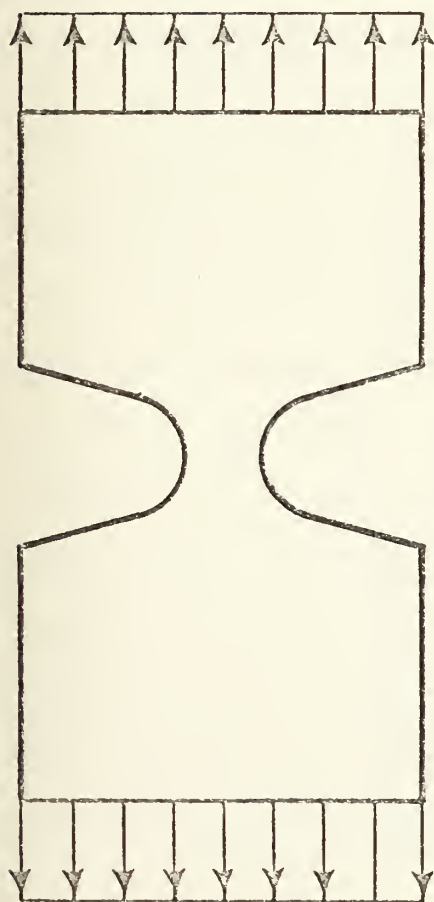
principle of Saint Venant, if the bar is several times longer than its width, as we assume and as is the case in practical applications, then only the static properties of the load, i.e., the net axial force and the moment (about, say, the central axis of the bar) are of importance. Thus what we have called a general loading can be treated by the superposition, in proper proportion, of a case with an axial force and no moment and a case with moment and no net axial load. Based on this, the four specific problems shown in Fig. 8 and described in Table I were selected for study.

TABLE I

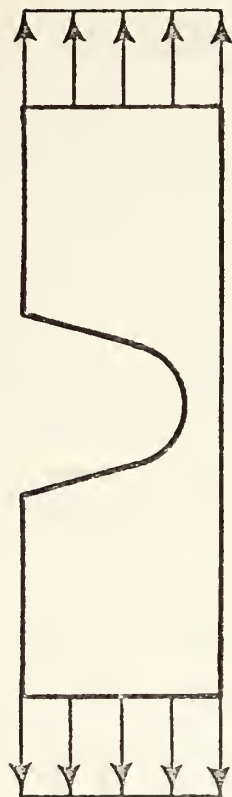
Problems Studied

<u>Problem Number</u>	<u>Notches</u>	<u>Loading</u>
1	Two	Axial Force
2	Two	Moment
3	One	Axial Force
4	One	Moment

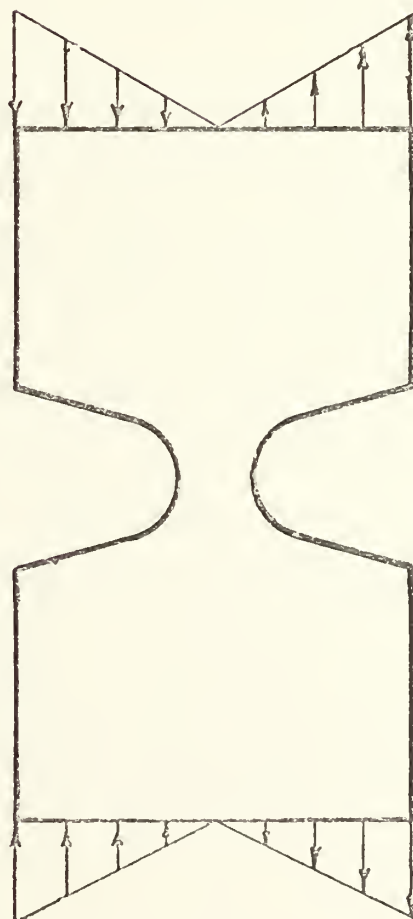
The general loading of the class of problems with two notches can be obtained by an appropriate superposition of problems 1 and 2. The maximum stress (σ_{\max}) always occurs at the base of one of the two notches and since they are symmetric, it is apparent that the maximum stress can always be calculated.



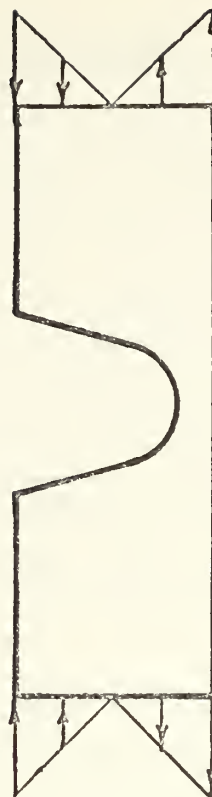
Problem 1



Problem 3



Problem 2



Problem 4

Fig. 8. The Four Problems

The general loading of the class of problems with one notch can similarly always be obtained by an appropriate superposition of problems 3 and 4. However the maximum stress does not always occur at the base of the notch. Consider first the bending of problem 4. Maximum tensile stress occurs on the straight boundary opposite the notch and maximum compressive stress at the bottom of the notch. Superimposing problem 3 can bring the stress at the bottom of the notch to any value, say zero, producing maximum stress on the boundary opposite the notch.

Accordingly, for this class, data should be generated and made available both for the point at the bottom of the notch and also for the opposite point on the straight boundary.

C. ONE STRUCTURE

By taking advantage of symmetry, the four problems may be reduced to four cases each of which is completely described by the single geometry of Fig. 9 and one of four different sets of boundary conditions. Face B is a circular arc of radius R . Face C is a straight line inclined at angle θ . The other four faces, A, D, E and F, are straight lines parallel to the x or y axis. The length of face A is designated D , the length of face E is designated W , and the length of face F is designated L . We take $L = 5W$ so as to assure, by St. Venant's principle, that fine details of end loading do not influence the stress distribution in the notched portion of the bar.

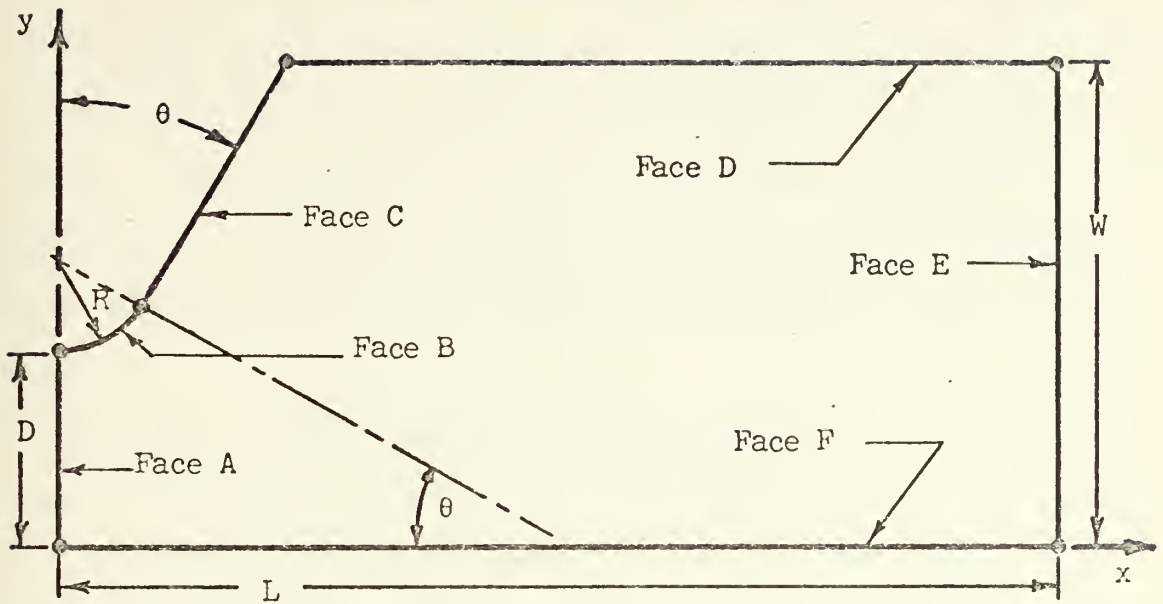


Fig. 9. Structure faces

The geometry of the structure can now be adequately described by the dimensionless ratios $\frac{R}{W}$, $\frac{D}{W}$ and θ .

D. FOUR SETS OF BOUNDARY CONDITIONS

The four cases to be described here and summarized in Tables II and III are equivalent to the four problems described earlier. Cases c and d are problems 3 and 4 directly. Appropriate superposing of two cases a and of two cases b along face F yield problems 1 and 2 respectively.

At this point we delineate the boundary conditions corresponding to each of the four cases. It is evident that we have to specify values of the displacements u and v along the faces A, B, C, D, E and F and/or the values of the forces


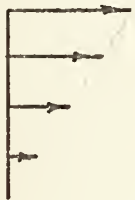

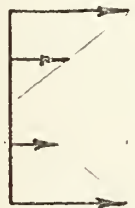
F_x and F_y applied along these faces by external agencies. Along faces B, C and D there are no externally applied forces and the displacements u and v are not specified (that is, they are unknowns which will be solved for by the FEM program). All internal points of the structure, likewise, have no specified values of u or v and are not externally loaded.

Because of the symmetry in all four cases, we specify that $u = 0$ all along face A. Along face F, for cases c and d, there are no boundary forces and values of u and v are unspecified. For case a, face F is along a line of symmetry and we take $v = 0$ all along face F. For case b, the condition of antisymmetry is satisfied by taking $u = 0$ at every point along face F. In neither of these cases are there any prescribed boundary forces along face F. In all four cases, the point which marks the intersection of faces A and F is restrained so that $u = v = 0$.

Loadings are applied on face E. The displacements along face E are unspecified. All forces F_y are zero. Values of F_x along this face are such that they produce the required loadings as shown in Table II.

A summary of boundary conditions for faces A, B, C, D and F is given in Table III. The conditions are given as triples (u, v, F_x) . All values of F_y are zero. An asterisk (*) indicates that no value is specified.

TABLE II
EXTERNAL LOADING ALONG FACE E

Loading	Case Number	Static Effect	
		F_x	M
	a	P	$\frac{PW}{2}$
	b	$-\frac{3P}{2}$	$-PW$
	c	P	0
	d	0	$-PW$

The displacements along face E are unspecified. All forces F_y are zero.

TABLE III
BOUNDARY CONDITION SPECIFICATION

Face	Case 1	Case 2	Case 3	Case 4
A	(0,*,*)	(0,*,*)	(0,*,*)	(0,*,*)
B,C,D	(*,*,0)	(*,*,0)	(*,*,0)	(*,*,0)
F	(*,0,0)	(0,*,*)	(*,*,0)	(*,*,0)

IV. SOFTWARE SELECTION

A. BASIC PROGRAM SELECTION

The purpose of the study was not only to obtain some useful data (i.e., SCF's) to supplement and refine that already available through other sources, but also to perfect computer software for generating such data and to establish its reliability. Reliable, efficient programs capable of solving the two-dimensional plane stress problem and three-dimensional stress problem have been written and are available. Some of them are proprietary but many appear in the literature and portions of others have been published. Unfortunately, mainly due to the state of the art in the field of computer science, most programs are machine dependent and therefore could not be considered for use in this investigation.

The two programs selected were developed at the Naval Postgraduate School. PLISOP [4] is a two-dimensional finite element program capable of solving the plane stress problem. It utilizes isoparametric elements which means that curved boundaries can be represented. All data handling in this program is confined to the main core storage of the computer. The program has internal documentation which includes instructions for its use. TRISOP [10] is a three-dimensional finite element program utilizing isoparametric elements. Because of the large amount of data implicit in the three-dimensional analysis, much of the program coding deals exclusively with

handling the data. Most of the storage is outside the computer main core on direct-access devices which provides for the storage of large volumes of data. The price paid for this expanded storage is the large computational time needed. Internal documentation includes instructions for its use.

Prior to the start of this investigation both of these programs had been debugged on the IBM-360 computer available for use in this study and solutions to a number of problems had been compared to the classically obtained solutions to demonstrate that the programs are capable of producing very good approximations when used correctly. The remainder of this section deals specifically with the two-dimensional program. Cf. Appendix C for remarks concerning the use of TRISOP.

B. MESH GENERATION

The first step in employing a FEM program for the solution of a specific problem is to provide appropriate input data, describing the problem, in the form called for by the specifications of the particular FEM program employed. This requires the preparation of a very large volume of data. Material properties and program options must be selected, of course, but the great preponderance of the input has to do with geometry. The user must discretize the structure into elements and describe these elements and their inter-connection to the program. Coordinates for each node used (specific points on the element boundaries) must be provided along with load boundary conditions. The displacement boundary conditions constitute the third large block of information

required. The elements and nodes are numbered for identification using numbering conventions dictated by the coding of the FEM program. Specified data card format must be adhered to rigidly. The discretization ultimately selected for most of this study would require over 600 data input cards.

Manual preparation of such a volume of data is unthinkable. However this problem is not new and others have dealt with it before and have provided programs to accomplish the task. Such a program is called a mesh generator. It is written to accept a gross description of the structure under consideration (Fig. 12) and its basic function is to superimpose a grid, establishing the elements (Fig. 11) required. Coordinates of all nodes are calculated. Elements and nodes are numbered according to the criteria of the FEM program which the mesh generator serves. The program output is in the form of a deck of punched data cards. The deck, compatible with the FEM program, is in two parts: element descriptions (element connectivity cards) and nodal coordinates (element node cards).

PLIMEG is a computer program originally written by J.R. Adamek as part of his NPS thesis [1] for the purpose of simplifying the preparation of input to PLISOP. Modifications to Adamek's program were made as a part of the present study in order to make it more useful for the purpose of inputting data for the notch stress intensification problem and making optimal use of the computer facilities in solving the problem.

The basic input to PLIMEG is a description of the geometry of the problem, divided, by the author, into several large subdivisions, referred to as superelements, or, briefly, as SEL's. The coordinates of the SEL corner points are specified, the connectivity is indicated; and, in an appropriate fashion, the geometry between corner points is specified. Other inputs to PLIMEG are m and n, the number of subdivisions required along two adjacent SEL boundaries. The numbers m and n must be consistent on any boundary common to two SEL's.

Internally, the program PLIMEG now establishes additional nodal points within each SEL, dividing each SEL into $m \times n$ smaller elements — the finite elements themselves. The output data deck is compatible with PLISOP. A program option may be used to obtain a graphical output depicting the completed grid.

The subdividing done in PLIMEG is actually accomplished in a non-dimensional coordinate system (ξ, η) and the grid established there is mapped into the SEL by a coordinate transformation.

C. MODIFICATIONS TO PLIMEG

1. Stress Gradient Considered

The structure considered in the study (Fig. 9) is of interest because of the stress concentration. That concentration implies a large gradient which, in turn, demands small elements in the finite element discretization. The use of a uniformly fine mesh is undesirable from the standpoint of the number of equations that must ultimately be solved. Not only

is the solution more time consuming but the maximum number of elements is directly dependent on machine storage capacity. The IBM-360, using PLISOP, imposes an upper limit of slightly over 180 quadratic elements, and even that size of problem can only be considered by special treatment.

Noting that the high stress gradient is very localized, it is possible however, to use small elements in that immediate area and larger elements where the gradient is smaller. By extension, bands of different size elements may be used. This technique has been successfully employed by many users. Pfeifer [13], for example, uses the three-dimensional stress analysis program (TRISOP) in this way to solve the problem of a concentrated force on the boundary of a semi-infinite body. His results compare well with Boussinesq's classical solution.

Accepting the usefulness of graded element size, a logical next step is to devise a way to vary element size progressively as the stress gradient changes. This was accomplished by modifying PLIMEG. Entering the program at the point where the nondimensional grid has been established, the element corner nodes, represented by (ξ_i, η_i) can be systematically moved by use of the relationships:

$$\xi_i = (\xi_{\max} - \xi_{\min}) \frac{\exp[a_{\xi}(\xi_i - \xi_{\min})] - 1}{\exp[a_{\xi}(\xi_{\max} - \xi_{\min})] - 1} - 1$$

$$\eta_i = (\eta_{\max} - \eta_{\min}) \frac{\exp[a_{\eta}(\eta_i - \eta_{\min})] - 1}{\exp[a_{\eta}(\eta_{\max} - \eta_{\min})] - 1} - 1$$

A wide range of element size variation is provided for by allowing the user to specify the exponential coefficients a_{ξ} and a_{η} as PLIMEG input values. The intermediate nodes are inserted on the new grid lines thus established, equally spaced between corner nodes (one if quadratic elements are used and two if cubic elements are used). From this point the coordinate transformation and other details of PLIMEG are as originally programmed. Mesh generation as originally programmed and as modified is illustrated in Fig. 10 for a representative general SEL. Note that PLIMEG, as modified, provides the capability of dividing a SEL into any specified number of increments with any specified exponential coefficient (positive, negative, or zero) in both the ξ and η directions, each completely independent from the other.

2. Curved Boundary Node Relocation

Isoparametric elements are used both for the SEL description and the elements in the completed mesh. Three element types are used. Each is capable of representing a different degree of variation along an element boundary. The element types, with their common names and nodal description are shown in Table IV. The maximum degree of polynomial which can be exactly represented by each element is given. If straight line, parabolic, and/or cubic boundaries determine the geometric shape of the structure, they may be exactly represented by proper choice of SEL type. If more complex curves are needed to describe the structure, or if there are discontinuities, additional SEL's can be used to meet the requirements of the particular use.

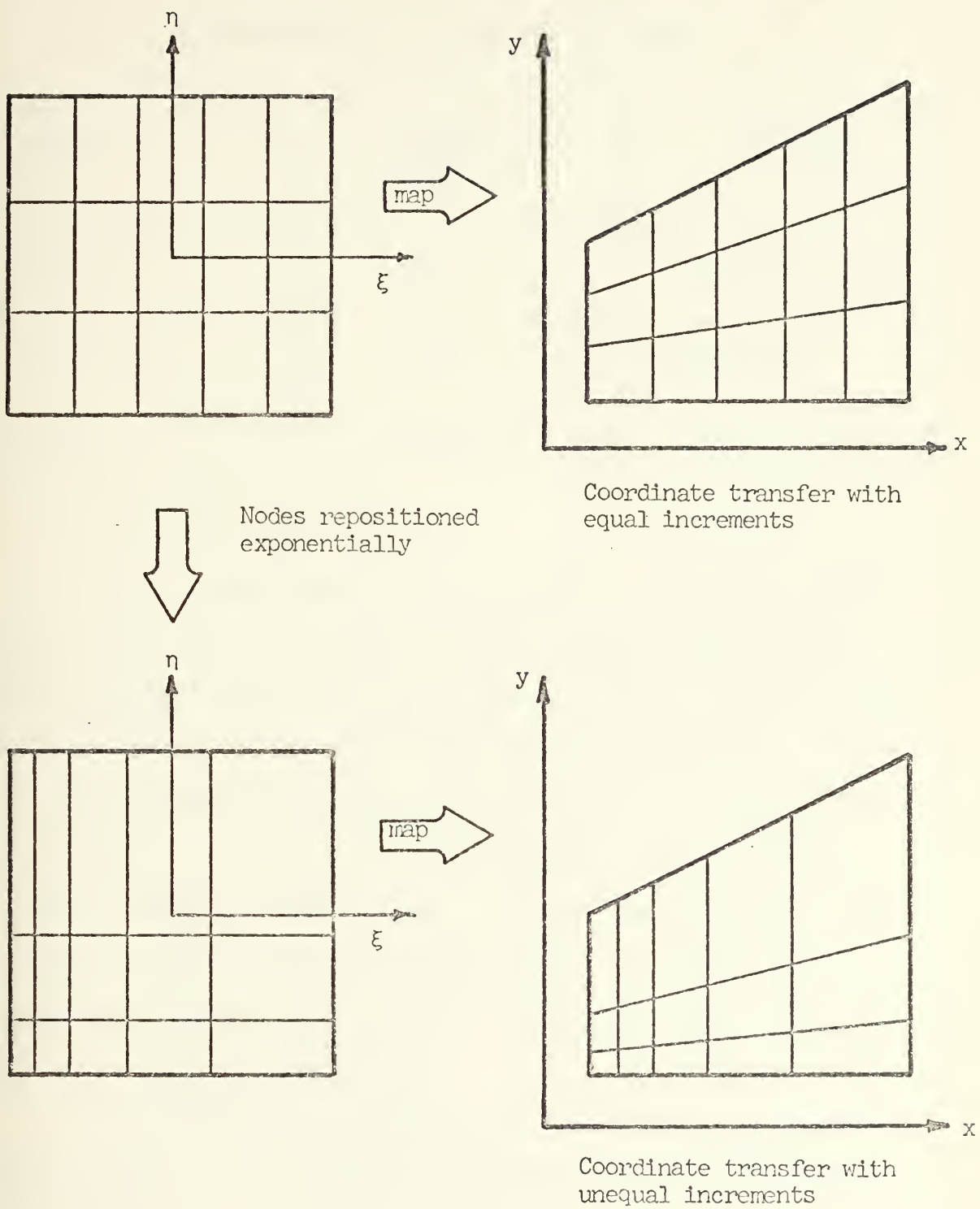


Fig. 10. Mesh generation with and without equal element size

TABLE IV

ISOPARAMETRIC ELEMENT TYPES USED

Common Name	Number of Nodes	Exactly Represents
Linear	Four	Straight Line
Quadratic	Eight	Parabola
Cubic	Twelve	Cubic Polynomial

It is important to note that SEL boundaries which cannot be exactly described by the element type chosen (i.e., are of higher order than the element used to describe them) become slightly distorted in the mapping procedure. Except for those boundaries which coincide with the boundaries of the structure, this is of no consequence. The structure boundary nodes, however, must be corrected to locate them properly in the real coordinate system. A provision to accomplish this for the curved boundary of Face B (Fig. 9) has been included in PLIMEG.

A representative mesh, as used in this study, is shown in Fig. 11. Quadratic elements are used throughout this study.

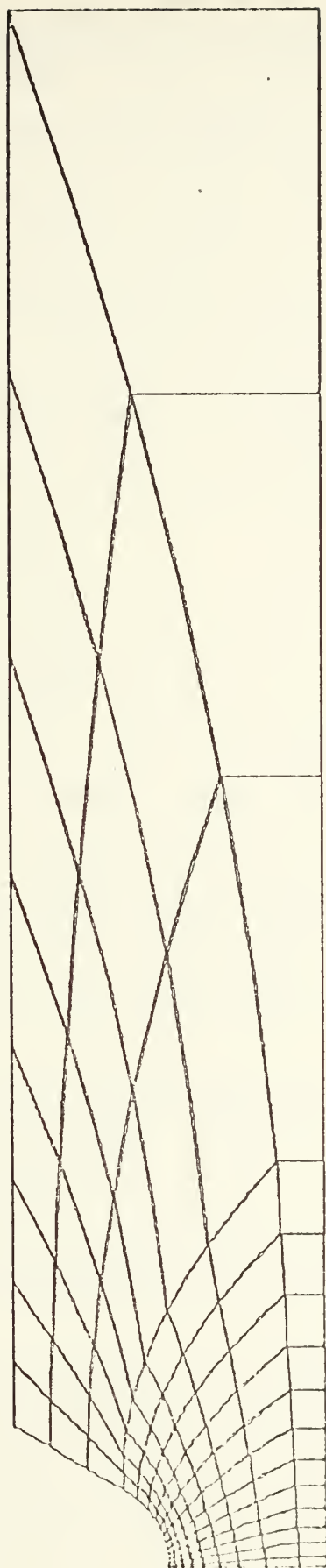


Fig. 11. A sample mesh as used

3. Boundary Condition Calculations

Boundary conditions for the structure are in two categories — force and displacement. As established in Section III D , there are two sets of force conditions and four sets of deflection conditions. These are easily coded into PLIMEG where the appropriate input data for the FEM program is prepared. A particular set of boundary conditions is imposed by a code number which exactly corresponds to one of the four problems outlined in Section III B.

D. SUBROUTINE PROBLM

The test structure, divided into the SEL arrangement utilized, is illustrated in Fig. 12. SEL numbers and SEL node numbers are indicated. The SEL arrangement was selected after considerable experimentation with other arrangements, based on the following considerations:

1. Small elements are required at the base of the notch because of the high stress gradient there.
2. Large elements are adequate away from the notch, specifically at the end of the structure where loads are applied.
3. Storage capacity of the computer limits maximum number of elements to not more than 180.
4. Extreme element corner angles (i.e. near 0° or 180°) must be avoided.
5. Each SEL must be a four-sided figure.
6. Relying on the principle of Saint-Venant, a single element boundary may be used to represent the loaded end.

The coordinates of most of the nodes are obvious after certain key nodes are located. The origin is at node 27. Nodes 1, 4, 7, 20, and 33 are established by the parameters

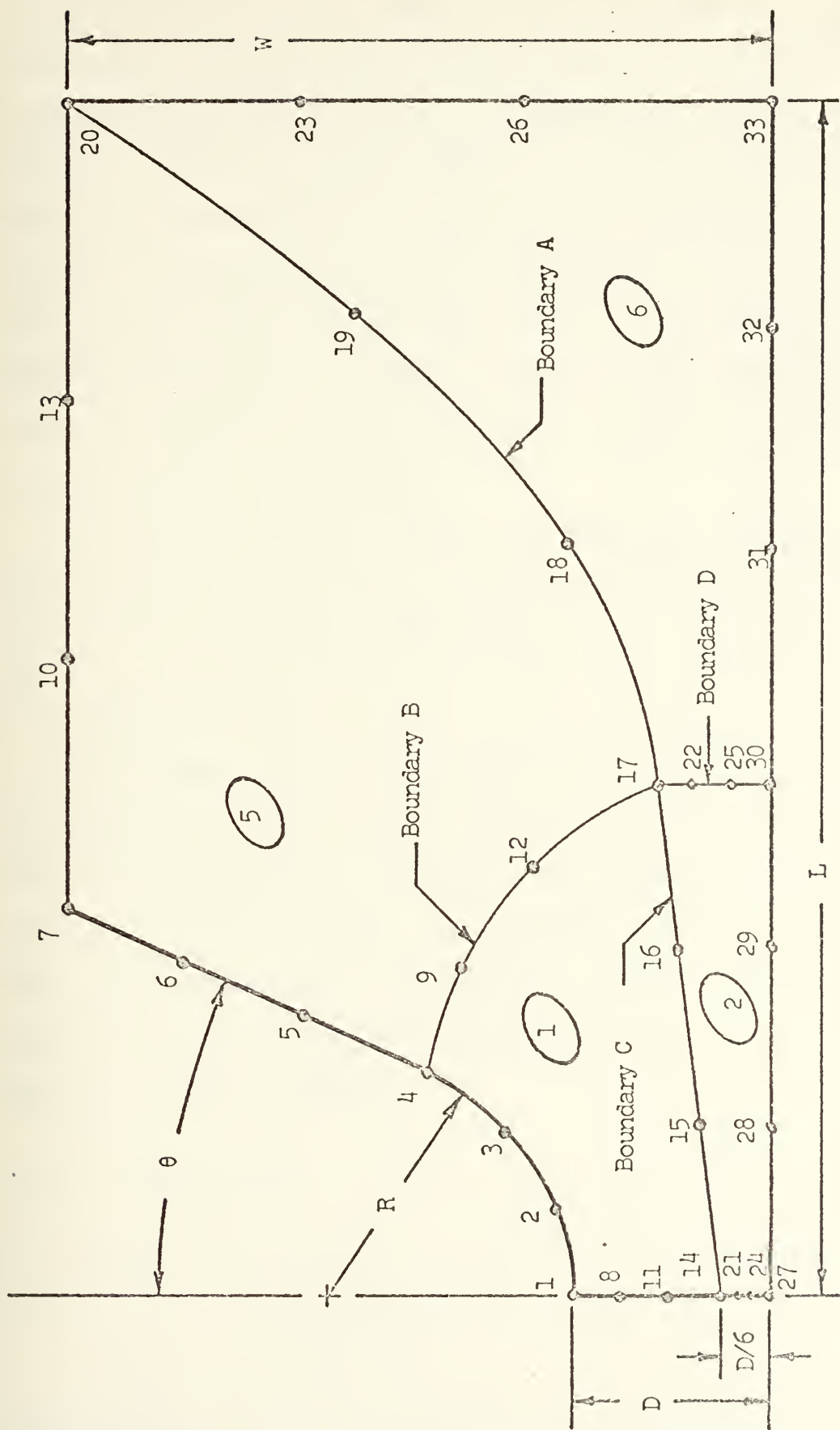


Fig. 12. Structure SEL's and boundary nodes. SEL identification numbers appear in ovals. (Not to scale)

directly (R/W, D/W, θ), when $L = 5W$ is provided. The x coordinate of node 30 was established at $W+R$ and the y coordinate of node 14 at $D/6$. Boundary A is an arc of the parabola passing through nodes 14 and 20 with zero slope at node 14. Boundary B is an arc of another parabola through nodes 4 and 17 perpendicular to boundary A at node 17. Boundaries C and D are straight lines. Intermediate nodes, where indicated, are located at the $1/3$, $2/3$ points along the curve establishing the boundary. Table V is a summary of the SEL node coordinates.

The program PROBLM, written to calculate SEL node coordinates uses the above criteria and requires a single card input: parameters R/W, D/W and θ .

E. SUBROUTINE ANS

The answer required for each problem is the stress concentration factor which is calculated in subroutine ANS. This program produces a single card reporting problem parameters and the stress concentration factor associated with them. The stress concentration factors reported are based on the following definitions of σ_{nom} .

Case 1, uniform loading:

$$\sigma_{nom} = P/A$$

where:

P = total load applied *

$A = 2D$ = net width of the bar

*Actually here and elsewhere, loads are per unit thickness.

TABLE V

SEL Node Coordinates

<u>Node</u>	<u>SEL's</u>	<u>x coordinate</u>	<u>y coordinate</u>
1	1	0	D
2	1	$R \sin(30^\circ - \theta/3)$	Note (1)
3	1	$R \sin(60^\circ - 2\theta/3)$	Note (1)
4	1,5	$R \cos \theta$	$(D+R) - R \sin \theta$
7	5	$x_4 + (W-y_4) \cot \theta$	W
9	1,5	$x_4 + (x_{17}-x_4)/3$	Note (3)
12	1,5	$x_4 + 2(x_{17}-x_4)/3$	Note (3)
14	1,2	0	D/6
17	1,2,5,6	$R + W$	Note (2)
18	5,6	$x_{17} + (x_{20}-x_{17})/3$	Note (2)
19	5,6	$x_{17} + 2(x_{20}-x_{17})/3$	Note (2)
20	5,6	$5W$	W
27	2	0	0
30	2,6	$R + W$	0
33	6	$5W$	0

Notes:

- (1) Determined by circular arc of radius R through 1,4.
- (2) Determined by parabola A through 14, 20 with zero slope at 14.
- (3) Determined by parabola B through 4, 17 perpendicular to parabola A at 17.
- (4) Points not listed are on straight line boundaries equally spaced between corner nodes.

Case 2, bending moment:

$$\sigma_{\text{nom}} = Mc/I$$

where:

M = total moment applied

c = D = distance from neutral axis

I = $2D^3/3$ = moment of inertia

Case 3, uniform loading:

$$\sigma_{\text{nom}} = P/A$$

where:

P = total load applied

A = D = net width of the bar

Case 4, bending moment

$$\sigma_{\text{nom}} = Mc/I$$

where:

M = total moment applied

c = D/2 = distance from neutral axis

I = $D^3/12$ = moment of inertia

F. PROGRAM MAIN

The four programs: PROBLM (establishes SEL node coordinates based on parameters), PLIMEG (discretises the structure and computes boundary conditons), PLISOP (solves the

stress problem) and ANS (calculates the stress concentration factor) are joined together by MAIN. All card output, except the single card from subroutine ANS, is suppressed. Input data and intermediate results are passed within the program in common blocks and via computer direct-access devices. The functions of the main program are to read and store the input data, call the various subroutines in turn, provide output of the solution cards and prints, and to increment the problem parameters so as to run through a related series of evaluations.

V. PROGRAM OPERATION

A. INPUT

The problem input data deck consists of nine cards, a typical example of which is shown in Fig. 13. Card 1 lists the problem parameters: R/W , D/W , and θ . Cards 2 and 3 are title cards which may contain any message to identify the run. Card 4 lists the mesh parameters: number of SEL's, number of nodes in each element (not SEL), problem identification number and an indicator for plotting the mesh. Cards 5 through 8, are SEL connectivity cards. Each card lists the number of increments to be used in the ξ and η directions, their respective exponential coefficients, and a listing of the nodes, appropriately ordered, defining the corners of the SEL. Card 9 lists the solution parameters: number of materials, an indicator for the plane stress solution, and a code for the numerical integration technique.

The job control language cards (JCL) needed to make the program operational, details of card format, and program options are discussed in Appendix D.

B. OUTPUT

Although the output required in this particular application is a single number (SCF), a great deal more is available. All of the input data is echo checked and the following important data passed between subroutines is printed:

00.300	0.5000	30.000										
THIS IS A SAMPLE INPUT DECK -- CARD COLUMNS ARE INDICATED ON THE NEXT CARD												
12345678901234567890123456789012345678901234567890	1	2	14	17	4	1	12	1.0	-1.0			
	12	1	27	30	17	1	4	1.0	-1.0			
	12	14	17	20	7	1	12					
	3	17	30	33	20	1	12					
	1			0	2							

FIG. 13 SAMPLE INPUT DECK

SEL node coordinates.

Element node coordinates with the load boundary conditions as imposed.

Element connectivity.

Displacement boundary conditions.

Material properties.

Displacements u and v for each node.

Reactions at the nodes where displacement boundary conditions were imposed.

A force equilibrium check which is the result of summing all x -direction and all y -direction reactions.

Average stress components at each node.

Average strain components at each node.

Stress concentration factor.

Although the stress concentration factor is independent of Young's modulus and Poisson's ratio, the values 30×10^6 and 0.3 respectively were coded into the program as representative of common engineering materials. The average stress and strain components are computed and printed in two ways: the cartesian coordinate components (σ_x, σ_y , and τ_{xy}) and the principal values (σ_1, σ_2 , and τ_{\max}) with the inclination of the principal axes (ϕ).

Other output in the form of data cards and the plotted mesh has already been mentioned.

VI. PROGRAM OUTPUT ANALYSIS

A. EQUILIBRIUM

Static equilibrium is maintained in the finite element solution of all problems studied. As indicated earlier, the equilibrium of forces is quickly checked from program output by comparing the imposed loading with the reaction summations printed by PLISOP as "equilibrium check".

The check on moment summation is slightly less convenient. Program output, including loads and reactions at all nodes, and the coordinates of nodes, is available but the actual arithmetic must be done by hand. These external calculations were made for several representative problems. The results were as required: moments and forces sum to zero.

B. MAXIMUM STRESS LOCATION

Using the program output, the location of the maximum principal stress was determined for several parameter combinations. In every case the maximum occurred tangent to the edge at the bottom of the notch.

C. CONVERGENCE

To investigate convergence behavior, we first identify the rows and columns of the SEL divisions used. The columns are referred to as band A and band B; the rows as band C and band D (Fig. 14). In what follows, band D always consists of one row of elements. This limit was imposed because

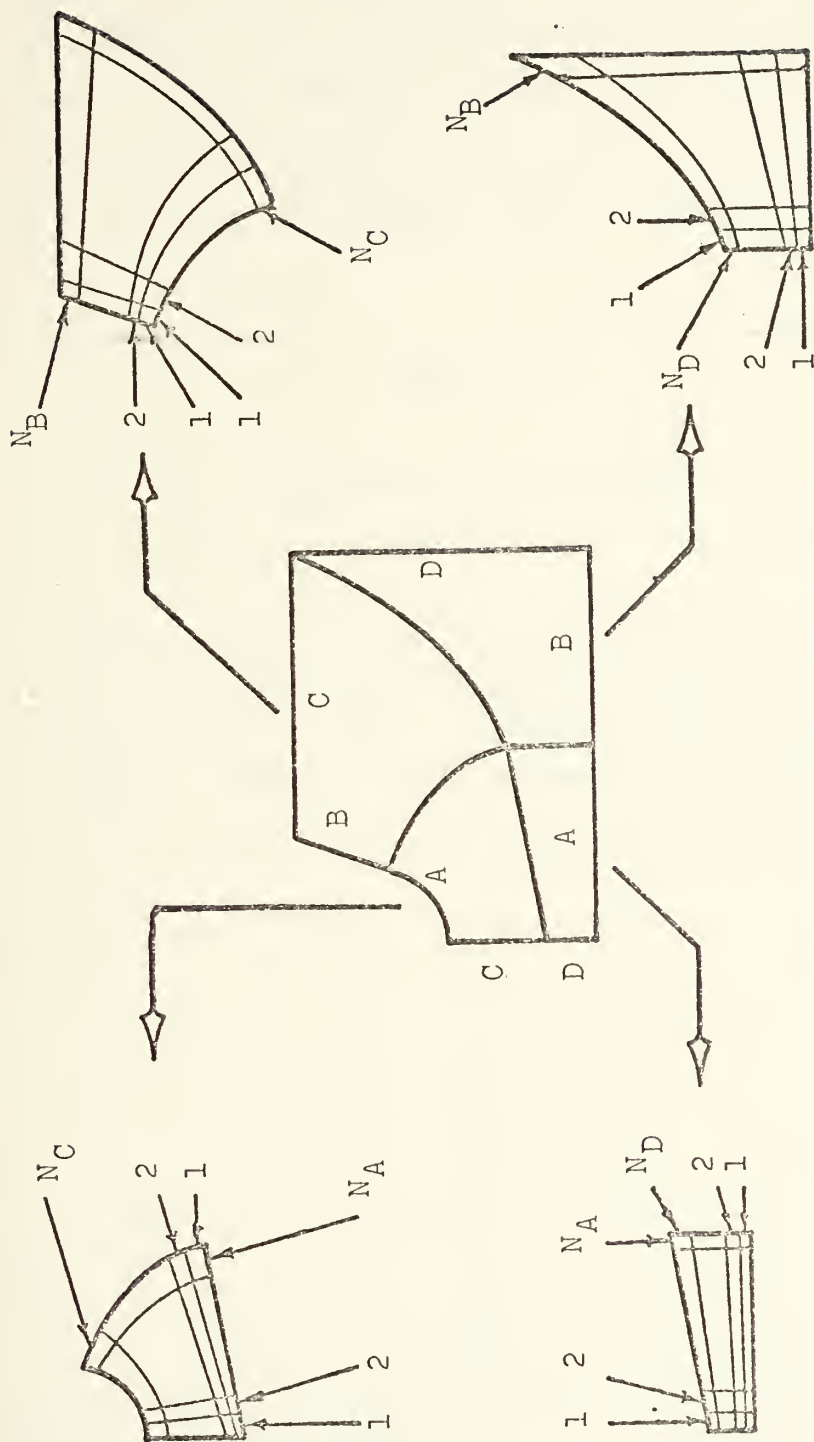


Fig. 14. SEL bands for convergence study (Numbers 1,2,...,N_A, etc., indicate band numbering).

of core storage availability in the computer used.

The refinements were accomplished by first assigning a base number to each of the other bands, then multiplying by a successively larger integer for each new mesh. Table VI shows the number of elements per band and total elements in the mesh. The mesh ultimately used is included for comparison.

TABLE VI

Convergence Subdivisions

$$N_{\text{total}} = (N_A + N_B)(N_C + N_D) \text{ (Refer to Fig. 14)}$$

Band Division	First Run (1)	Second Run (2)	Third Run (2)	Fourth Run (2)	Final Data Runs (3)
N_A	3	6	9	12	12
N_B	2	4	6	8	3
N_C	2	4	6	8	8
N_D	1	1	1	1	1
Total Elements	15	50	105	180	135

- (1) This division was used primarily to verify correct performance of program.
- (2) These divisions were used to verify and evaluate convergence.
- (3) This division was used for volume data generation as an optimal compromise giving good accuracy and satisfactory computer turnaround.

The refinement was done for several combinations of the problem parameters. Figure 15 is a representative plot of the stress concentration factor vs. (reciprocal of) total elements in the mesh for two combinations of the parameters as shown. In both cases only the three finest meshes used in the convergence study (50, 105 and 180 elements) are shown. Fitting a straight line through the points and extrapolating back to the axis of ordinates, an approximation for the converged result can be obtained. The value obtained using 135 elements (see below) has been added. Note that it plots on this same straight line.

Consider the upper curve shown which represents the case of a shallow notch. The extrapolated value for stress concentration factor is $SCF = 1.773$. The 180 element result is less than 0.8% high while the 135 element mesh used is less than 1% high. Results from studies using other parameter combinations, including $\theta \neq 0$, showed the same convergence pattern.

The mesh of 135 elements was chosen for data runs because that size mesh requires approximately $3/4$ of the computer core storage space available. From a practical standpoint data collection proceeded without undue special arrangements in the computer center. The larger number of elements required elaborate special consideration by operating personnel which was not warranted by the 0.2% difference in the results.

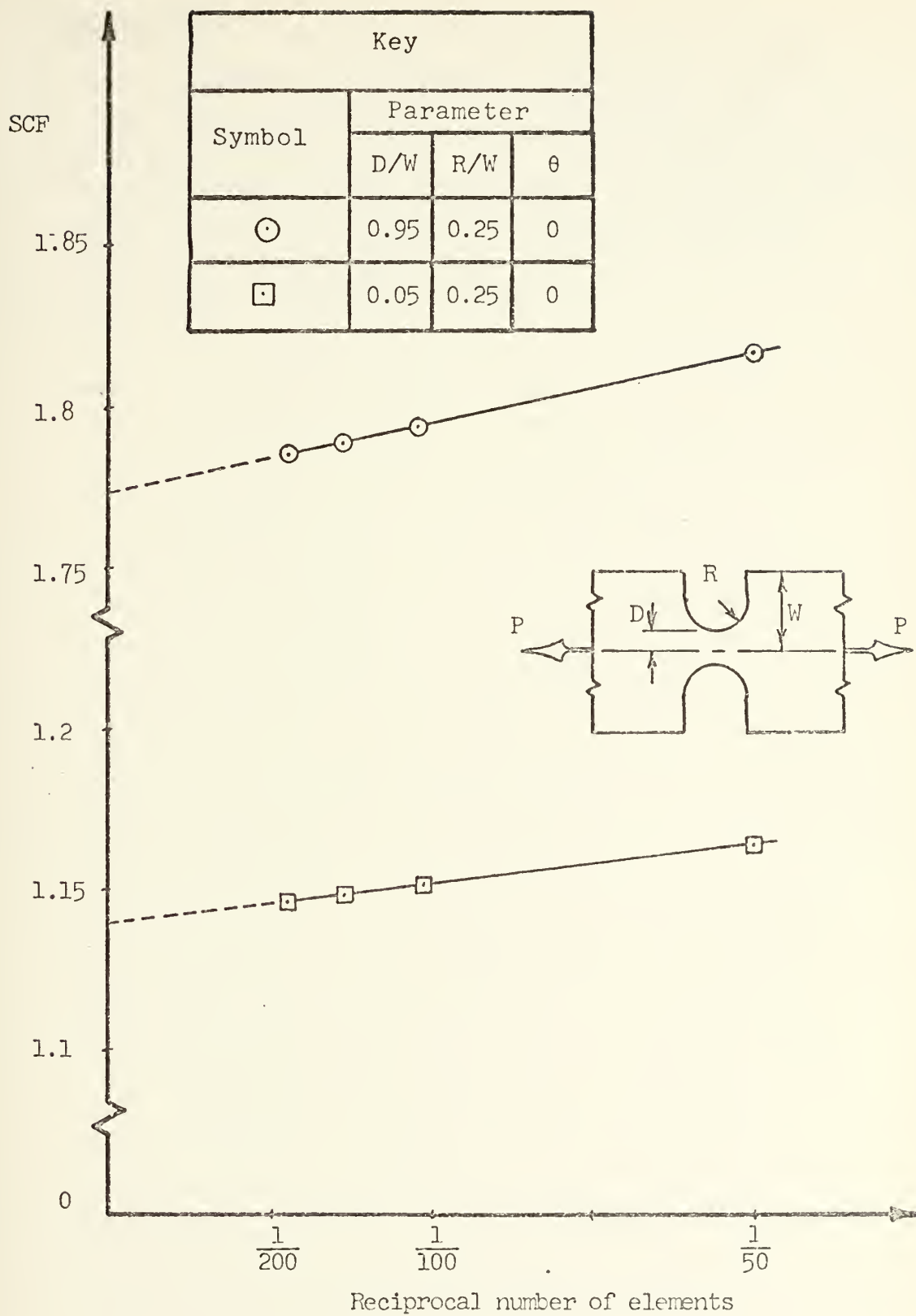


Fig. 15. Convergence Plot

D. CORRELATIONS

The data collected is discussed in the next section. As will be seen, experimental data from the literature correlates very well with values of SCF calculated. The trends established are verified and the experimental values are sometimes identical to three significant figures.

VII. DISCUSSION OF RESULTS

A. RESULTS PRESENTED

The SCF's presented in Appendix A document a representative variation of the parameters for problem 1. It is obvious that either $\theta = 90^\circ$ or $D/W = 1$ constitutes a bar with no notch and results in stress concentration factor = 1. Several computer runs with D/W very small showed that as D/W approaches zero, SCF indeed did approach unity.

To establish the curves, $D/W = 0.1$ was taken as the initial value and incremented by adding 0.2 through $D/W = 0.9$. Likewise, R/W was incremented by steps of 0.05 from 0.1 through 0.5. θ was incremented by steps of 15° from 0° through 60° .

The data are presented as several families of curves. Each family has a specified θ associated with it. The curves are plotted as SCF vs. D/W with R/W as a parameter for each family. Linear interpolation between the curves may be used without appreciable error. Interpolation between the families for $\theta = 60^\circ$ and $\theta = 90^\circ$, where stress concentration factor is one, should not be attempted. Data points actually calculated are indicated by a cross. The curves through these points were generated by fitting a sixth order polynomial through them.

Only one run was made to prove the programing for problem 2; no data for this case are presented. One run was also made for each of problem 3 and 4. The data collected are presented

in Section VII D in the form of a correlation with experimental data from the literature.

Time was not available for more extensive data collection. However, now that the software has been perfected and proved, it is a perfectly straightforward task to obtain additional data as computer time becomes available. Appendix D suggests the parameter ranges which should be investigated.

B. EFFECT OF NOTCH DEPTH

Selected data from the studies of problem 1 are plotted in Fig. 16. The parameter D/R is constant. Experimental data plotted is from Flynn and Roll; however Kikukawa's data shows the same trends. The data in the experiments was for the symmetrically located U-shaped notches as in problem 1, with $\theta = 0$. Both Neuber's results and Flynn and Roll's experimental data are included for the hyperbolic shaped symmetric notches with the same parameters.

The general close agreement between the FEM and experimental values for the U-shaped notch is easily seen. The largest difference noted is for $W/D = 4.33$ where the difference is less than 2%.

We might examine the difference by utilizing an aspect ratio defined as effective length from the notch to point of load application divided by notch depth. Table VII compares this value. As can be seen, the calculations allow a much more favorable (i.e., larger, and thus more realistic) ratio than that provided in the experiment.

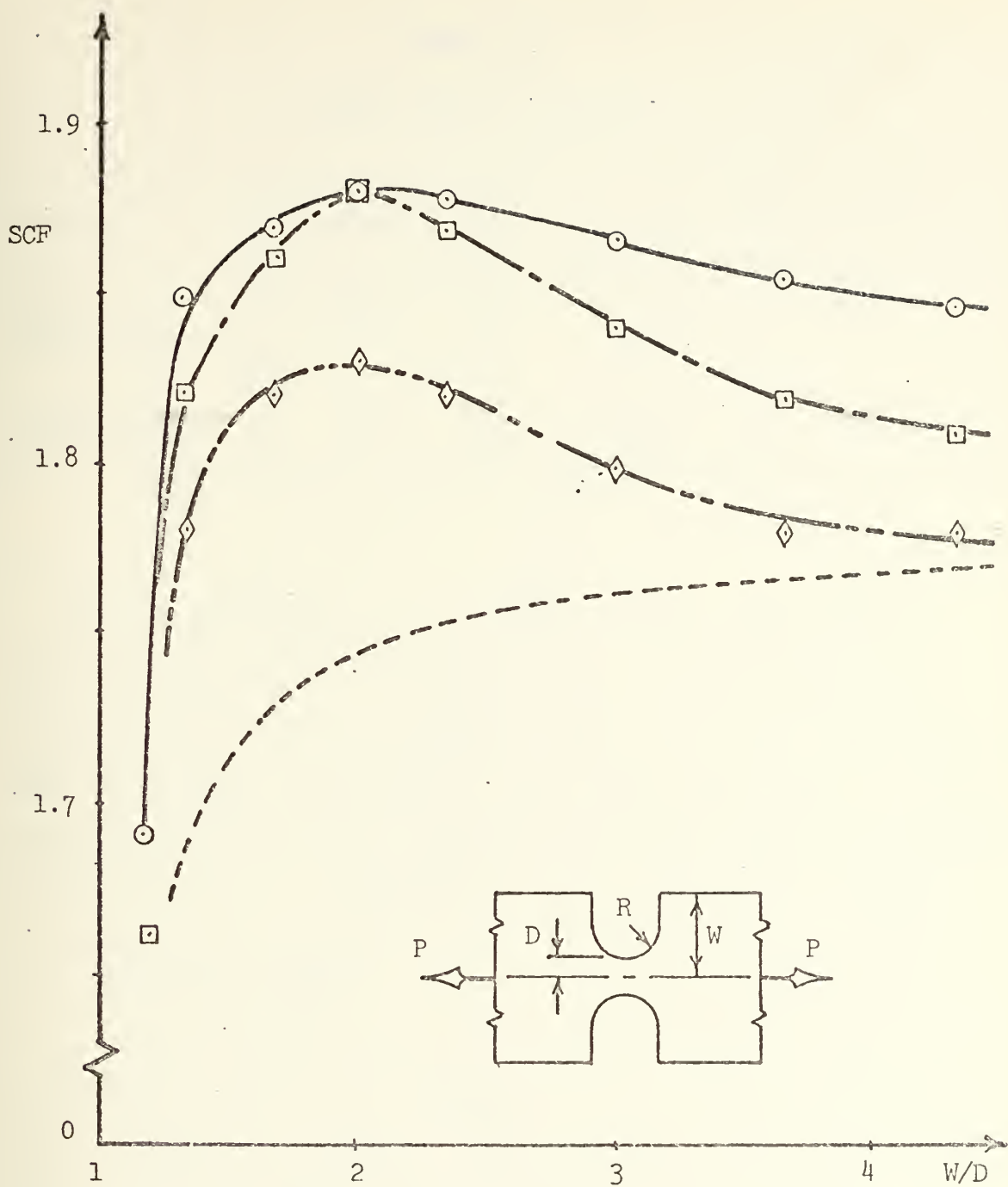


Fig. 16. Effect of notch depth on SCF for $R/W = 1.5$

- Numerical U-notch (Finite Element)
- Experimental U-notch (Flynn & Roll)
- ◇—◇ Experimental Hyperbolic notch (Flynn & Roll)
- Analytical Hyperbolic notch (Neuber)

TABLE VII

Aspect Ratio $L/(W - D)$

Source	W/D = 2	W/D = 3	W/D = 4.33
FEM Calculations	10	7.5	6.5
Experiments	8.6	4.33	2.6

The maximum point on the curve in Fig. 16 occurs at $W/D = 2$, a relatively shallow notch. Experimental data matches at this point exactly. Note, the error that would be made if Neuber's hyperbolic notch result was used for such a notch is more than 7%. Experimental data presented by Flynn and Roll point to a systematic error in Neuber's results.

C. EFFECT OF ANGLE θ

The data plotted in Fig. 17 compares the stress concentration factor for $\theta = 60^\circ$ (SCF_{60}) to the stress concentration factor for $\theta = 0^\circ$ (SCF_0). The parameter used is W/D . Two experimentally determined curves show that increasing the angle of the V from 0° to 60° decreases the SCF_{60} . This effect is more profound as the W/D ratio is increased (i.e., for deeper notches).

Replotting the data as in Fig. 18 shows the variation of SCF_{60} with changing W/D for constant SCF_0 . Note the close correlation of the experimental data and FEM data.

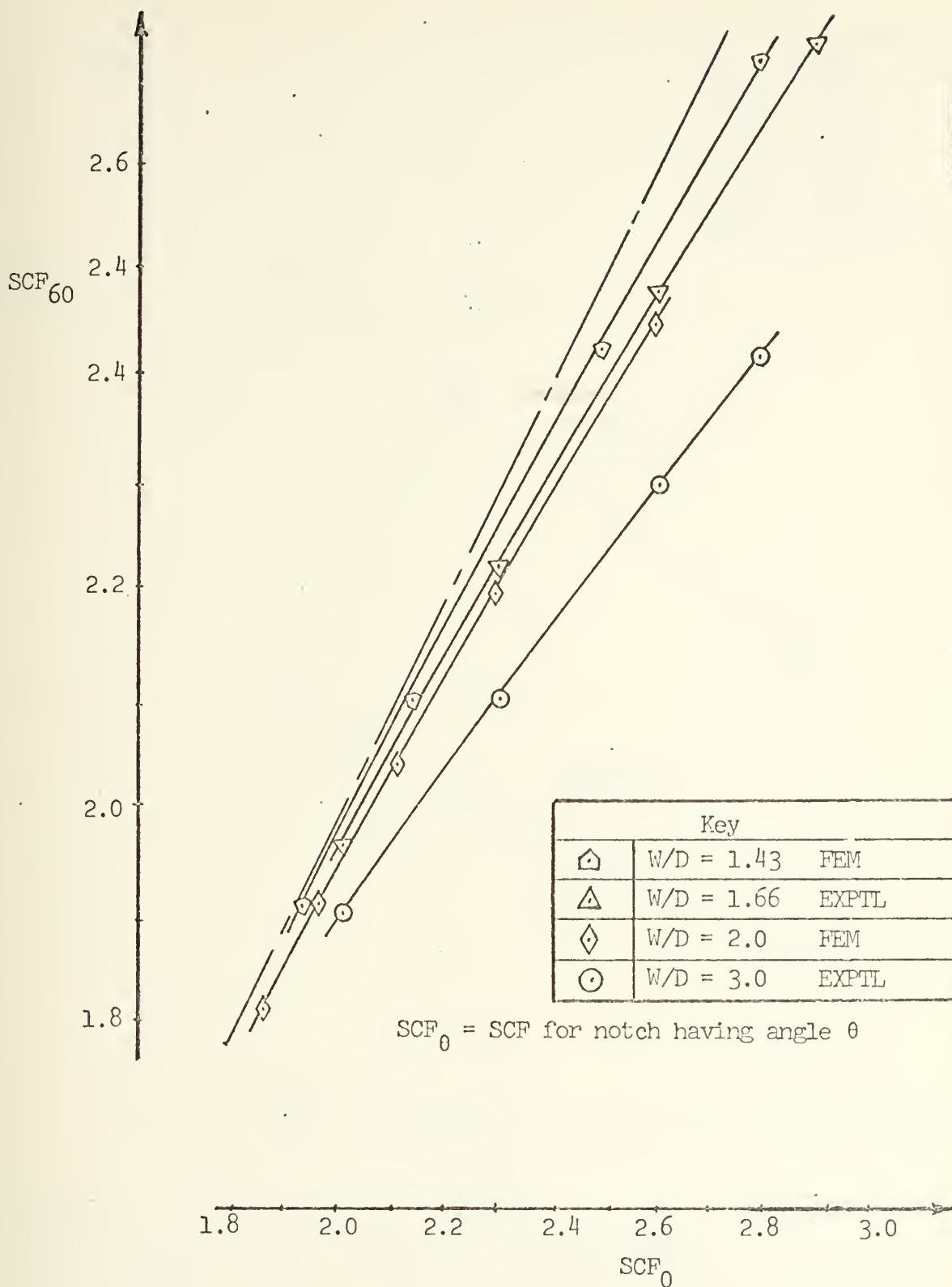


Fig. 17. Effect of V angle on SCF. The dot-dash line ($SCF_{60} = SCF_0$) is included for reference to emphasize that SCF_{60} is always less than SCF_0 for any value of the other parameters. Similar data could be plotted for other values of θ .

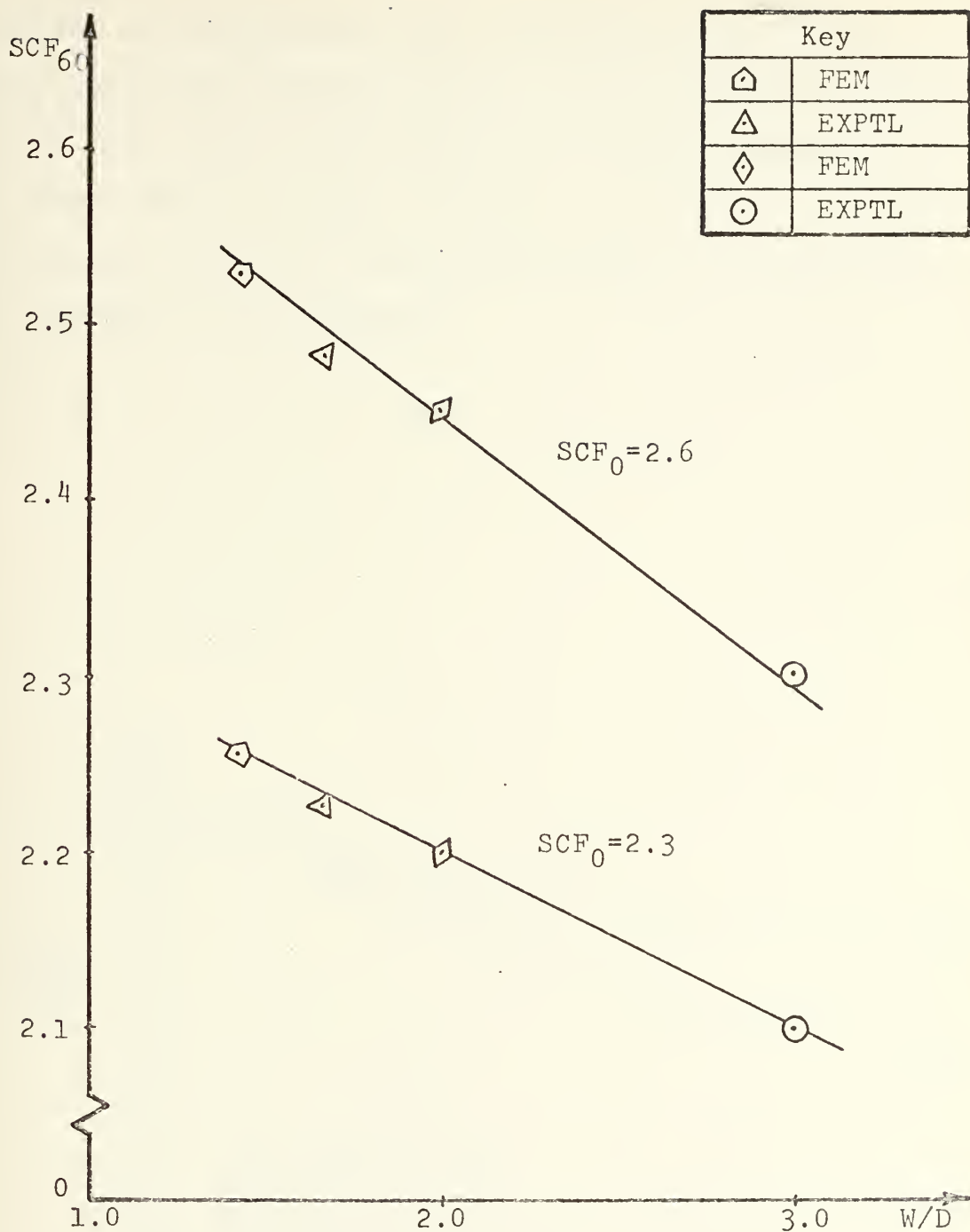


Fig. 18. Effect of W/D on SCF_{60} These lines represent profiles (for $SCF_0 = 2.3$ and $SCF_0 = 2.6$) of the data shown in Fig. 17. The same plot symbols are used as in Fig. 17.

Figure 19 demonstrates that increasing the angle θ reduces the stress intensification and this effect is more profound for smaller radius notches than for notches where the bottom radius is large. That is, the SCF for a given notch may be reduced by increasing either R or θ while the other parameters are unchanged.

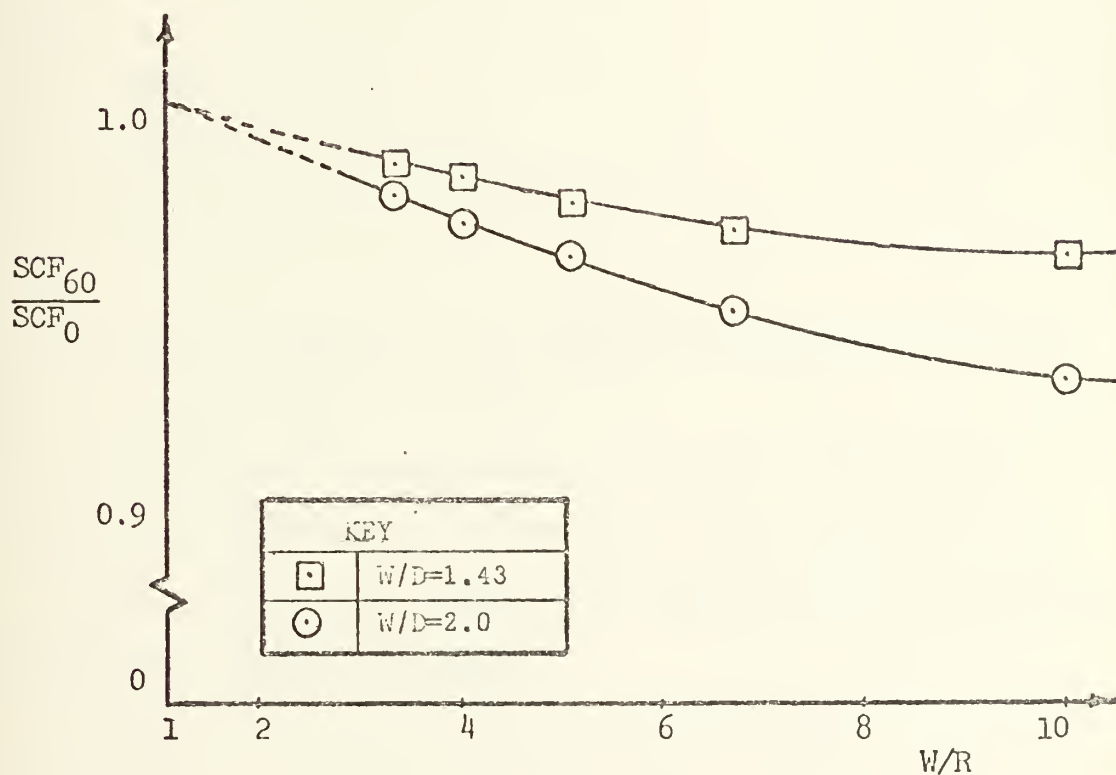


Fig. 19. Effect of angle θ on SCF as function of radius

D. SINGLE NOTCH GEOMETRY

The only experimental data available dealing with the single notch geometry is that presented by Cole and Brown [5]. Their data is for a particular case of loading such that the line of action of the applied force is through the midpoint of the net width of the bar. By an appropriate combination of the SCF's calculated for problems 3 and 4 this loading can be reproduced as shown in Fig. 20. The defining relationship for SCF as used by Cole and Brown is:

$$SCF_* = \frac{\sigma_{\max}}{P/D}$$

where

σ_{\max} = maximum stress

P = total load applied

D = net width

The defining relationships for problem 3 (SCF_3) and problem 4 (SCF_4) are contained in Section IV E.

For the parameter values $D/W = 0.5$, $R/W = 0.1$ and $\theta = 0^\circ$, Cole and Brown report $SCF_* = 1.95$. The computed results are $SCF_3 = 7.85$, $SCF_4 = 1.98$. Making the appropriate substitutions and solving for maximum stress:

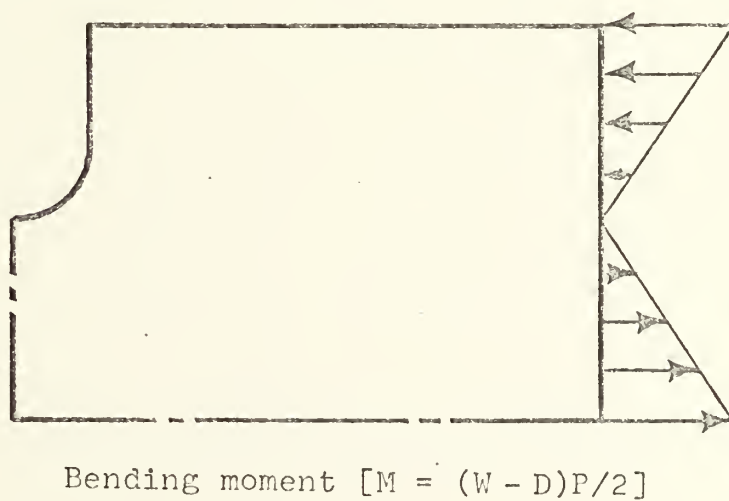
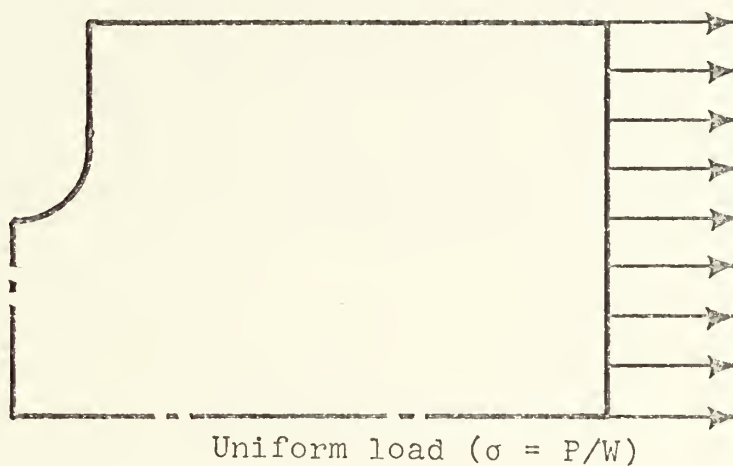
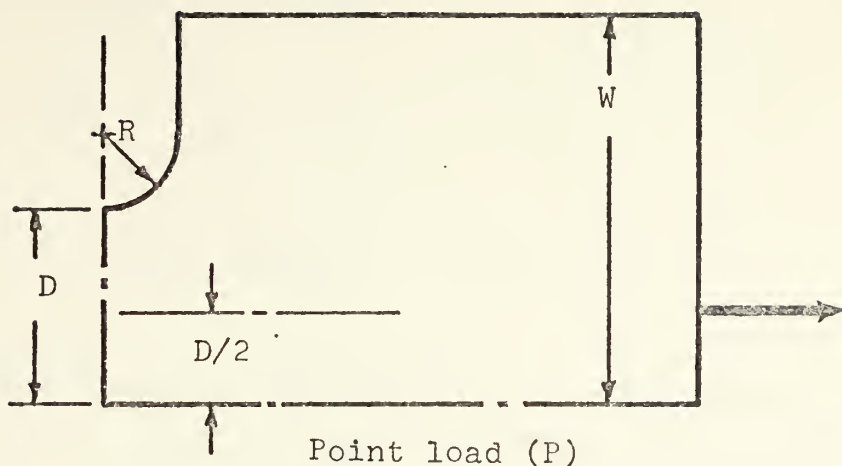


Fig. 20. Bar with one notch only. A point load decomposed into constant and linearly varying components. St. Venant's principle accounts for the absence of higher order components.

$$\begin{aligned}
\sigma_{\max} &= \text{SCF}_3 \left(\frac{P}{D} \right) - \text{SCF}_4 \left(\frac{Mc}{I} \right) \\
&= (\text{SCF}_3 - 3 \text{SCF}_4) \left(\frac{P}{D} \right) \\
&= 1.91 \left(\frac{P}{D} \right) = \text{SCF} \left(\frac{P}{D} \right)
\end{aligned}$$

Thus the FEM analysis gives $\text{SCF} = 1.91$ compared to Cole and Brown's 1.95. There is approximately 2% difference in the results. A special computer run with this specific loading gave $\text{SCF} = 1.91$ also. This calculation served to verify superposability of the two cases and the correctness and internal consistency of the programming and the inputs.

VIII. CONCLUSIONS AND RECOMMENDATIONS

A. CONCLUSIONS

The FEM program as presented in this thesis can be used to calculate the stress concentration factor for the specific problems listed, over a wide range of the parameters used. Further, by appropriate superposing of these four specific problems, the SCF can be calculated for bars which are notched either on one side only or symmetrically on both sides and are subjected to general tensile and bending loads.

One of the conclusions from an analysis of the data obtained for problem 1, the case of the symmetrically notched bar subjected to a tensile load only, and a comparison with tabulations and recommendations in the literature is that the three parameters (minimum radius of curvature, gross width of the bar, and net width of the bar) do a rather good job of characterizing the geometry of the notch, in the sense that interpolated values of the SCF obtained from available data agree rather well with the more accurate values obtained by FEM analysis in this study.

However, the analysis also shows that there are some small but systematic deviations that are assignable to the fact that these three parameters are not sufficient to characterize the geometry of the notch completely. The data presented in Appendix A accordingly provides a more complete and accurate representation of SCF's in this case than was previously available.

The stress concentration factors presented in the literature for several specific cases of U-shaped and V-shaped notches are essentially correct. However, the data presented is limited, mainly because of the difficulties associated with experimental investigations. This program overcomes those difficulties and can solve for a single SCF in less than three minutes of computer time as compared to several hours by accepted experimental methods.

B. RECOMMENDATIONS

Accordingly, it is recommended that the program described herein be used to determine SCF's for problems 1 through 4 and that the results be published for general use. Appendix D presents a specific plan for obtaining the necessary results.

Further, if interest in other notch shapes warrants it, this program should be appropriately modified and the SCF's calculated and published.

An axi-symmetric stress analysis program has been written by Bahkshandehpour [3] as part of his NPS thesis. That program could be similarly adapted to calculate SCF's for general axisymmetric geometries having notches.

APPENDIX A

CURVES OF RESULTS

The stress concentrations presented in this appendix are for the problem of symmetrically located, round bottom, V-shaped notches subjected to uniform tensile loading. The data collected is plotted as crosses. A sixth order polynomial is shown fitted through these points.

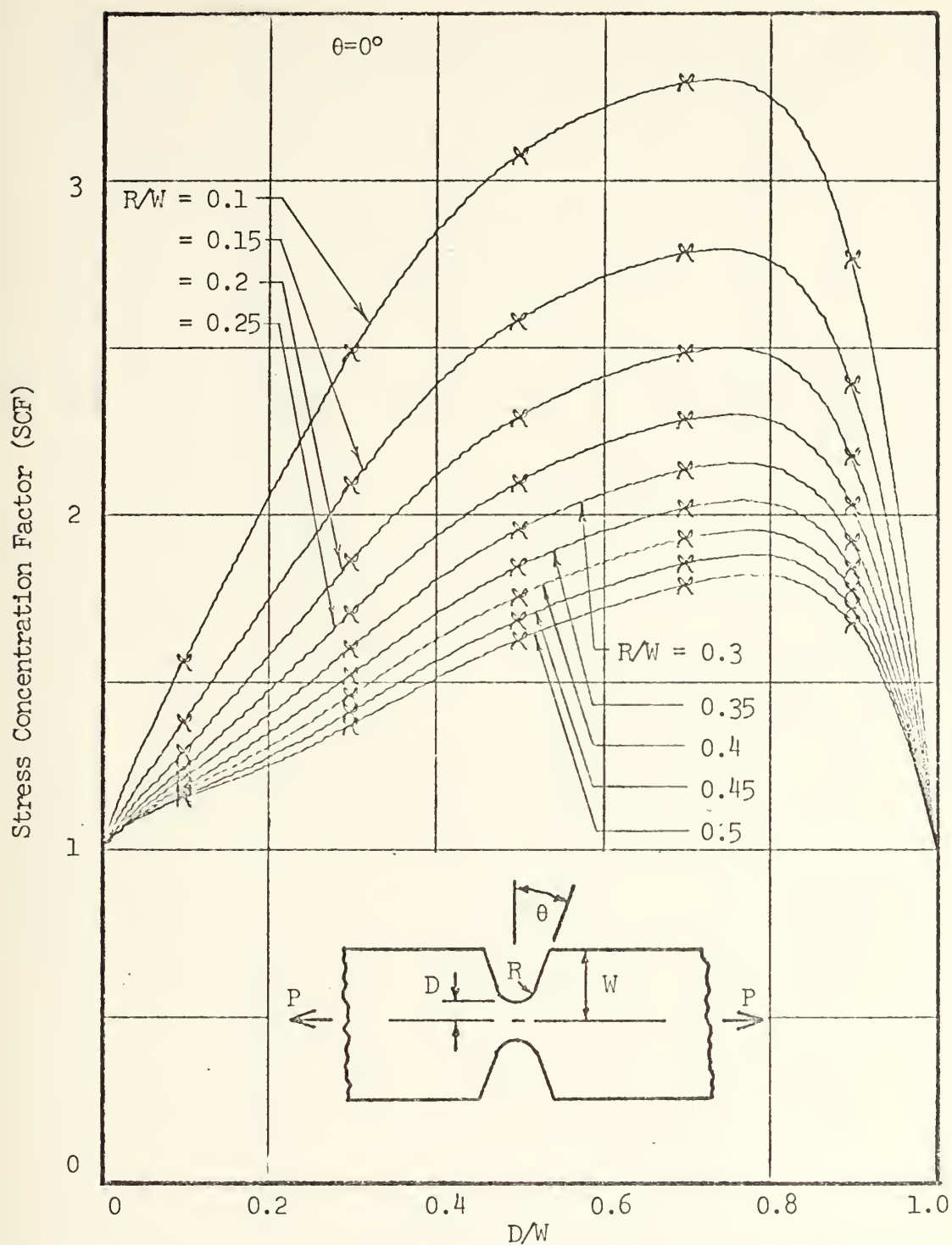
The curves are plotted as SCF vs. D/W using R/W as a parameter with each family representing a single θ value, where

R = radius of the bottom of the notch

D = net half width of the bar

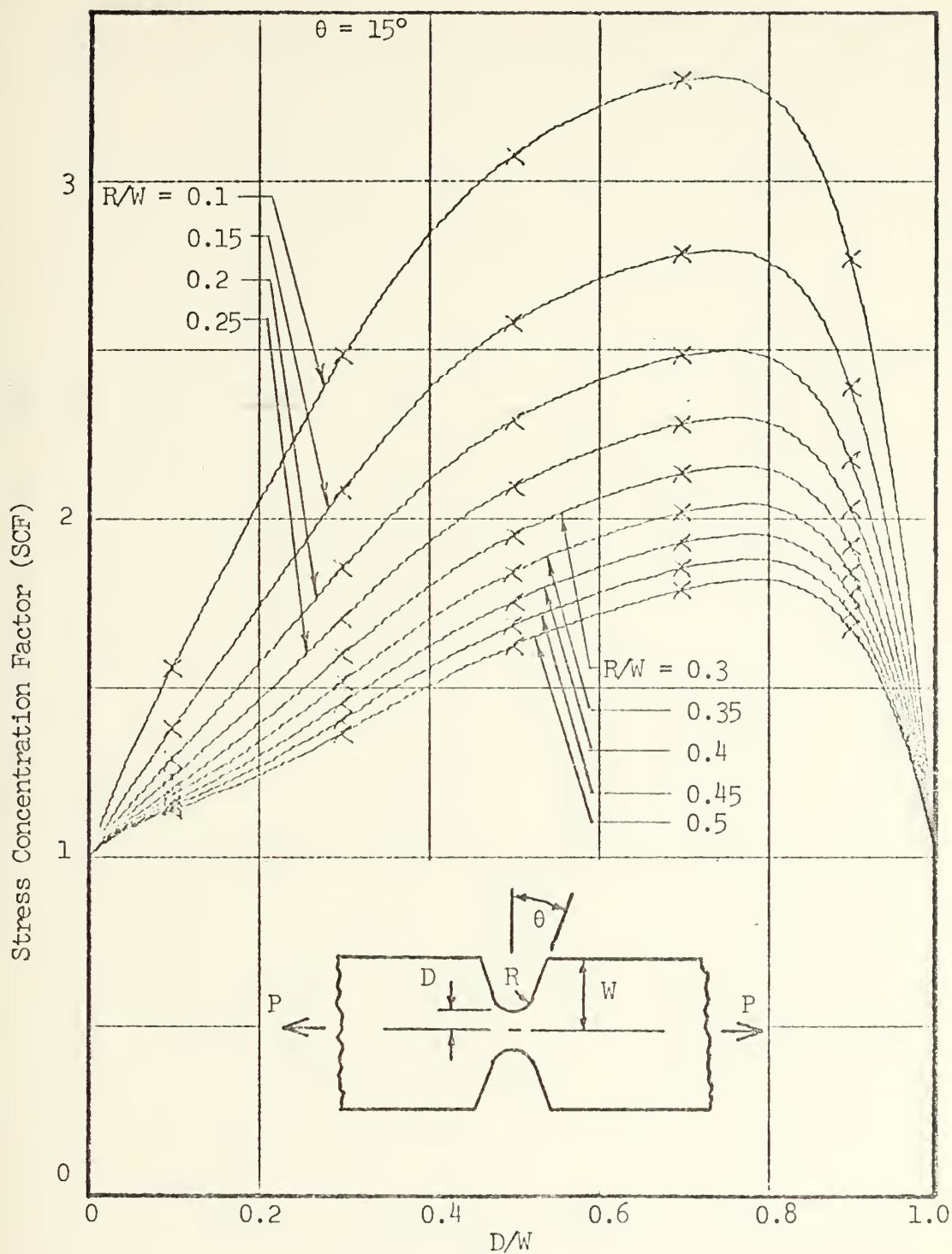
W = gross half width of the bar

θ = half included angle of the V



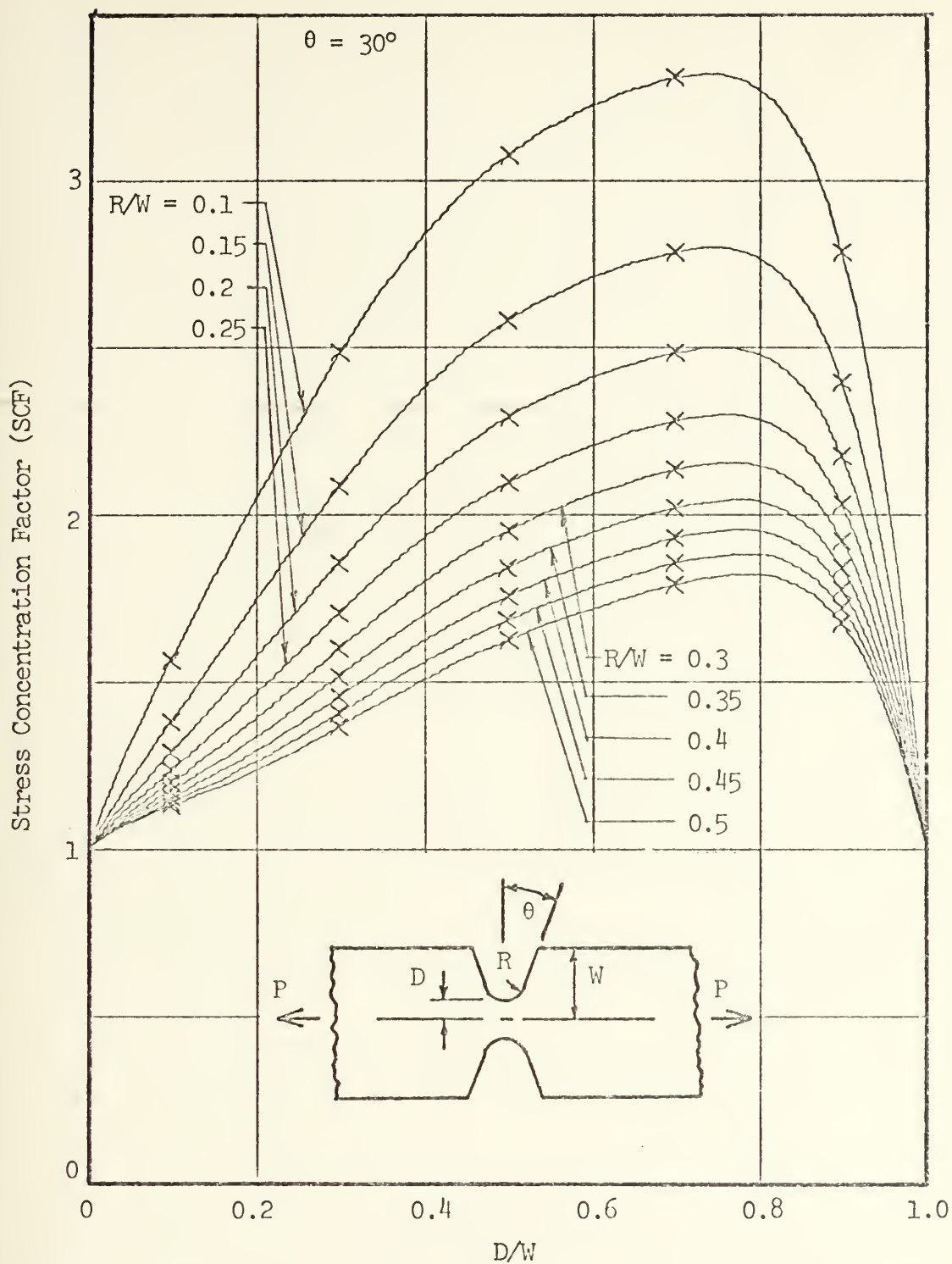
Plane stress values of SCF for $\theta = 0^\circ$.

x indicates FEM data. $\sigma_{\max} = \text{SCF} \left(\frac{P}{2D} \right)$



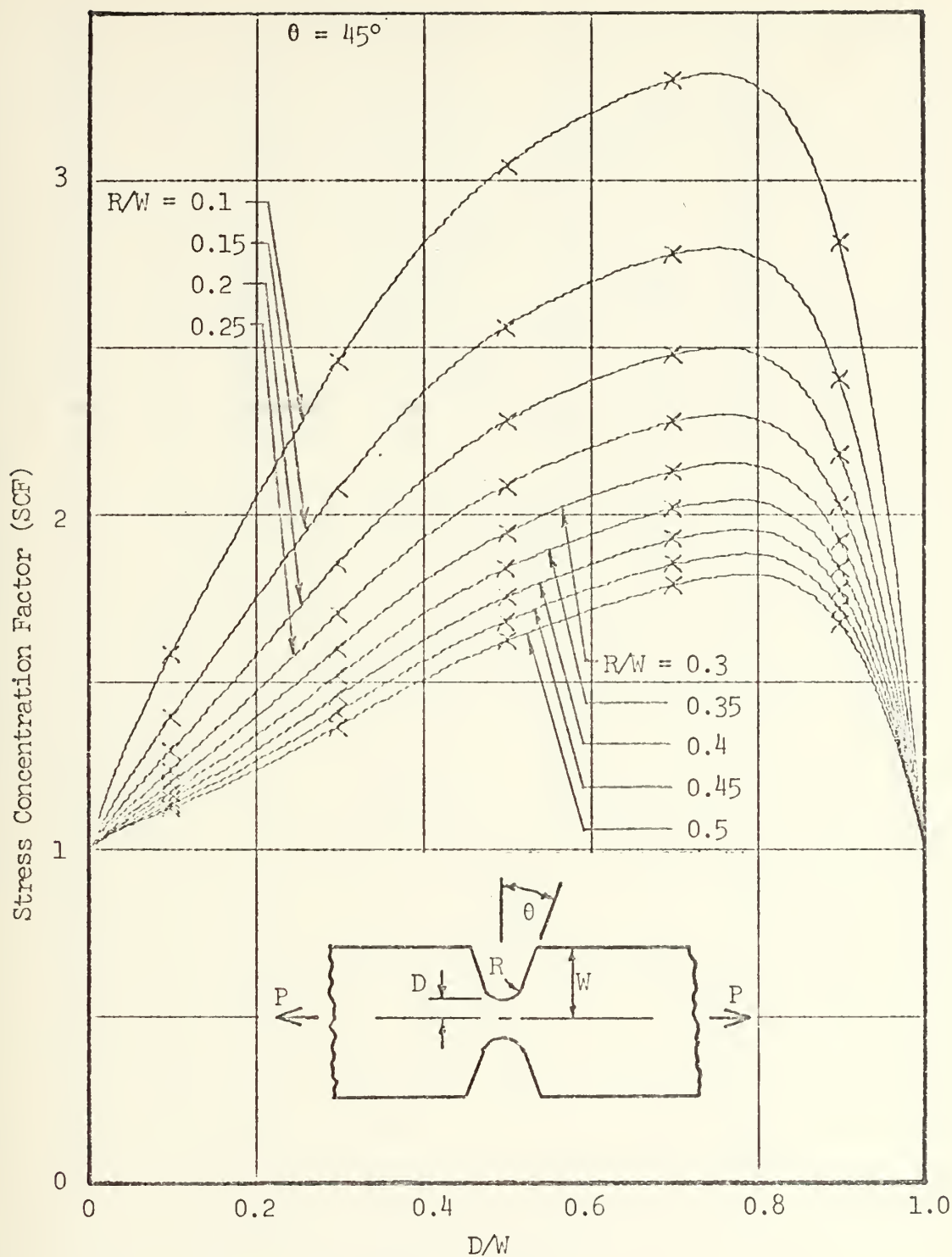
Plane stress values of SCF for $\theta = 15^\circ$.

x indicates FEM data. $\sigma_{\max} = \text{SCF} \left(\frac{P}{2D} \right)$



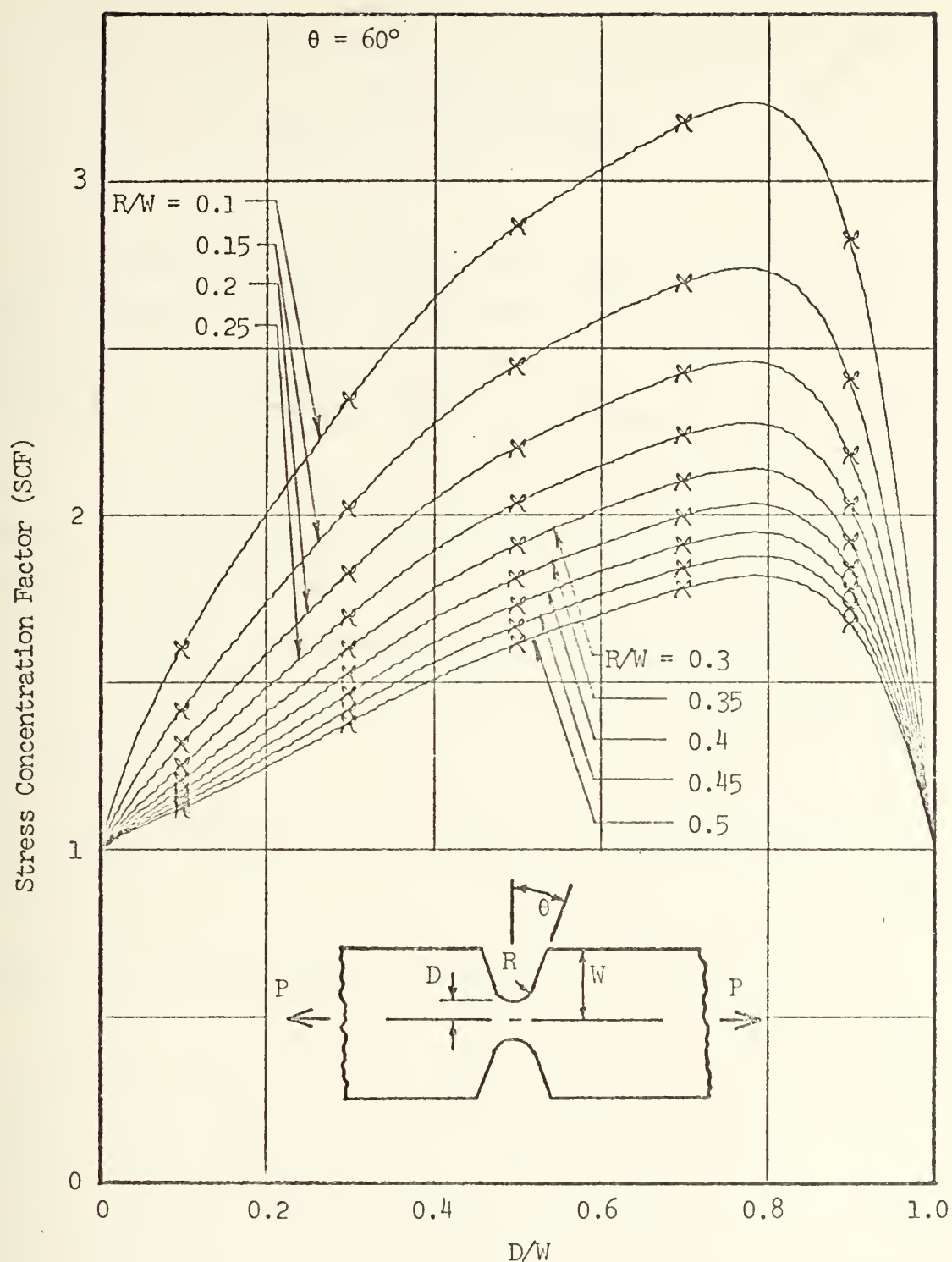
Plane stress values of SCF for $\theta = 30^\circ$

x indicates FEM data. $\sigma_{\max} = \text{SCF} \left(\frac{P}{2D} \right)$



Plane stress values of SCF for $\theta = 45^\circ$.

x indicates FEM data. $\sigma_{\max} = \text{SCF} \left(\frac{P}{2D} \right)$



Plane stress values of SCF for $\theta = 60^\circ$.

x indicates FEM data. $\sigma_{\max} = \text{SCF} \left(\frac{P}{2D} \right)$

APPENDIX B

NEUBER'S NOTCH ANALYSIS

This appendix is included since we have been unable to find a reference which quotes these useful and important results in a brief and clear fashion.

We are concerned with the two-dimensional case of an axial load transmitted in the y-direction through the net section of a thin bar (plane stress case) having a hyperbolic boundary. All quantities which follow are for unit thickness.

To describe the geometry and to provide a basis for the solution for elastic stress distribution, Neuber employed the mapping

$$z = c \cosh \zeta, \quad \zeta = \cosh^{-1}(z/c) = \ln[(z/c) + (z^2/c^2 - 1)^{1/2}] \quad (\text{B1a,b})$$

where z and ζ are complex variables

$$z = x + iy, \quad \zeta = \xi + i\eta \quad (\text{B2a,b})$$

and i is the imaginary unit. In real terms this results in

$$x = c \cosh \xi \cos \eta; \quad y = c \sinh \xi \sin \eta \quad (\text{B3a,b})$$

$$\xi = \frac{1}{2} \cosh^{-1}(G+H), \quad \eta = \frac{1}{2} \cos^{-1}[G-H] \quad (\text{B4a,b})$$

where

$$G = (x^2 + y^2)/c^2; \quad H^2 = G^2 + 2(y^2 - x^2)/c^2 + 1 \quad (\text{B5a,b})$$

This mapping provides a correspondence between the xy cartesian system of coordinates and a $\xi\eta$ system useful for defining the geometry of the notch. Lines of constant ξ are ellipses

$$\left(\frac{x}{c \cosh \xi}\right)^2 + \left(\frac{y}{c \sinh \xi}\right)^2 = 1 \quad (B6)$$

while lines of constant η are the hyperbolas

$$\left(\frac{x}{c \cos \eta}\right)^2 - \left(\frac{y}{c \sin \eta}\right)^2 = 1 \quad (B7)$$

Figure B-1 shows the pattern of the $\xi\eta$ network.

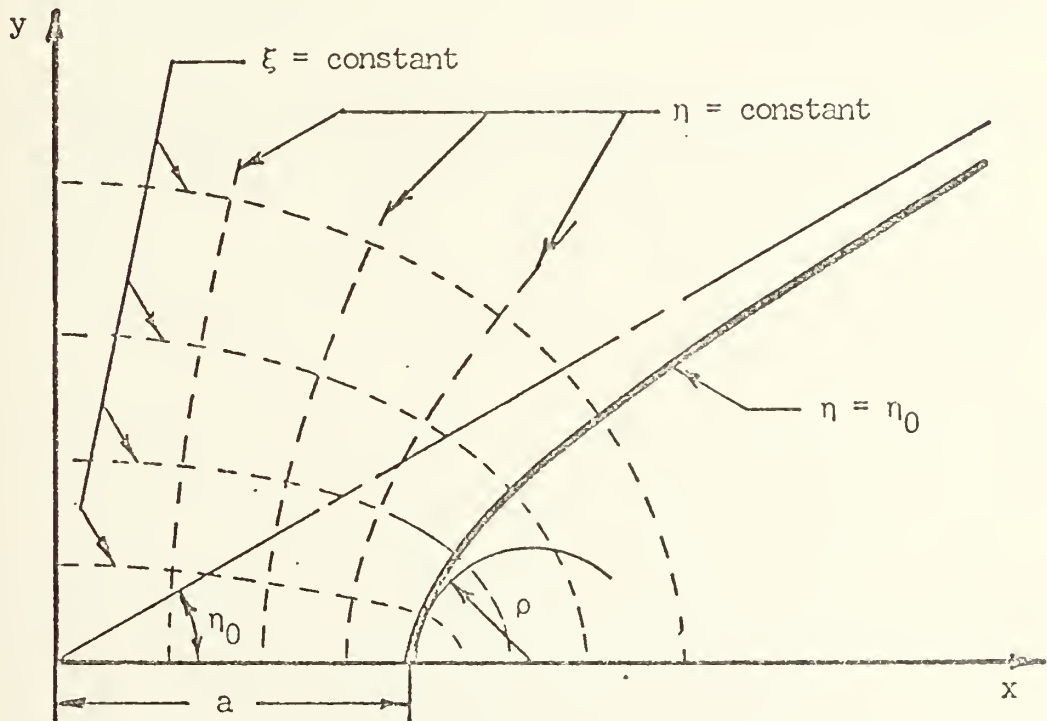


Fig. B1. Neuber's hyperbolic, symmetric notches in an infinite plate.

A complex Airy stress function is used to solve the elasticity problem so that

$$\sigma_{\eta} \equiv \tau_{\xi\eta} \equiv 0 \quad (B8)$$

along the notch boundary which is the hyperbola

$$x^2 - y^2 \cot^2 \eta_0 = c^2 \cos^2 \eta_0 \quad (B9)$$

corresponding to the value $\eta = \eta_0$. The half width at the base of the notch is the value of x when $y = 0$. We denote this by a , so that we are able to evaluate

$$c = a \sec \eta_0 \quad (B10)$$

This choice of c selects a definite shape, namely that which has net width $2a$ and whose hyperbolic boundary has asymptotes

$$y = \pm x \tan \eta_0 \quad (B11)$$

It is significant to note that except for a change of overall scale, the value of η_0 is the single parameter which defines the geometry of the notch. The two "halves" of the hyperbolic boundary are fixed relative to each other by the fact that their mutual asymptotes intersect at the origin $x = y = 0$.

One of the most significant derived quantities is the minimum radius of curvature of the hyperbola, ρ , which occurs at the base of the notch.

$$\rho = a \tan^2 \eta_0 . \quad (B12)$$

The solution, not given in detail here, permits finding the stress state $(\sigma_x, \sigma_y, \sigma_{xy})$ or $(\sigma_\xi, \sigma_\eta, \tau_{\xi\eta})$ at any point of the field. A constant, b , is involved in this solution. For our purposes we need only the stresses along the line $y = 0$, viz:

$$\begin{aligned} \sigma_x &= \sigma_\eta = 2b \csc^3 \eta (\sin^2 \eta - \sin^2 \eta_0) \\ \sigma_y &= \sigma_\xi = 2b \csc^3 \eta (\sin^2 \eta + \sin^2 \eta_0) \\ \tau_{xy} &= \tau_{\xi\eta} = 0 \end{aligned} \quad (B13,a,b,c)$$

One of the results we will use in Appendix C is the sum

$$\sigma_x + \sigma_y = 4b \csc \eta \quad (B14)$$

along $y = 0$.

To determine the constant b , we note that the tensile force (per unit thickness) transmitted in the y -direction is

$$P = 2 \int_0^a \sigma_y \, dx \quad (B15)$$

Substituting Eq. (B13b) and solving for b , we get

$$b = (P \cos \eta_0) / 2a(\pi - 2\eta_0 + \sin 2\eta_0) \quad (B16)$$

Substituting Eq. (B16) into (B13b), and evaluating at $\eta = \eta_0$, we get the maximum tensile stress (at the base of the notch) to be

$$\sigma_{\max} = (2P \cot \eta_0)/a(\pi - 2\eta_0 + \sin 2\eta_0) \quad (\text{B17})$$

The nominal tensile stress is

$$\sigma_{\text{nom}} = \frac{P}{2a} \quad (\text{B18})$$

and the stress concentration factor is

$$\text{SCF} = \sigma_{\max}/\sigma_{\text{nom}} = (4 \cot \eta_0)/(\pi - 2\eta_0 + \sin 2\eta_0) \quad (\text{B19})$$

In terms of the ratio of minimum radius of curvature ρ and net half-width a , we have

$$\text{SCF} = 4/k[\pi - 2 \arctan k + 2k/(1+k^2)] \quad (\text{B20})$$

where

$$k = \rho/a \quad (\text{B21})$$

This shows the SCF in terms of the ratio of two evidently significant and measurable geometric dimensions.

APPENDIX C

THREE DIMENSIONAL EFFECT

1. PREAMBLE

Before proceeding with this discussion, the following points should be made clear. First, there is every reason to place full reliance upon the accuracy of the determinations made by the two-dimensional FEM program, that is, to assert that these calculations accurately represent the theoretical two dimensional problem (plane stress, as presented here). From this standpoint, the study of three dimensionality is intended only to assess the validity of photoelastic determinations which were compared to the FEM determinations, and we in no way depend upon three dimensional behavior in presenting, with great confidence, our results for the two dimensional case. However, one cannot evade the responsibility of making some sort of evaluation of the effect of finite thickness upon determinations valid, strictly speaking, only for cases of zero thickness or infinite thickness.

2. A SPECIFIC PROBLEM

In addition to other difficulties of photoelastic evaluations, there is an inherent error which is due to the fact that all photoelastic models have finite thickness so that the conditions of plane stress are violated, at least to some extent.

To a first approximation, as shown by Timoshenko and Goodier [15], the variation of a two-dimensional stress field, due to finite thickness, may be obtained by employing, instead of the usual Airy stress function $\phi_0(x,y)$, satisfying

$$\nabla^4 \phi_0 \equiv 0 \quad , \quad \frac{\partial^2 \phi_0}{\partial x^2} = \sigma_y \quad , \quad \frac{\partial^2 \phi_0}{\partial y^2} = \sigma_x \quad , \quad \frac{\partial^2 \phi_0}{\partial x \partial y} = -\tau_{xy} \quad (C1a,b,c,d)$$

a modified function

$$\phi(x,y;z) = \phi_0(x,y) - \frac{\nu z^2}{2(1+\nu)} \theta_0(x,y) \quad (C2)$$

where

$$\theta_0(x,y) = \nabla^2 \phi_0 = \frac{\partial^2 \phi_0}{\partial x^2} + \frac{\partial^2 \phi_0}{\partial y^2} \quad (C3)$$

The (modified) stresses

$$\sigma_x = \frac{\partial^2 \phi}{\partial y^2} \quad ; \quad \sigma_y = \frac{\partial^2 \phi}{\partial x^2} \quad ; \quad \tau_{xy} = - \frac{\partial^2 \phi}{\partial x \partial y} \quad (C4a,b,c)$$

obtained from this modified stress function, thus have a parabolic dependence upon the third dimension, and, in general,

agree with the elementary (strictly two-dimensional) solution only on the plane of symmetry, $z \equiv 0$.

Note that θ_0 is the first tensor invariant of the elementary solution, that is

$$\theta_0 = (\sigma_x)_0 + (\sigma_y)_0 \quad (C5)$$

where we have added the subscript 0 to indicate that these are the elementary or unmodified stresses.

In photoelastic experiments, the light beam is affected by the distance-average stress-state and this differs somewhat from the stress-state at mid thickness. It is the latter, however, which corresponds to the theoretical plane stress distribution which the photoelastic evaluation is intended to reveal.

To determine the correction it is necessary to have, locally, second derivatives of the first tensor invariant. This involves two-fold differentiation of a stress field which itself has been determined, usually, by graphical or numerical integration procedures. The problem is somewhat easier to deal with at points on the free edge. Here there is only one stress, namely that in a direction parallel to the free edge, with which we are concerned, and all that is required is two-fold differentiation of θ_0 in a direction normal to the edge. Nevertheless, it is quite unlikely that sufficiently accurate stress determinations will have been made on the interior of the model area to permit a reliable evaluation of the second derivative needed.

In the particular case with which we are concerned in this thesis, namely the matter of stress concentrations at the bottom of notches, we can construct a plausible theoretical means of obtaining the desired information. This procedure, and experimentally accomplished equivalent procedures are, however, of doubtful accuracy and probably do no more than give a very rough estimate of the proper correction which, fortunately, usually is not large.

The problem, specifically, is to determine $\frac{d^2\theta_0}{dn^2}$

where θ_0 is the sum of principal stresses and n is the direction normal to the boundary at the point at which the correction is to be made. The evaluation is at the boundary.

3. PROCEDURES TO SOLVE THE PROBLEM

The following procedures suggest themselves. First, one can use the photoelastic stress information, properly integrated so as to obtain the stress-sum, and perform two-fold differentiation. Or, still proceeding experimentally, one can perform another experiment, using an interferometric procedure, to get the isopachic lines, which provide a direct experimental evaluation of the (average) stress-sum, and then differentiate the field twice in the normal direction. Third, one can analytically determine the desired second derivatives by studying an available theoretically exact solution to a geometry which "matches" that of the case under investigation. Fourth, one can construct a photoelastic model of such a geometry for which an analytic solution is available and infer

the desired correction by comparing photoelastic results with the theoretical results and then apply the same correction to the case under investigation.

Although superficially these procedures seem reasonable, each has flaws of fatal or near-fatal magnitude. The first two methods described do indeed relate to the geometry of the case at hand rather than to some substitute geometry. Thus, in theory, they are capable of providing the desired information. However, the fact that a stress-sum field must be constructed with sufficient accuracy that a second derivative can be relied upon indicates the need for a degree of precision considerably beyond what might be regarded as normally achievable.

The third and fourth methods are essentially the same — one is dealing with a substitute geometry for which a theoretical result is available. In the third method one needs a more detailed mathematical representation of the solution; in the fourth method all that is required is the theoretical value of the edge stress — and a second photoelastic determination. In each of these methods however, the reliance is upon the assumption that the second derivative of the stress-sum is the same for the substitute geometry as for the case of interest, or at least that the ratio of this second derivative to the edge stress itself is the same for the two cases.

One is quite disinclined to believe that there is any real justification for such reliance. If the substitute geometry

(with known analytic solution) is sufficiently close to the actual geometry that one may rely upon the coincidence of the second derivative of the stress sum, then indeed there should be even closer coincidence between the edge stresses themselves so that a photoelastic investigation is not called for at all. It is the very fact that the geometry of interest does not coincide with a geometry for which there is an available analytic solution that causes us to make the photelastic study in the first place.

However, even though we may have deep and quite reasonable doubts concerning the accuracy of our evaluation or estimate of the second derivative of the stress-sum (or its equivalence in other terms), nevertheless, for thin photoelastic models there is reason to believe that the corresponding variation in edge stress through the thickness of the model is "small" so that a greater degree of error may be tolerated in this estimate than would be tolerable in the basic evaluation of the edge stress.

Our own study of this matter has involved (1) analytical differentiation of the stress-sum field for a known geometry "approximating" that of the case under study, (2) numerical differentiation of the stress-sum field obtained by use of a two-dimensional FEM program, and (3) actual use of a three-dimensional FEM program.

In the following paragraphs we concern ourselves with a U-shaped notch. The radius of the bottom of the notch is $R = 0.2$ inch, the gross half width of the bar is $W = 1.3$ inches, the net half width is $D = 0.3$ inch and the half thickness is 0.125 inch. The angle θ , as used in the text, is $\theta = 0^\circ$.

a. Analytical Differentiation

1. Neuber's Deep Notch

The geometry of Neuber's hyperbolic notch in an infinite plate is shown in Fig. B1. Equations B13 and B14 in Appendix B give the following expressions for stress:

$$(\sigma_y)_0 = 2b \csc^3 \eta (\sin^2 \eta + \sin^2 \eta_0) \quad (C6)$$

$$\theta_0 = (\sigma_x + \sigma_y)_0 = 4b \csc \eta \quad (C7)$$

Letting $\csc \eta = (1 - u^2)^{-1/2}$ and designating $\frac{d}{d\eta}$ by ' , we get

$$\theta_0'' = 4b (1+2u^2)(1-u^2)^{-5/2} \csc^2 \eta_0 / D^2 \quad (C8)$$

Along $y = 0$, σ_y varies both with respect to x and z ; letting

$$c = \nu/2(1+\nu) \quad ,$$

we get from eq. (C4):

$$\sigma_y = (\sigma_y)_{2D} - c \theta'' z^2 \quad (C10)$$

Taking $2\lambda = t$, the thickness, and evaluating the constant, b:

$$p = 4 \int_0^D \int_0^\lambda \sigma_y dz dx \quad (C11)$$

$$b = p \cos \eta_0 / 4\lambda D [G - 3H/2] \quad (C12)$$

$$\text{where } G = \pi - 2\eta_0 + \sin 2\eta_0 \quad (C13)$$

$$H = \lambda^2 c \cot^3 \eta_0 / D^2 \quad (C14)$$

From eq. (C10)

$$(\sigma_y)_{\max} = 4b \csc \eta_0 \quad (C15)$$

$$(\sigma_y)_{\text{edge}} = (\sigma_y)_{\max} - c \theta_0'' \lambda^2 \quad (C16)$$

Letting

$$\Delta\sigma_y = (\sigma_y)_{\max} - (\sigma_y)_{\text{edge}} \quad (C17)$$

$$\frac{\Delta\sigma_y}{(\sigma_y)_{\max}} = H \csc \eta_0 (1 + 2 \cos \eta_0) \quad (C18)$$

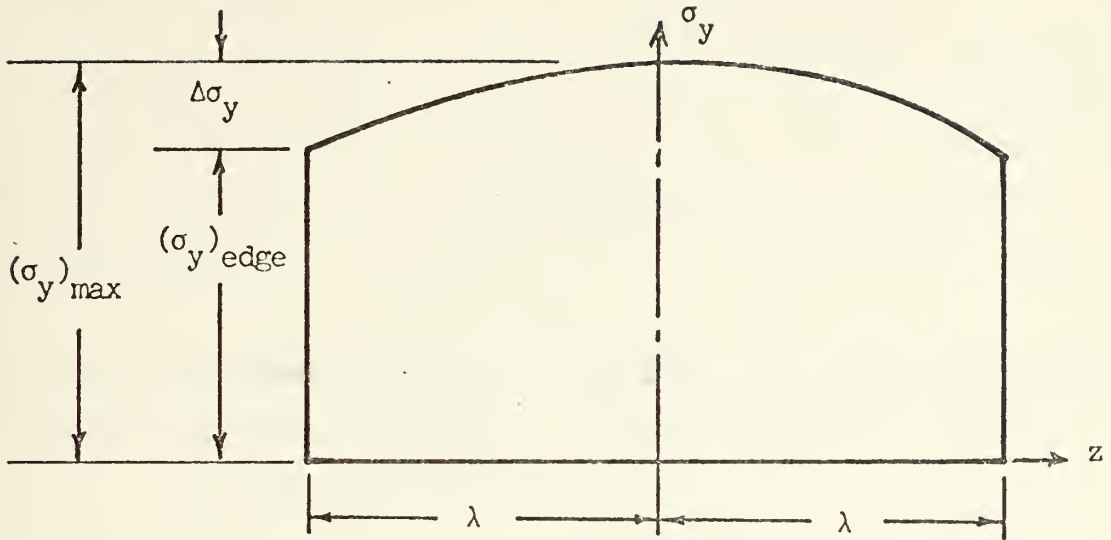


Fig. C1. Stress profile through the thickness

Figure C1 shows the stress profile through the model thickness. The photoelastician sees σ_y averaged through the thickness 2λ :

$$(\sigma_y)_{\text{ave}} = (\sigma_y)_{\text{max}} - \frac{\Delta\sigma_y}{3} \quad (\text{C19})$$

Consider the case: $D = 0.3$, $\rho = 0.2$, $\lambda = 0.125$,
 $\rho = D \tan^2 \eta_0$. We find

$$\bar{\theta}_0'' = 18.85$$

$$(\sigma_y)_{\text{ave}} = 0.982 (\sigma_y)_{\text{max}} \quad (\text{C.20})$$

(Here and later $\bar{\theta}_0''$ denotes the evaluation of θ_0'' at the base of the notch.)

That is to say the photoelastic evaluation of stress provides an uncorrected value for $(\sigma_y)_{\text{max}}$ that is nearly 2% low.

2. Circular Hole in a Plate

One substitute geometry which suggests itself is that of a circular hole in a plate under uniaxial tension. Figure C2 shows a round hole in a large plate.

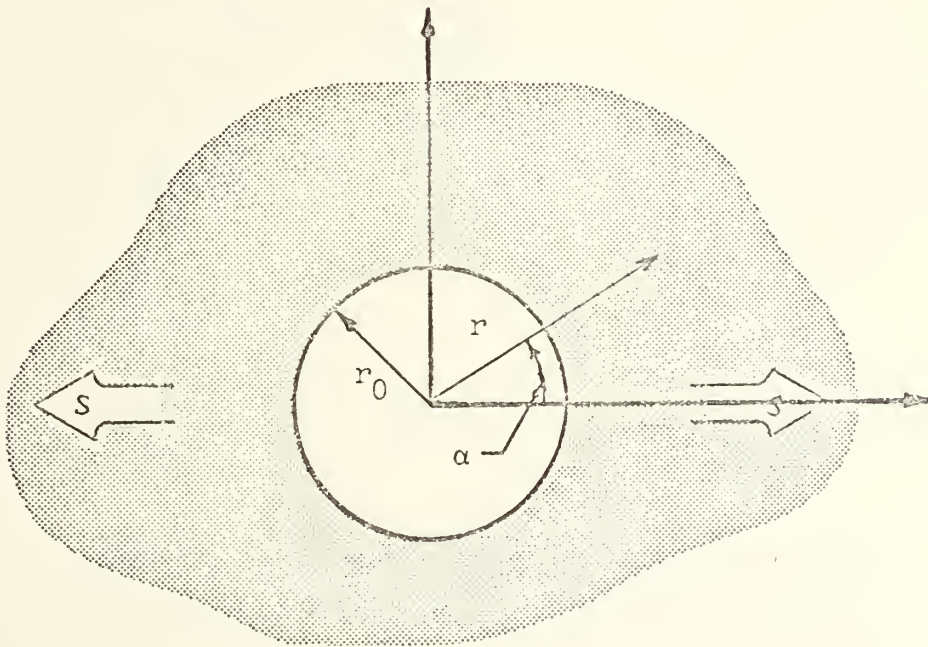


Fig. C2. Circular hole in an infinite plate

If the plate is large in comparison with the size of a circular hole the following relations hold:

$$\sigma_r = S[(1-R^2) + (1+3R^4-4R^2)\cos 2\alpha]/2 \quad (C21)$$

$$\sigma_\alpha = S[(1+R^2) - (1+3R^4)\cos 2\alpha]/2 \quad (C22)$$

$$\theta_0 = \sigma_r + \sigma_\alpha = S(1 - 2R^2 \cos 2\alpha) \quad (C23)$$

$$\text{where } R = r_0/r \quad (C24)$$

Introducing the three-dimensional behavior, we have

$$(\sigma_\alpha) = \frac{\partial^2 \phi}{\partial r^2} = \frac{\partial^2 \phi_0}{\partial r^2} + cz^2 \frac{\partial^2 \theta_0}{\partial r^2} \quad (C25)$$

and evaluating at the edge ($r = r_0$), we get

$$\begin{aligned} (\sigma_\alpha)_{\text{edge}} &= \sigma_0 + \Delta\sigma_0 \\ &= [S-2S \cos 2\alpha] + [6S(z/r_0)^2 \nu \cos 2\alpha/(1+\nu)] \quad (C26) \end{aligned}$$

Table C1 shows evaluations of this formula at various points around the hole, in terms of the ratio λ/r_0 where λ is the half thickness.

TABLE C1
EDGE STRESS AROUND HOLE.

α	σ_0/S	$\frac{\Delta \sigma_0}{S} / \frac{\lambda^2}{r_0^2}$	$\frac{\Delta \sigma_0}{\sigma_0} / \frac{\lambda^2}{r_0^2}$
0	-1	1.38	-1.38
15	-0.732	1.20	-1.64
30	0	0.69	∞
45	1	0	0
60	2	-0.69	-0.35
75	2.732	-1.20	-0.44
90	3	-1.38	-0.46

Inserting the numerical data as previously used: $r_0 = 0.2$,
 $\lambda = 0.125$; and solving at $\alpha = 90^\circ$:

$$(\sigma_\alpha)_{\text{edge}} = 0.82 \sigma_0 \quad (\text{C27})$$

Proceeding as before:

$$\bar{\theta}_0'' = 99.79$$

$$(\sigma_\alpha)_{\text{ave}} = 0.94 (\sigma_\alpha)_{\text{max}} \quad (\text{C28})$$

A more precise analysis using Howland's [8] formulation yields essentially the same result. It is apparent that if a circular hole is used to infer the needed correction, as suggested in Section 3 above, SCF's reported for the U-shaped notch will be slightly high. This is apparently the procedure used by Flynn and Roll in their experiments.

4. NUMERICAL DIFFERENTIATION FROM 2D FEM

For this evaluation, we deal directly with the U-shaped notch. The same numerical data was used to facilitate direct comparisons. Our objective is to take the FEM computed values of $\sigma_x + \sigma_y$ at the nodes along the line normal to the notch, fit a polynomial through the values obtained and compute the second derivative in the normal direction. Figure C3 shows the notch.

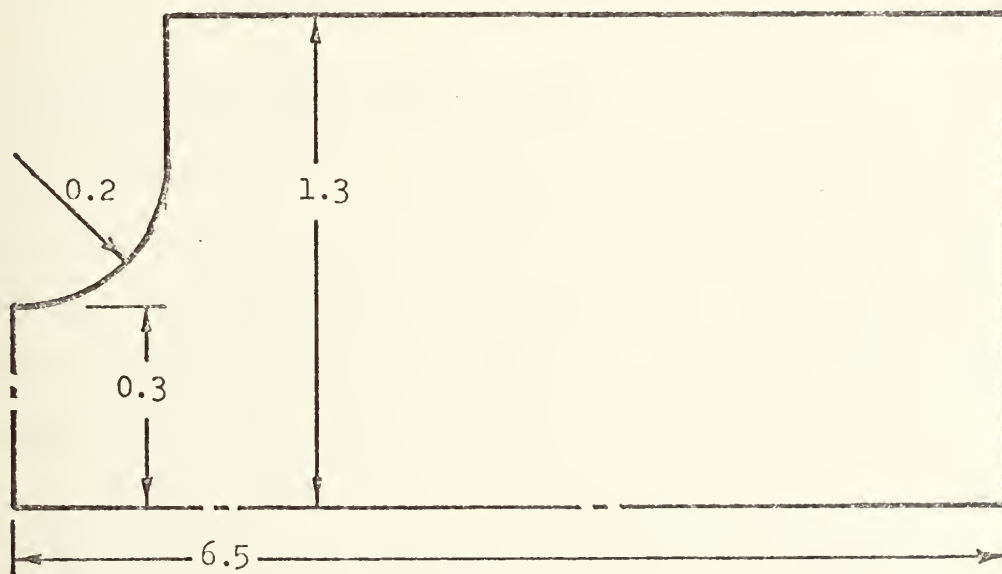


Fig. C3. Symmetric U-shaped notches (not to scale)

Examination of the stress-sum profile reveals that a smooth curve is not obtained even with the finest mesh used. (This is primarily because of a minor systematic inherent discrepancy between the FEM evaluation of stress at a midside node and at a corner node.) Choosing the element corner nodes only, a fourth degree, least square polynomial can be calculated. Examination of the second derivative of this polynomial reveals that it is slowly converging to some value with each successive refinement of the mesh. Viewing each of these results as a term in a convergent sequence, a convergence-accelerating procedure due to Shanks [14] was used to estimate θ_0'' at the base of the notch. The numerical result was:

$$\overline{\theta_0''} \approx 10$$

$$(\sigma_x)_{\text{ave}} = 0.994 (\sigma_x)_{\text{max}} \quad (\text{C29})$$

5. DIRECT COMPARISON FROM 3D FEM

The FEM program used in this study was TRISOP [10]. Quadratic elements were used for the solution. The mesh was generated by TRIMEG [1], modified in the same way as the two dimension mesh generator (PLIMEG), to progressively vary the element size. The mesh in the x-y plane was the same as that used in the 2D solutions. Two equal size elements were used for the half thickness in the z direction. Because of symmetry about the midthickness plane, it was sufficient to consider only half the plate. The half thickness of the bar (previously designated λ) was 0.125. Figure C4 shows the notch.

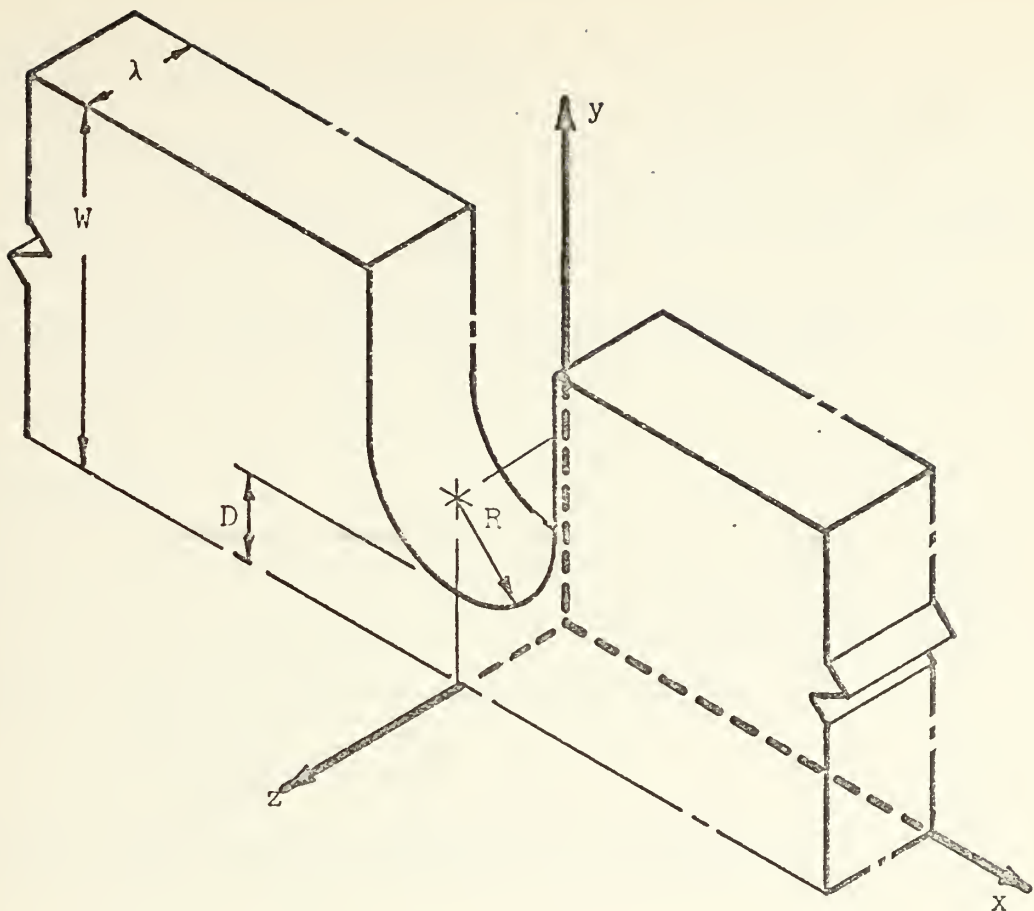


Fig. C4. U-shaped notches. (xy , yz , zx planes are planes of symmetry. The planes $z = \pm\lambda$ are outside faces, the planes $y = \pm w$ are the unnotched boundaries)

Each computational run involved nearly three and one-half hours of computer time. Because of this only a few runs were made to insure proper program operation and gather this data. Since a large data gathering task was not contemplated here, the mesh generator and FEM program were not coupled together. All data input to the mesh generator was manually prepared. All calculations subsequent to determination of nodal stresses was done outside the computer.

A parabola was fitted through the values σ_x at the corner nodes along the line $y = a = 0.3$. The result of this procedure,

cast again in familiar terms was

$$\bar{\theta}_0'' = 14.98$$

$$(\sigma_x)_{\text{ave}} = 0.991 (\sigma_x)_{\text{max}} \quad (\text{C30})$$

The former value was inferred from the coefficients in the parabolic fit.

6. CONCLUSION

We are now in a position to compare the various results and estimate the importance of the three-dimensional effect. The aspect ratio of the bar considered here is

$$\text{AR} = \frac{\text{thickness}}{\text{width}} = \frac{0.25}{2.6} \approx 0.1 \quad (\text{C31})$$

The results obtained are summarized in Table C2.

TABLE C2
Results of Three-Dimensional Analyses

Method	$\sigma_{\text{ave}}/\sigma_{\text{max}}$	$\bar{\theta}_0''$	Remarks
Neuber notch	0.982	18.85	Two derivatives of analytical stress-sum.
Hole in plate	0.94	99.79	Two derivatives of analytical stress-sum.
2D FEM	0.994	10	Two derivatives of the curve fit through stress-sum from numerical data.
3D FEM	0.991	14.98	Parabola fit through numerical computations of σ_x .

As can be seen from the results presented here, the effect of three-dimensionality is indeed small. The two-dimensional and three-dimensional FEM studies compare closely enough to permit extracting the third dimension effect from PLISOP. The extraction is not easy. However, the procedure outlined is readily accomplished with the computer and requires much less computational time than does the execution of TRISOP.

We see also from these results that an indiscriminate adjustment of photoelastically obtained values of SCF based on the SCF for a known geometry may cause overcorrection. The overcorrection is small, however, and the error causes conservative estimates, that is, one overestimates the ratio $(\sigma_{\max}/\sigma_{\text{ave}})_{\text{notch}}$.

APPENDIX D

SUGGESTIONS FOR PRODUCING ADDITIONAL NUMERICAL RESULTS

Stress concentration factors for the four problems presented in this thesis can easily be calculated by using the program in Appendix F. For all four problems the useful range of the parameter D/W is from zero to one and the range of θ is from 0° to 90° . Note that either $D/W = 1$ or $\theta = 90^\circ$ describes a bar with no notch and results in $SCF = 1$. D/W may be incremented in steps of 0.2 (program statements AA 01340 and AA 01200) and θ in steps of 15° (program statements AA 01380 and AA01180) for all problems to provide sufficient data. The incrementing step selected in the program for R/W is 0.05 (program statements AA 01360 and AA 01190).

The SCF's for problem 1 over the full range of D/W , all θ up to 60° and R/W from 0.1 to 0.5 are presented in Appendix A. To duplicate this information for the other three problems, all that is needed is three additional computer runs. The sample input deck of figure 13 of the text may be duplicated and used with a single change for each new problem. The entry on card 4 in columns 11-15 will be changed to 2, 3 and 4 for each successive run.

Each computer run will require 12.5 hours and will provide the raw data (a deck of punched cards, each listing the problem parameters and corresponding SCF) paralleling

the data plotted in Appendix A. A simple plotting routine will be needed to plot the data.

In Section III C of the text, we pointed out that the SCF at two points are of interest for problem 4, namely the point at the bottom of the notch and also the opposite point on the straight boundary. As presented, this program calculates only the first of these for each new problem. To make the information more complete, an investigator should add the card "Y(15) = SSJNT(19,1)" following PP 0930. Following SS 00090 add the card "SCF2 = SCF * Y(15)/Y(14)"; change present card SS 00130 by adding ",SCF2"; change present card SS 00140 to "FORMAT (6D15.8)".

APPENDIX E

PROGRAM USER'S MANUAL

This user's manual is intended to be used with the program listed in Appendix F.

A user familiar with neither computer coding or the Finite Element Method (FEM) of numerical solution can, with the aid of this manual:

1. execute the program listed to solve the four specific problems presented in the body of this thesis.

A user familiar with both computer coding and FEM, in addition to the above, can:

2. change the boundary conditions applied to the structure.
3. change the shape of the notch in a minor way.
4. change the program dimensions to suit the user's needs.
5. modify the program to solve a different, parameterized problem.

1. TO EXECUTE THE PROGRAM

The job control language cards needed are listed in Figure E1. No explanation of their make-up will be attempted in this manual other than to comment that some of the cards listed beginning with //FTXXF001 provide the direct access storage needed by the program. Others provide linkages needed to print, plot, and punch cards.

A sample input deck is included in Figure E1. The entries on the cards are listed in Table E1 in detail. Figure E2 (identical with Figure 9 in the text) is a sketch of the structure considered.

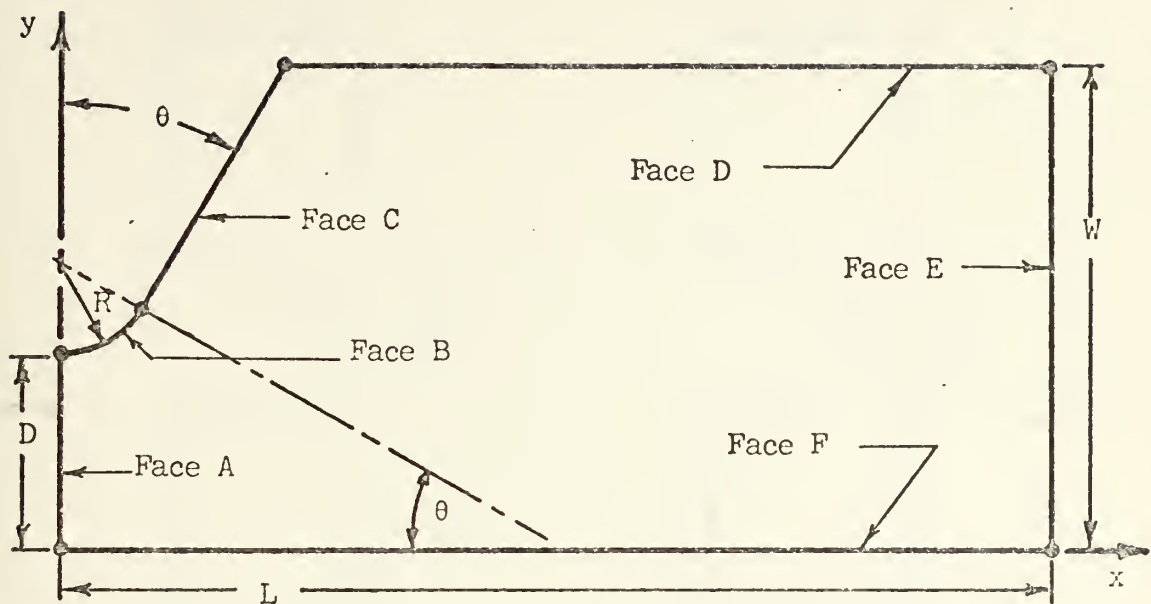


Fig. E2. Structure Faces

Figure E3 (identical with Figure 8 in the text) shows the four problems solved. The user must make some selections and can change other numbers; however some entries on these cards should not be changed. They are indicated by:

User must choose --()--

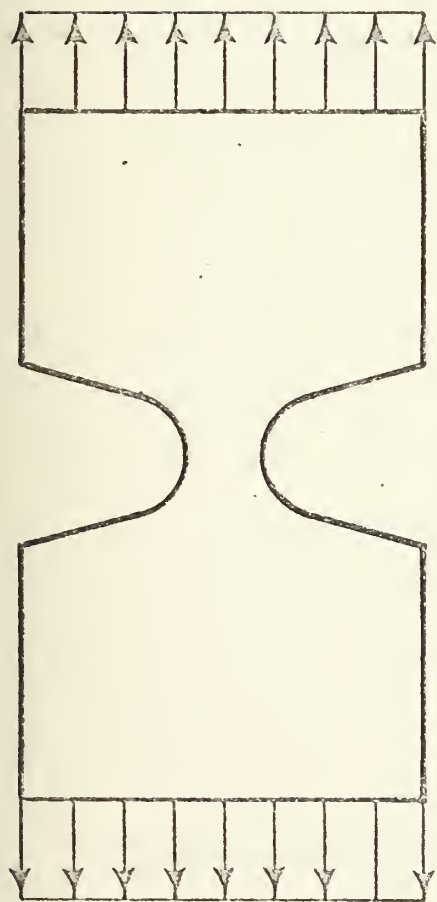
User may choose ()

User may not choose *()*

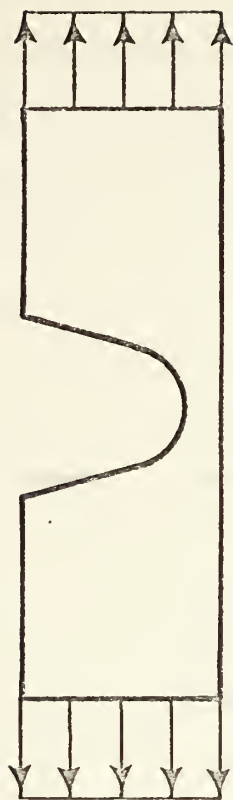
Some additional explanatory material may be found in the thesis by Adamek [1].

Notes to Accompany Figure E1 and Table E1.

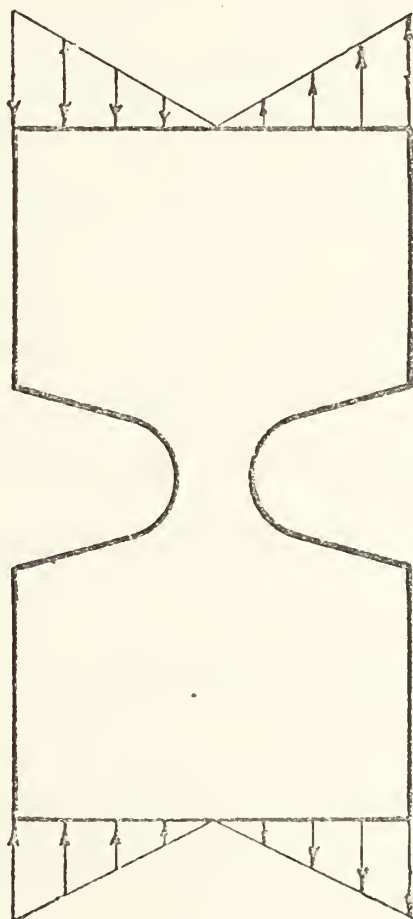
- a. Card 4: If NPL0T= 1 or 2, only a single problem is solved. This is done to avoid unnecessarily drawing the same mesh



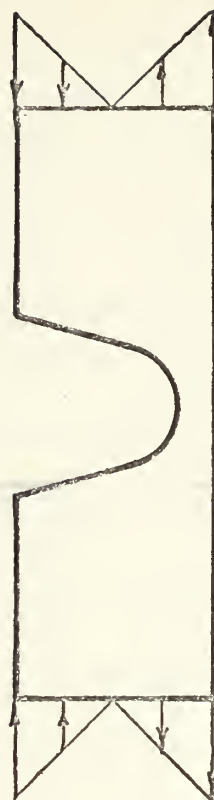
Problem 1



Problem 3



Problem 2



Problem 4

Fig. E3. The Four Problems

with only minor modification 225 times. This also provides the capability to stack as many problems as desired in one data run. If NPLOT \neq 0, at the end of calculations for each problem, control returns to the reading section of MAIN to begin a new problem.

- b. Program PLIMEG has an ordering of SEL's with which the present use conforms. This means that here we use only SEL's numbered 1, 2, 5, and 6. Cards 5, 6, 7, and 8 relate to SEL's numbered 1, 2, 5, and 6, in that order.
- c. Cards 5-8: Element size increases with coordinate direction for positive EXPX and EXPY. For the smallest element to lie at the base of the notch EXPX should be positive and EXPY should be negative. If the values shown are not used the stresses calculated may be farther from the converged result than 1% shown in the body of this thesis.
- d. Cards 5-8: ROWS must be the same for SEL's 1 and 5 and for SEL's 2 and 6. Likewise for EXPY.
- e. Cards 5-8. CLMNS must be the same for SEL's 1 and 2 and SEL's 5 and 6. Likewise for EXPX.
- f. Cards 5-8: Dimension statements in the program limit the ROWS and CLMNS as follows; ROWS: $SEL1 + SEL2 \leq 9$; CLMNS: $SEL1 + SEL5 \leq 15$.
- g. Card 9: Card columns not listed are not used and should be left blank.
- h. Card 9: For a discussion of NGP see reference [16], Chapter 8. For this formulation NGP = 2 is adequate.

TABLE E1

LIST AND DESCRIPTION OF INPUT DECK

<u>Card Number</u>	<u>Card Columns</u>	<u>Variable Name</u>	<u>Explanation</u>
1			problem parameters
	1-10	(RW)	radius/gross width ratio
	11-20	(DW)	net/gross width ratio
	21-30	(TH)	Notch semi-angle (degrees)
2			identification
	1-48	-(TITLE)-	as desired by user
3			additional identification
	1-48	-(TITLE)-	as desired by user
4			mesh parameters
	1-5	*(NSEL)*	number of SEL's
	6-10	*(NPT)*	number nodes per element
	11-15	-(NPUNCH)-	1 indicator for problem 1
			2 indicator for problem 2
			3 indicator for problem 3
			4 indicator for problem 4
	16-20	-(NPLOT)-	0 indicator for no plots
			1 indicator for printer plot
			2 indicator for CALCOM PLOT
5-8			super element deck
	1-5	*(SELNR)*	SEL identification number
	6-10	(ROWS)	number of columns (divisions in y direction) in this SEL
	11-15	(CLMNS)	number of columns (divisions in x direction) in this SEL

TABLE E1 (Continued)

<u>Card Number</u>	<u>Card Columns</u>	<u>Variable Name</u>	<u>Explanation</u>
	16-20	*(Node A)*	upper left corner node number
	21-25	*(Node B)*	lower left corner node number
	26-30	*(Node C)*	lower right corner node number
	31-35	*(Node D)*	upper right corner node number
	36-40	*(TYPE)*	material identification number
	41-45	*(NPTSB)*	number of boundary nodes in this SEL
	46-50	*(CON)*	code for interconnection between SEL - for use see thesis by Adamek [H]
	51-60	(EXPX)	exponential coefficient XI direction
	61-70	(EXPY)	exponential coefficient ETA direction
9			FEM parameters
	11-15	*(NMAT)*	number of materials in the structure
	26-30	(NSTRES)	2 dimension assumption made: 0 for plane stress 1 for plane strain
	31-35	(NGP)	number of Gauss points used in the integration

Computer time required may be estimated by knowing that the compile and link steps require approximately two minutes total and each problem executes in three minutes. Core requirement with this configuration is 690K. The core requirement may be reduced to 615K if cards with serial numbers GG 00530, GG 00740 and GG 00750 are removed from the deck. This removes the plotting capabilities from the program. If NPLOT= 1 or 2 is used, the program terminates by "end of file on unit 5" (the card reader is empty) after the last problem is solved.

2. TO CHANGE BOUNDARY CONDITIONS

Computations for the load boundary conditions and codes indicating the displacement specifications are entirely contained in subroutine COORD. The serial numbers on all FORTRAN statements used to calculate boundary conditions begin with the three digits EEX or EEY. These instructions assume that the user can calculate externally applied forces F_x and F_y to describe the loading desired.

Nodal displacement specifications may be imposed in any of several ways. Each specification is indicated by a code assigned to one specific node. The array NBC (454,2) is used to transmit the coded information. NBC (I,1) is the node number at which the I^{th} displacement specification applies and NBC (I,2) is the code for that specification taken from the following list.

- 1: A roller on an x axis (i.e., $v = 0$)
- 2: A roller on a y axis (i.e., $u = 0$)
- 3: A fixed node (i.e., $u = v = 0$)

A cumulative tally of the number of nodes where a displacement specification has been imposed is contained in the variable NPBC and the tally appears in the output.

At least one nodal displacement must be specified in each of the two coordinate directions in order to prevent rigid body motion which might result in meaningless outputs.

The cards which must be modified are serialized EEY. The actual changes to be made are left to the user.

3. TO CHANGE THE SHAPE OF THE NOTCH

Only a minor change can be accomplished easily. The notch shape is modified but no modification of the SEL arrangement is contemplated. That is, we only wish to relocate SEL nodes 1 through 7 (Fig. E4, identical with Fig. 12 in the text) and subsequently to generate an appropriate FEM mesh. It is assumed that the same problem parameters (R/W , D/W , θ) are used.

In subroutine PROBLM, the x and y coordinates of nodes 1 through 7 must be re-coded. The FORTRAN statements that must be changed can easily be identified by the user. Some computational short cuts may be useful under certain conditions. Before introducing the shortcuts, however, the user must understand the data string output by this subroutine.

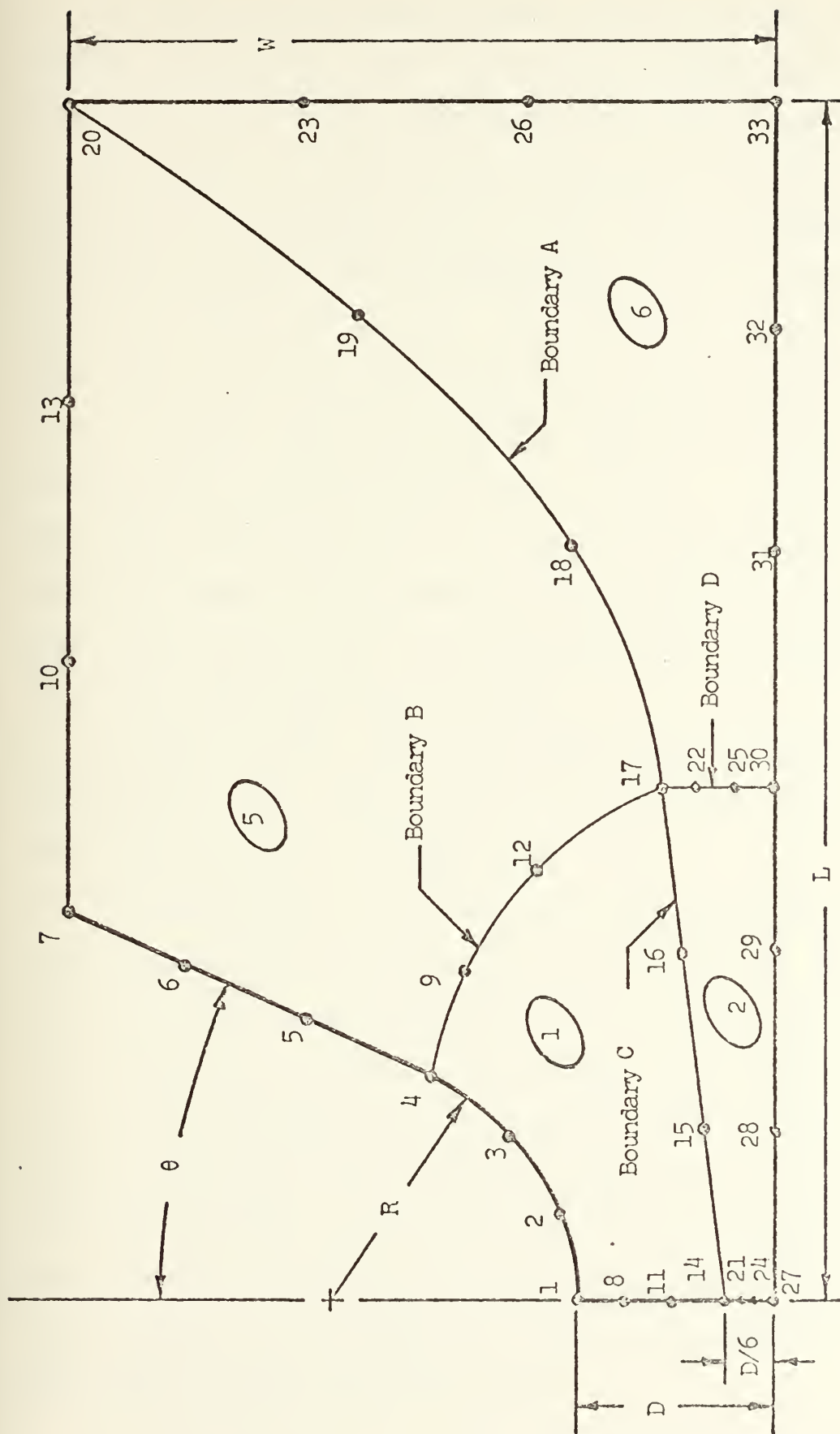


Fig. E4. Structure SEL's and boundary nodes. SEL identification numbers appear in ovals. (Not to scale)

We refer to each data string written on direct access device 10 as a node card which has the format (3I5, 2D25.16). The first three numbers (integers) are the number of the SEL (variable J), the node number (variable K) and the short-cutting code (Variable I or L). The other two numbers (Real*8) are the x and y coordinates of node K (variables X(K) and Y(K) respectively). The node cards are grouped by SEL number and the groups arranged in increasing numerical order. Within each SEL group the cards are arranged according to the SEL connectivity. That is, the node in the upper right hand corner first, followed by one card for each node used to describe the SEL, ordered in counter-clockwise fashion. In this program SEL's 1, 5, and 6 have 12 nodes each; SEL 2 has 4 nodes.

In what follows, some familiarity with PLIMEG and PLISOP is assumed. The coded numbers are described and/or calculated as shown in Table D2.

The shortcutting code referred to above may be used if the SEL boundary between any two corner nodes is a straight line. L=5 for 12 node elements (or L=4 for 8 node elements; not used in this program) causes PLIMEG (the mesh generator itself) to calculate the coordinates of these intermediate nodes. Therefore the coordinates need not be calculated in subroutine PROBLM. Card serial BB 00790 is an example of the use of the shortcutting code. Note that where the short-cutting code L is not used, I= 0 must be specified as has been done in card serial BB 00830.

The structure boundary nodes along the circular arc (points 1 through 4) are corrected (see page 38 of text) in subroutine COORD. A user modifying subroutine PROBLM must also recode the corrections made by cards serialized EEZ. The variables CORD(N, 1) and CORD(N, 2) are the x and y coordinates of node N respectively.

4. TO CHANGE DIMENSIONING

The cards listed in Table E2 include all of the controllable dimension statements in the program. Each is an exact reproduction of its parent card in the program except that the dimension numbers, where appropriate, have been replaced by a code: NR2 through NR15. By calculating the numbers represented by these codes, preparing a new dimension deck and replacing the parent cards in the program with the new cards (on the basis of serial number) a user may tailor the program size to meet his needs.

The designations included in the name column are variable names used in PLIMEG and PLISOP. If several different versions of the dimension deck might be required, the computer terminal can be advantageously used. This can be done by reading the coded deck into the system, then using up to fourteen change commands to change the codes to the previously calculated numbers, and then ordering a new punched deck.

If several problems requiring different dimensions are to be solved, they can all be solved using a program with the largest of the dimensions. From the standpoint of

efficient computer usage, however, it is better to dimension the program to fit each job.

A rough estimate of core storage required (in K BYTES) may be arrived at by making the following computation:

$$\text{CORE} = \frac{2 * \text{NO4} * \text{NO10}}{128} + 180$$

5. TO MAKE MAJOR MODIFICATION

A major modification to the program involves, primarily, a complete rewrite of subroutine PROBLM. The guidance of Section 3, together with a good working knowledge of PLIMEG, can be extended to accomplish this. The user may be guided by carefully studying the preceding portions of this appendix.

TABLE E1 CONTROLLABLE DIMENSION STATEMENTS

THIS IS THE GENERAL VERSION OF THE DIMENSION DECK
THE FOLLOWING CONSTANTS MUST BE SUPPLIED:

CCCCCCCCCCCCCCCCCCCCCCCCCCCC

NO2 --- (NGROW*NGCOL)*NO11

NO3 --- MAXMAT

NO4 --- MAXNJT

NO5 --- (NGCOL+1)*NGROW

NO6 --- NGCOL

NO7 --- NGROW

NO8 --- MAXNEL

NO9 --- 2*MAXNJT

NO10 --- (NBAND*GE.11)

LINEAR ----- = 2*(ROWS+3)

QUADRATIC ----- = 2*(3*ROWS+5)

CUBIC ----- = 2*(5*ROWS+7)

NODES/ELEMENT (4, 8 CR 12)

NO11 --- NODES/ELEMENT

NO12 --- MAXNJT+1

NO13 --- 2*(NODES/ELEMENT)

NO14 --- 3*(NODES/ELEMENT)

NO15 --- GAUSS POINTS MAX

CCMMGN/STAT/WR,DR,TH,W,X(33),Y(33),EXPX(NO2),EXPY(NO2)

CCMMGN/CORD1/CORD(N04,4),ELCON(N03,4),NBC(NC4,2)

CCMMGN/MESH1/ NSCON(N05,9),MS(NC5,8),MEL(N05,4)

CCMMGN/COORD(12,2),ELAST(3,3),SS(N014,N013),SN(N014,N013)

CCMMGN/STAT/WR,DR,TH,W,X(33),Y(33),EXPX(NO2),EXPY(NO2)

DIMENSION NCT(TITLE(12))

CCMMGN/TITLE(12)

CCMMGN/INT/NPT,NEL,NPUNCH,NSTOP,NJT,NPLOT,NKIND,NSEL,NGROW,NGCOL,

1 NCLOAD,NPBC

CCMMGN/MESH1/ NSCON(N05,9),MS(NC5,8),MEL(N05,4)

CCMMGN/CORD1/CORD(NC4,4),ELCON(N03,4),NBC(NC4,2)

CCMMGN/CORD2/BOUND(N02,2)

CCMMGN/STAT/WR,DR,TH,W,X(33),Y(33),EXPX(NO2),EXPY(NO2)

DATA MAXBJT/ND4/

NGROW=NO7

NGCOL=NO6

CCMMGN/MESH1/ NSCON(NC5,9),MS(NC5,8),MEL(NC5,4)

CCMMGN/MESH2/ NCR(N06),NRR(N07)

CCMMGN/MESH3/ NCON(N08,14)

DATA MAXNEL/NO8/MAXNJT/NO4/

CCMMGN/MESH1/ NSCON(N05,9),MS(NC5,8),MEL(NC5,4)

CCMMGN/MESH2/ NCR(N06),NRR(N07)

CCMMGN/MESH3/ NCON(N08,14)

CCMMGN/CORD1/CORD(N04,4),ELCON(NC3,4),NBC(NC4,2)

CCMMGN/CORD2/BOUND(N02,2)

CCMMGN/STAT/WR,DR,TH,W,X(33),Y(33),EXPX(NO2),EXPY(NO2)

DIMENSION X(N04),Y(N04),RANGE(4)

CCMMGN/MESH1/ NSCON(N05,9),MS(NC5,8),MEL(NC5,4)

AAW000690

AAW000700

AAW000710

AAW000720

BBW000040

CCW001180

CCW001190

CCW001200

CCW001210

CCW001220

CCW001230

CCW001240

CCW001250

CCW001260

CCW001270

CCW001280

DDW00110

DDW001120

DDW001130

DDW001140

EEW000120

EEW000130

EEW000140

EEW000150

EEW000160

EEW000170

GGW000070

GGW000080


```

COMMON/ MESH2/ NCR(N06), NRR(N07)
COMMON/ MESH3/ NCON(N08,14)
COMMON/ CORD1/ CORD(N04,4), ELCON(N03,4), NBC(N04,2)
COMMON/ SOL/ BGK(N09,N010), ALOAD(NC9), ABGN
COMMON/ UNT1/ NEL,NJT,NMAT,NCON(N08,14), NSTRES,NGP,
1 LM(N011), LJT(N011), NTLD,LTBY,NTIN
COMMON/ CORD1/ COARD(N04,2), CLOAD(N04,2), ELCON(N03,4), NBC(N04,2)
DIMENSION REACT(N012,2), NCODE(NC4)
EQUIVALENCE (BGK(1,1), REACT(1,1))
NEL=N08
NJT=N04
NMAT=N03
MBD=N010
COMMON/ UNT1/ NEL,NJT,NMAT,NCLoad,NPBC,NCON(NC8,14), NSTRES,NGP,
1 LM(N011), LJT(N011), NTLD,LTBY,NTIN
COMMON/ CORD1/ COARD(N04,2), CLOAD(N04,2), ELCON(N03,4), NBC(N04,2)
DIMENSION STK(N012,N013), AK(N013,N013), B(3,N013)
COMMON/ SOL/ BGK(N09,N010), ALOAD(NC9), ABGN
COMMON/ UNT1/ NEL,NJT,NMAT,NCLoad,NPBC,NCON(N08,14), NSTRES,NGP,
1 LM(N011), LJT(N011), NTLD,LTBY,NTIN
COMMON/ CORD1/ COARD(N04,2), CLOAD(N04,2), ELCON(N03,4), NBC(N04,2)
DIMENSION AK(N013,N013), STK(N013,N013), B(3,N013)
DIMENSION XI(N015), AIA(N015,N015)
COMMON/ CORD1/ COARD(N04,2), ELAST(3,3), SS(N014,N013), SN(N014,N013)
1 DIMENSION COORD(12,2), ELAST(3,3), SS(N014,N013), WI(2,12), B(3,N013)
COMMON/ COORD(12,2), ELAST(3,3), SS(N014,N013), SN(N014,N013)
COMMON/ SOL/ A(N09,N010), B(N09), ABGN
COMMON/ SOL/ A(N09,N010), B(N09), ABGN
COMMON/ SOL/ BGK(N09,N010), DISP(NC9), ABGN
COMMON/ STAT/ WR,DR,TH,W,X(33), EXPX(N02), NSTRES,NGP,
1 LM(N011), LJT(N011), NTLD,LTBY,NTIN
COMMON/ UNT1/ NEL,NJT,NMAT,NCLoad,NPBC,NCON(NC8,14), NSTRES,NGP,
COMMON/ CORD1/ COARD(N04,2), CLOAD(N04,2), ELCON(N03,4), NBC(N04,2)
COMMON/ COORD(12,2), ELAST(3,3), SS(N014,N013), SN(N014,N013)
DIMENSION SSJNT(N04,7), SNJNT(N04,7), SSEL(N014), SSEL(N014),
1 DSPEL(N014)
COMMON/ SOL/ BGK(N09,N010), ALOAD(NC9), ABGN
COMMON/ UNT1/ NEL,NJT,NMAT,NCLoad,NPBC,NCON(NC8,14), NSTRES,NGP,
1 LM(N011), LJT(N011), NTLD,LTBY,NTIN
COMMON/ CORD1/ COARD(N04,2), CLOAD(N04,2), ELCON(N03,4), NBC(N04,2)
COMMON/ SOL/ BGK(N09,N010), DISP(NC9), ABGN
COMMON/ UNT1/ NEL,NJT,NMAT,NCLoad,NPBC,NCON(NC8,14), NSTRES,NGP,
1 LM(N011), LJT(N011), NTLD,LTBY,NTIN
COMMON/ CORD1/ COARD(N04,2), CLOAD(N04,2), ELCON(N03,4), NBC(N04,2)
DIMENSION REACT(N012,2)
COMMON/ STAT/ WR,DR,TH,W,X(33), EXPX(N02)

```


TABLE E1 (Continued)
EXPLANATIONS OF
DIMENSIONING CODES

<u>Code</u>	<u>Name</u>	<u>Explanation</u>
NO3	MAXMAT	The maximum number of materials to be considered
NO4	MAXNJT	The maximum number of nodes to be considered
NO6	NGCOL	The maximum number of columns in the basis SEL grid
NO7	NGROW	The maximum number of rows in the basic SEL grid
NO8	MAXNEL	The maximum number of elements to be considered
NO11	NJT	The maximum number of nodes per element (4, 8, or 12)
NO15	NGP	The maximum number of Gauss points to be used in the integrations (2 through 5)
NO2	NBAND	NGROW * NGCOL * NO 11
NO5		(NGCOL + 1) * NGROW
NO9		2 * MAXNJT
NO10		The half bandwidth of the stiffness matrix calculated from: IF NO11= 4, NBAND= 2 * (ROWS + 3) IF NO11= 8, NBAND= 2 * (3 * ROWS + 5) IF NO11= 12, NBAND= 2 * (5 * ROWS + 7) Note: ROWS is the maximum number of rows of elements in the completed mesh
NO12		MAXNJT + 1
NO13		2 * NO11
NO14		3 * NO11

[illegible]

PROGRAMMED, TESTED AND USED BY L. J. SMITH AT THE
NAVAL POSTGRADUATE SCHOOL, SPRING, 1974

THIS PROGRAM INCORPORATES THE PROGRAMS PLISOP, WRITTEN BY G. CANTIN, MARCH, 1972 AND PLIMEG, WRITTEN BY J. R. ADAMEK, DEC., 1972.

END OF RECORD OF MODIFICATIONS.

THIS PROGRAM CALCULATES THE STRESS CONCENTRATION FACTOR FOR 'V'-NOTCHED BARS (1 NOTCH AND 2 SYMMETRIC NOTCHES) BASED ON GROSS WIDTH, NET WIDTH, BOTTOM RADIUS OF NOTCH AND ANGLE OF THE 'V' SUBJECTED TO UNIFORM LOAD OR BENDING MOMENT.

A USER'S MANUAL APPEARS AS APPENDIX D OF THE THESIS
CONCENTRATION FACTORS FOR CIRCULAR NOTCHES: BY L. J. SMITH, JUNE 1974.

```

* JCL CARDS REQUIRED:
// (COLUMN ONE INDICATED BY ASTERISK)
// (STANDARD JOB CARD)
// EXEC FCRTCLG,REGION=690K
//FORT.SYSIN DD

```

(INSERT THE FORTRAN DECK HERE)

```
//GC.FT06F001 DD SPACE=(CYL,(4,1))
//GC.FT07F001 DD SYSOUT=B,SPACE=(CYL,(5,1))
//GC.SYSPLCTS DD SYSOUT=C,UNIT=SE=(FT05F001,FT06F001)
//GC.FT10F001 DD UNIT=SYSDA,SPACE=(TRK,(2,6))
//GC.FT11F001 DD UNIT=SYSDA,SPACE=(080,(0500,1)),DISP=(NEW,DELETE)
//GC.FT12F001 DD UNIT=SYSDA,SPACE=(080,(0001,1)),DISP=(NEW,DELETE)
//GC.SYSIN DD *
//GC.FT13F001 DD UNIT=SYSDA,SPACE=(CYL,(0010,1)),DISP=(NEW,DELETE)
```

(INSERT THE INPUT DECK HERE)
(A SAMPLE INPUT DECK IS SHOWN BELOW)

*

(COLUMN ONE INDICATED BY ASTERISK)

0.190 0.500 30.000
THIS IS A SAMPLE INPUT DECK - 9X15 MESH
SYMMETRIC, U-SHAPED NOTCHES, UNIFORM LOAD

4	1	8	1	14	17	4	1	12	1.0	-1.0
1	12	1	14	27	30	17	1	1	1.0	
2	12	1	17	30	20	7	1	12		-1.0
3	12	4	17	30	33	20	1	12		
5	3	17	0			2				
6	1									

(END OF SAMPLE INPUT DECK. PROBLEMS MAY BE STACKED BY USING)
(MORE THAN ONE SUCH INPUT DECK AT THIS POINT. EXECUTION)
(TERMINATES EITHER BY BOMBING OR NORMAL TERMINATION. SEE USER'S)
(MANUAL, APPENDIX D OF THESIS. THE LAST CARD, FOLLOWING)
(INPUT DECK OR DECKS, IS A SLASH-STAR.)

EXPLANATION OF THE DATA DECK:
(NUMERALS IN PARENTHESES INDICATE VALUES EMPLOYED IN WORK DONE
IN THE AFOREMENTIONED THESIS.)

CARD 1 (3F10.2) PROBLEM PARAMETERS
1-10 RW: RADIUS / UNDISTURBED WIDTH (0.1)
11-20 DW: WAIST WIDTH / UNDISTURBED WIDTH (0.5)
21-30 TH: ANGLE OF INCLINATION (DEGREES) (30.0)

CARDS 2 & 3 (6A8) EACH CARD TITLE

CARD 4 (4I5) MESH PARAMETERS
1-5 NSEL: NUMBER OF SUPER ELEMENTS PER ELEMENT
6-10 NPNT: NUMBER OF NODES - UNIFORM LOAD
11-15 NPUNCH: 1 FOR SYMMETRIC - UNIFORM MOMENT
2 FOR ONE NOTCH - UNIFORM MOMENT
3 FOR ONE NOTCH - BENDING MOMENT
4 FOR ONE NOTCH - BENDING MOMENT

16-20 NPLOT: 0 FOR NO PLOTS
1 FOR PRINTER PLOT
2 FOR CALCOM PLOT

AA 00090
AA 00100
AA 00110
AA 00120
AA 00130
AA 00140
AA 00150
AA 00160
AA 00170
AA 00180
AA 00190
AA 00200
AA 00210
AA 00220
AA 00230
AA 00240
AA 00250
AA 00260
AA 00270


```

CARD 5-(NSEL+4) (1015,2F10.2) ONE PER SUPER ELEMENT
1-5 SELNR: SUPER ELEMENT IDENTIFICATION NUMBER
6-10 ROWS: NUMBER OF ROWS IN SUPER ELEMENT
11-15 CLMNS: NUMBER OF COLUMNS IN SUPER ELEMENT
16-20 NODE A: SUPER ELEMENT A *****
21-25 NODE B: CONNECTIVITY B *****
26-30 NODE C: COUNTERCLOCKWISE C *****
31-35 NODE D: (SEE NOTE) D *****

NOTE: SEL NUMBERING IS ARBITRARY. HOWEVER,
A NODE COMMON TO TWO OR MORE SELS MUST
RETAIN ITS NUMBER. (ALWAYS 1)
MATERIAL ID NUMBER. (ALWAYS 1)
NUMBER OF BOUNDARY NODES FOR THIS SEL
(NPTS B = 4, 8 OR 12)
IF SEL NOT CONNECTED TO ADJACENT SEL
AT MID SIDE NODES, ENTER ADJACENT SEL
NUMBER HERE. (NORMALLY BLANK)
EXPONENTIAL COEFF. - XI DIRECTION
EXPY: EXPONENTIAL COEFF. - ETA DIRECTION
61-70 EXPY: NOTE: ELEMENT SIZE INCREASES WITH
CG-COORDINATE DIRECTION FOR POSITIVE
EXPX AND EXPY

CARD (NSEL + 5) (1015) STRESS ANALYSIS PARAMETERS
1-10 NOT USED (LEAVE BLANK)
11-15 NMAT: ALWAYS 1
26-30 NSTRES: 0 FOR PLANE STRESS
31-35 NGP: NUMBER OF GAUSS POINTS DESIRED
36-50 IN THE INTEGRATION (2 THRU 5)
NOT USED (LEAVE BLANK)

IMPLICIT REAL*8 (A-H,O-Z)
COMMON/INT/NPT,NEL,NPUNCH,NSTOP,NJT,NPLOT,NKIND,NSEL,NGROW,NGCOL,
1 COMMON/TITL/TITLE(12)

FOR 9 X 15 QUADRATIC ELEMENT MESH - NOTCH PROBLEMS
COMMON/STAT/WR,DR,TH,W,X(33),Y(33),EXPX(48),EXPY(48)
COMMON/COORD1/COORD(454,4),ELCON(1,4),NBC(454,2)
COMMON/MESHI/ NSCON(20,9),MS(20,8),MEL(20,4)
COMMON COORD(12,2),ELAST(3,3),SS(24,16),SN(24,16)

7 REWIND 11
READ(5,15)RW,DW,TH

```

```

AA 00280
AA 00290
AA 00300
AA 00310
AA 00320
AA 00330
AA 00340
AA 00350
AA 00360
AA 00370
AA 00380
AA 00390
AA 00400
AA 00410
AA 00420
AA 00430
AA 00440
AA 00450
AA 00460
AA 00470
AA 00480
AA 00490
AA 00500
AA 00510
AA 00520
AA 00530
AA 00540
AA 00550
AA 00560
AA 00570
AA 00580
AA 00590
AA 00600
AA 00610
AA 00620
AA 00630
AA 00640
AA 00650
AA 00660
AA 00670
AA 00680
AAW00690
AAW00700
AAW00710
AAW00720
AA 00730
AA 00740
AA 00750

```

```

(1)
(0)
(2)

```



```

A=RW
B=DW
15 FORMAT(3F10.2)
READ(5,10) (TITLE(I),I=1,12)
WRITE(6,20) (TITLE(I),I=1,6)
WRITE(6,22) (TITLE(I),I=7,12)
20 FORMAT(1X,6A8)
22 FORMAT(1X,6A8)
READ(5,11) NSEL,NPT,NPUNCH,NPLCT
NCKIND=NPT/4
DC1000 N=1,NSEL
READ(5,11) I,(NSCON(I,J),J=1,9),EXPX(I),EXPY(I)
1000 WRITE(11,11) I,(NSCON(I,J),J=1,9)
10 FORMAT(1X,6A8)
11 FORMAT(10I5,2F10.2)
W=1.3D0
IJK=0
NR=NSCON(1,1)+NSCON(2,1)
NC=NSCON(1,2)
GC TO (101,102,103),NKIND
101 I1=0
I2=NR+2
I3=(NC-1)*(I2-1)+1
I4=0
I5=I2-1
I6=0
GC TO 104
102 I1=(NR*2)+2
I2=(NR*3)+3
I3=(NC-1)*(I2-1)+1
I4=(NC-1)*(I2-1)+11
I5=I2-1
I6=0
GC TO 104
103 I1=(NR*3)+2
I2=(NR*5)+4
I3=(NC-1)*(I2-1)+1
I4=(NC-1)*(I2-1)+12
I5=I2-1
I6=NR+1
104 WRITE(11,2999) I1,I2,I3,I4,I5,I6
2999 FORMAT(6I10)
DC1 I=1,5
DC2 L=1,10
DC3 K=1,5
WR=1/RW
R=WR*RW
DR=WR*DW
AA 00760
AA 00770
AA 00780
AA 00790
AA 00800
AA 00810
AA 00820
AA 00830
AA 00840
AA 00850
AA 00860
AA 00870
AA 00880
AA 00890
AA 00900
AA 00910
AA 00920
AA 00930
AA 00940
AA 00950
AA 00960
AA 00970
AA 00980
AA 00990
AA 01000
AA 01010
AA 01020
AA 01030
AA 01040
AA 01050
AA 01060
AA 01070
AA 01080
AA 01090
AA 01100
AA 01110
AA 01120
AA 01130
AA 01140
AA 01150
AA 01160
AA 01170
AA 01180
AA 01190
AA 01200
AA 01210
AA 01220
AA 01230

```



```

CALL PRCBLM
IF (X(1).EQ.10.00) GO TO 3
CALL PLIMEG
IF(IJK.NE.0) GO TO 6
IJK=IJK+1
READ(5,11)NNN,NNN,NMAT,NNN,NNN,NSTRES,NGP,NTLD,NTBY,NTIN
WRITE(11,11)NEL,NJT,NMAT,NCLOAD,NPBC,NSTRES,NGP,NTLD,NTBY,NTIN
CALL PLISOP
CALL ANS
IF(NPLOT.GT.0) GO TO 7
DW=DW+0.200
DW=B
RW=RW+0.0500
RW=A
TH=TH+15.00
1 STOP
9000 END

```

```

AA 01240
AA 01250
AA 01260
AA 01270
AA 01280
AA 01290
AA 01300
AA 01310
AA 01320
AA 01330
AA 01340
AA 01350
AA 01360
AA 01370
AA 01380
AA 01390
AA 01400

```

```

SUBROUTINE PROBLEM
IMPLICIT REAL*8 (A-H,O-Z)
COMMON/STAT/WR,DR,TH,W,X(33),Y(33),EXPX(48),EXPY(48)
REWIND 10
PI=3.1415926535900
R=W/WR
D=DP*WR
WRITE(6,2000) WR,DR,TH,W,D,R
TH=(PI*TH)/540.00
RU=R+D
X(1)=0.00
Y(1)=D
Y(7)=W
X(14)=0.00
Y(14)=D/3.00
X(20)=5.00*W
Y(20)=W
X(27)=0.00
Y(27)=0.00
X(33)=5.00*W
Y(33)=0.00
Y(30)=0.00
X(2)=RD-R*DSIN(PI/6.00-TH)
Y(2)=RD-R*DCOS(PI/6.00-TH)

```

```

BB 00010
BB 00020
BB 00030
BB 00040
BB 00050
BB 00060
BB 00070
BB 00080
BB 00090
BB 00100
BB 00110
BB 00120
BB 00130
BB 00140
BB 00150
BB 00160
BB 00170
BB 00180
BB 00190
BB 00200
BB 00210
BB 00220
BB 00230
BB 00240
BB 00250
BB 00260

```



```

BB 00270
BB 00280
BB 00290
BB 00300
BB 00310
BB 00320
BB 00330
BB 00340
BB 00350
BB 00360
BB 00370
BB 00380
BB 00390
BB 00400
BB 00410
BB 00420
BB 00430
BB 00440
BB 00450
BB 00460
BB 00470
BB 00480
BB 00490
BB 00500
BB 00510
BB 00520
BB 00530
BB 00540
BB 00550
BB 00560
BB 00570
BB 00580
BB 00590
BB 00600
BB 00610
BB 00620
BB 00630
BB 00640
BB 00650
BB 00660
BB 00670
BB 00680
BB 00690
BB 00700
BB 00710
BB 00720
BB 00730
BB 00740

```

```

TH=2.D0*TH
X(3)=R*DSIN(2.D0*PI/6.D0-TH)
Y(3)=R*DCOS(2.D0*PI/6.D0-TH)
TH=3.D0*TH/2.D0
X(4)=R*DCOS(TH)
Y(4)=R*DSIN(TH)
IF((Y(7)-Y(1)).LE.0.ID-3) GO TO 7
IF((Y(7)-Y(4)).LE.0.ID-3) GO TO 4
X(7)=X(4)+(W-Y(4))*DIAN(TH)
X(5)=X(4)+(X(7)-X(4))/3.D0
X(6)=X(4)+(X(7)-X(4))*2.D0/3.D0
Y(5)=Y(4)+(Y(7)-Y(4))/3.D0
Y(6)=Y(4)+(Y(7)-Y(4))*2.D0/3.D0
TH=180.D0*TH/PI
IF(X(7).GE.X(20)) GO TO 3
X(17)=W+R
X(30)=X(17)
DX=(X(20)-X(17))/3.D0
X(18)=X(17)+DX
X(19)=X(18)+DX
C=(W-D/6.D0)/(25.D0*W**2)
B=0.D0
DO 1 I=1,19
  Y(I)=D/6.D0+B*X(I)+C*X(I)**2
  C=(Y(17)-Y(4))/(X(17)**2-X(4)**2-2.D0*(X(17)-X(4))*X(4))
  B=-2.D0*X(4)*C
  A=Y(4)-X(4)*B-X(4)**2.D0*C
  DX=(X(17)-X(4))/3.D0
  X(9)=X(4)+DX
  X(12)=X(9)+DX
  DO 2 I=9,12,3
    Y(I)=A+B*X(I)+C*X(I)**2
    FORMAT(1,20X,W/R=,G10.2,/,
2    1,20X,D/R=,G10.2,/,
3    2,20X,THETA=,G10.2,/,
4    3,20X,WIDTH=,G10.2,/,
5    4,20X,DEPTH=,G10.2,/,
5    5,20X,RADIUS=,G10.2,/)
  L=5
  A=0.D0
  I=0
  J=1
  K=4
9998 FFORMAT(315,2D25.16)
      WRITE(10,9998)J,K,I,X(K),Y(K)
      K=3
      WRITE(10,9998)J,K,I,X(K),Y(K)
      K=2

```



```

4000 TH=180.D0*TH/PI
      FORMAT(' DEPTH TOO LARGE')
      RETURN
      END

```

```

BB 01710
BB 01720
BB 01730
BB 01740

```

```

SUBROUTINE PLIMEG
      MESH GENERATING PROGRAM FOR 'PLISUP',
      CODED BY J.R.ADAMEK, DECEMBER 1972, NAVAL POSTGRADUATE SCHOOL
      MODIFIED BY L.J.SMITH, MAY 1974, NAVAL POSTGRADUATE SCHOOL

```

```

CC 00010
CC 00020
CC 00030
CC 00040
CC 00050
CC 00060
CC 00070
CC 00080
CC 00090
CC 00100
CC 00110
CC 00120
CC 00130
CC 00140
CC 00150
CC 00160
CC 00170
CC 00180
CC 00190
CC 00200
CC 00210
CC 00220
CC 00230
CC 00240
CC 00250
CC 00260
CC 00270
CC 00280
CC 00290
CC 00300
CC 00310
CC 00320
CC 00330
CC 00340
CC 00350
CC 00360
CC 00370
CC 00380
CC 00390

```

```

      THE NECESSARY INPUT FOR THIS PROGRAM IS AS FOLLOWS:
      (PASSED VIA MAIN)

```

```

      CARD 1 AND 2, TITLE, FORMAT (6A8) EACH CARD.

```

```

      COL. 1 TO 48 BRIEF TITLE OF PROBLEM. USER'S NAME AND/CR BOX NO.
      MUST BE INCLUDED ON ONE OF THE CARDS IF CALCOMP
      OPTION INCLUDED. (SEE CARD 3)

```

```

      CARD 3, MESH PARAMETERS, FORMAT (4I5).

```

```

      CCL. 1 TO 5 (NSEL): NUMBER OF SUPER ELEMENTS.

```

```

      6 TO 10 (NPT): THE NUMBER OF NODAL POINTS PER ELEMENT.
      NPT= 4,8 OR 12

```

```

      11 TO 15 (NPUNCH): IF THIS IS ZERO OR BLANK, NO CARDS WILL
      BE PUNCHED. IF NPUNCH IS DIFFERENT FROM ZERO A DECK
      FOR CONNECTIVITY AND X,Y COORDINATES OF ALL JOINTS
      WILL BE PUNCHED. NPUNCH BLANK OR ZERO SHOULD ALWAYS
      BE USED UNTIL ONE IS SATISFIED WITH THE MESH.

```

```

      16 TO 20 (NPLOT): IF THIS IS ZERO OR BLANK, NO PLOTS WILL
      BE MADE. IF NPLOT IS (1) A PLOT WILL BE OBTAINED ON
      THE PRINTER (UTPLOT). IF NPLOT IS (2) A PLOT WILL BE
      OBTAINED ON CALCOMP PLOTTER.
      NPLOT SHOULD BE (1) UNTIL SATISFIED WITH MESH.
      ALL PLOTS WILL BE PLOTTED IN FIRST QUADRANT ONLY.

```

```

      SUPER ELEMENT DECK, TOTAL OF NSEL CARDS, FORMAT (10I5), LOAD IN
      ASCENDING ORDER OF SUPER ELEMENT NUMBERS.

```

```

CCCCCCCCCCCCCCCCCCCCCCCCCCCCCCCCCCCCCCCCCCCCCCCCCCCCCCCC

```



```

CC 00400
CC 00410
CC 00420
CC 00430
CC 00440
CC 00450
CC 00460
CC 00470
CC 00480
CC 00490
CC 00500
CC 00510
CC 00520
CC 00530
CC 00540
CC 00550
CC 00560
CC 00570
CC 00580
CC 00590
CC 00600
CC 00610
CC 00620
CC 00630
CC 00640
CC 00650
CC 00660
CC 00670
CC 00680
CC 00690
CC 00700
CC 00710
CC 00720
CC 00730
CC 00740
CC 00750
CC 00760
CC 00770
CC 00780
CC 00790
CC 00800
CC 00810
CC 00820
CC 00830
CC 00840
CC 00850
CC 00860
CC 00870

COL. 1 TO 5 (SEL NO.) SUPER ELEMENT IDENTIFICATION NUMBER.
      6 TO 10 (ROW): NUMBER OF ROWS IN SUPER ELEMENT.
     11 TO 15 (COL): NUMBER OF COLUMNS IN SUPER ELEMENT.
     16 TO 20 (NODE A): ***** A ***** D
     21 TO 25 (NODE B): * SUPER ELEMENT *****
     26 TO 30 (NODE C): * CONNECTIVITY *****
     31 TO 35 (NODE D): * COUNTERCLOCKWISE *****
                       * (SEE NOTE) *****
                       * B ***** C *****
NOTE: NUMBERING OF SUPER-ELEMENT CORNER NODES IS
ARBITRARY. HOWEVER, CORNER NODES WHICH ARE
CONNECTED TO OTHER CORNER NODES, MUST HAVE
THE SAME NUMBER.
      36 TO 40 (TYPE): MATERIAL IDENTIFICATION NUMBER FOR
                       SUPER ELEMENT.(SEE 'PLISOP' INST)
     41 TO 45 (NPTSB): NUMBER OF SUPER ELEMENT BOUNDARY NODES.
                       NPTSB = 4, 8 OR 12
     46 TO 50 (CGN): IF SUPER ELEMENT IS CONNECTED TO AN
                       ADJACENT SUPER ELEMENT BELOW OR TO THE
                       RIGHT ONLY AT THE CORNER NODES AND NOT IN
                       BETWEEN, ENTER ADJACENT SUPER ELEMENT
                       NUMBER HERE. OTHERWISE LEAVE BLANK.

SUPER ELEMENT BOUNDARY DECK, TOTAL OF NPTB CARDS, (315,2625.17)

NPTB=SUM OF BOUNDARY NODES OF ALL SUPER ELEMENTS.
ORDER IS COUNTER CLOCK-WISE STARTING AT NODE COMMON
WITH (XI,ETA)=(1,1). IF MORE THAN ONE SUPER ELEMENT,
LOAD ITS BOUNDARY AFTER THAT OF FIRST SUPER ELEMENT
IN SAME NODAL ORDER AS ABOVE. ORDER OF SUPER ELEMENTS
SAME AS FOR SUPER ELEMENT DECK.

COL. 1 TO 5 (SEL NO.): SUPER ELEMENT IDENTIFICATION NUMBER.
      6 TO 10 (NODE NO.): ARBITRARY NUMBERING OF SUPER ELEMENT
                           BOUNDARY NODES. MAY OR MAY NOT BE THE
                           SAME NUMBERING SCHEME AS
                           FOR CONNECTIVITY.

```



```

C
46
47
48
49
50
51
52
53
55

DC 70 K=1,NSELT
IF (NSCON(K,2).EQ.0) GO TO 70
I4=NSCON(K,8)+I3-I
DC 60 I=I3,I4
READ (10,25) NBSEL,NBNGDE,NCT(I),(BOUND(I,J),J=1,2)
WRITE (6,28) NBSEL,NBNGDE,NCT(I),(BOUND(I,J),J=1,2)
IF (NBSEL.LT.NBS1) NSTOP=1
NBS1=NBSEL
NCTI=NCT(I)
GC TO (46,46,46),NCTI
GO TO 47
PHI=.314159265358979D1*BOUND(I,2)/1.8D2
RAD=BOUND(I,1)
BCUND(I,1)=RAD*DCOS(PHI)
BOUND(I,2)=RAD*DSIN(PHI)
GO TO (50,48,49),NCTI
GC TO 50
READ (5,26) XCC,YCC
WRITE (6,29) XCC,YCC
BOUND(I,1)=BOUND(I,1)+XCC
BOUND(I,2)=BOUND(I,2)+YCC
II=I-I-1
III=I-I-2
IIII=I-I-3
IF (II.LE.0) II=1
IF (IIII.LE.0) IIII=1
IF (II.EQ.NLAST).AND.(I.EQ.I4) GO TO 51
GO TO 52
II=I-I-1
IIII=II-1
IIIIII=II-1
IF (NCT(II).EQ.5) GO TO 53
IF (NCT(IIII).EQ.5).AND.(NCT(IIIIII).EQ.5) GO TO 55
GO TO 60
NB1=I-I-1
NB2=II+1.EQ.IIIII) NB2=II-7
IF (NCT(II).EQ.III,1)=(BOUND(NB1,1)+BOUND(NB2,1))/2.0D0
BOUND(II,2)=(BOUND(NB1,2)+BOUND(NB2,2))/2.0D0
GO TO 60
NB1=I-I-2
NB2=II-1
NB3=II+1.EQ.IIIII) NB3=II-11
IF (NCT(II).EQ.III,1)=BOUND(NB1,1)-BOUND(NB3,1)
BMIDX=BOUND(NB1,2)-BOUND(NB3,2)
BMIDY=BOUND(II,1)-BOUND(NB1,1)-BMIDX/3.0D0
BOUND(II,2)=BOUND(NB1,2)-BMIDY/3.0D0

```



```

60 BCUND(11,1)=BCUND(NB1,1)-2*BMIDY/3.0D0
CC 02320
CC 02330
CC 02340
70 CC 02350
CC 02360
CC 02370
CC 02380
CC 02390
75 CC 02400
CC 02410
CC 02420
CC 02430
CC 02440
CC 02450
CC 02460
CC 02470
CC 02480
95 CC 02490
CC 02500
CC 02510
CC 02520
CC 02530
CC 02540
CC 02550
CC 02560
CC 02570

BCUND(11,1)=BCUND(NB1,1)-2*BMIDY/3.0D0
BCUND(11,2)=BCUND(NB1,2)-2*BMIDY/3.0D0
CC 02320
CC 02330
CC 02340
CC 02350
CC 02360
CC 02370
CC 02380
CC 02390
CC 02400
CC 02410
CC 02420
CC 02430
CC 02440
CC 02450
CC 02460
CC 02470
CC 02480
CC 02490
CC 02500
CC 02510
CC 02520
CC 02530
CC 02540
CC 02550
CC 02560
CC 02570

111,15,/, DATA REJECTED***NUMBER OF BOUNDARY NODES GREATER THCC
RETURN
NSTOP=0
CALL CONN
IF (NSTOP.EQ.1) RETURN
CALL COORD
IF (NPLOT.NE.0) CALL GRID
9000 RETURN

```

```

C SUBROUTINE CONN
C THIS SUBROUTINE DETERMINES ELEMENT CONNECTIVITY FOR 4,8 AND 12
C NODAL ELEMENTS. OUTPUT IS PRINTED AND AN OPTION TO PUNCH IN
C FORMAT COMPATIBLE WITH "PLISOP" IS INCORPORATED.
C
IMPLICIT REAL*8 (A-H,O-Z)
INTEGER*4 INF1,INF2,INF3,INFB
DIMENSION NLC(14,3), LCON(14)
COMMON/INT/NPT,NEL,NPUNCH,NSTOP,NJT,NPLOT,NKIND,NSEL,NGROW,NGCOL,
1 NCLoad,NPBC
COMMON/MESH1/ NSCON(20,9),MS(20,8),MEL(20,4)
COMMON/MESH2/ NCR(4),NRR(4)
COMMON/MESH3/ NCON(135,14)
DATA MAXNEL/135/,MAXNJT/454/
111,12,13,14,10,11,12,13,14,7,8,9,10,11,12,13,14,5,6,7,8,9,10,
111,12,13,14,10,11,12,13,14,7,8,9,10,11,12,13,14,5,6,7,8,9,10,
FORMAT (///, CONNECTIVITY MATRIX,/, ELEMENT NUMBER ,64X, KINDD
20

```



```

10,IX,'TYPE',//)
21 FORMAT (//,' NUMBER OF ELEMENTS=',I4,/,', NUMBER OF JOINTS=',I4)
25 FORMAT (5X,I3,11X,14I5)
26 FORMAT (15I4)
C
C
C      NUMBER OF ROWS AND COLUMNS IN EACH GRID COLUMN.
K=1
REWIND 10
DO 60 I=1,NGCOL
  NRR(I)=0
  NCR(I)=0
  DO 50 J=1,NGROW
    NRR(I)=NRR(I)+NSCON(K,1)
    IF (NCR(I).NE.0) GO TO 50
    IF (NSCON(K,2).NE.0) NCR(I)=NSCON(K,2)
    K=K+1
  CONTINUE
50
60
C
C
C      ZERO CONNECTIVITY MATRIX
DO 80 I=1,MAXNEL
  DO 70 J=1,14
    NCON(I,J)=0
  CONTINUE
70
80
C
C
C      SUPER ELEMENT CONNECTIVITY
K=1
DO 100 I=1,NGCOL
  IF (NCR(I).EQ.0) GO TO 95
  J1=NGROW
  IF (I.EQ.NGCOL) J1=NGROW-1
  DO 90 J=1,J1
    IF (NSCON(K,1).EQ.0) GO TO 90
    L=K+1
    M=K+NGROW
    IF (NSCON(K,4).NE.NSCON(L,3)) GO TO 86
    MS(K,4)=1
    MS(L,1)=1
    IF (NSCON(K,5).NE.NSCON(L,6)) GO TO 87
    MS(K,5)=1
    MS(L,8)=1
    IF (I.EQ.NGCOL) GO TO 90
    IF (NSCON(K,6).NE.NSCON(M,3)) GO TO 88
    MS(K,7)=1
    MS(M,2)=1
    IF (NSCON(K,5).NE.NSCON(M,4)) GO TO 90
86
87
88

```



```

DD 00660
DD 00670
DD 00680
DD 00690
DD 00700
DD 00710
DD 00720
DD 00730
DD 00740
DD 00750
DD 00760
DD 00770
DD 00780
DD 00790
DD 00800
DD 00810
DD 00820
DD 00830
DD 00840
DD 00850
DD 00860
DD 00870
DD 00880
DD 00890
DD 00900
DD 00910
DD 00920
DD 00930
DD 00940
DD 00950
DD 00960
DD 00970
DD 00980
DD 00990
DD 01000
DD 01010
DD 01020
DD 01030
DD 01040
DD 01050
DD 01060
DD 01070
DD 01080
DD 01090
DD 01100
DD 01110
DD 01120
DD 01130

```

```

90 MS(K,6)=1
95 MS(M,3)=1
100 K=K+1
C GC TO 100
C K=K+NGROW
C CONTINUE
C
C ELEMENT CONNECTIVITY
C
NCL=1
KK=1
MM1=1
II=0
DO 500 I=1,NGCOL
  LI=NCR(I)
  IF (LI.EQ.0) GO TO 470
  II=II+1
  DO 450 L=1,LI
    LL1=NKIND
    LL2=NKIND+1
    IF (L.EQ.LI) LL1=LL2
    DO 430 LL=1,LL1
      L3=0
      IF ((LL.EQ.1).AND.(L.EQ.1)) L3=1
      NKINDI=NKIND
      IF ((LL.NE.1).AND.(LL.NE.LL2)) NKINDI=1
      K=KK
      M1=MM1
      DO 400 J=1,NGROW
        IF (NSCON(K,1).EQ.0) GO TO 390
        KA=K-1
        KB=NSCON(K,9)-1
        KL=K-NGROW
        KL1=KL-1
        KL2=KL+1
        KR=K+NGROW
        KR1=KR-1
        IF (LL.NE.LL2) GO TO 145
        IF ((MS(K,7).EQ.0).AND.(MS(K,8).EQ.1)).AND.(MS(KA,6).EQ.1))
          1 NCL=NCL-1
        IF ((MS(K,6).EQ.1).AND.(MS(K,7).EQ.1))
          1 AND.((KR.NE.NSCON(K,9))) GO TO 135
        GO TO 140
      M1=M1+NSCON(K,1)
      GC TO 390
    IF (MS(K,7).EQ.1) NCL=NCL-1
    M2=M1+NSCON(K,1)-1
    IF (M2.GT.MAXNEL) GO TO 700
  135
  140
  145

```



```

147.      DC 350 M=M1,M2      GO TO 148
      IF (LL.NE.1) GO TO 147
      IF (L.NE.M1) MEL(K,1)=M
      IF (M.EQ.M1) MEL(K,2)=M
      IF (L.NE.L1) GO TO 148
      IF (M.EQ.L1) MEL(K,3)=M
      IF (M.EQ.M1) MEL(K,4)=M
      IF (M.EQ.M2) MEL(K,4)=M
      IF TO (150,200,250),NKIND
148      C
      C
      C      LINEAR ELEMENTS
150      GO TO (160,185),LL
160      NCON(M,1)=NC1
      NCON(M,2)=NC1+1
      IF (L.EQ.1) GO TO 165
      NCON(MM2,4)=NCON(M,1)
      NCON(MM2,3)=NCON(M,2)
      MM2=MM2+1
      GO TO 300
      IF (L.EQ.1) GO TO 300
      IF ((MS(K,2).EQ.0).AND.(MS(K,3).EQ.0)) GO TO 300
      IF (M.NE.M1) GO TO 171
      MM3=MEL(KL,3)
      MM4=MEL(K,1)
      IF ((MS(K,2).EQ.1).AND.(MS(K,3).EQ.1)) GO TO 172
171      GC TO 300 NSCON(KL,9)) GO TO 300
172      IF (K.EQ.1) NCON(MM3,4)=NCON(MM4,1)
      NCON(MM3,3)=NCON(MM4,2)
      MM3=MM3+1
      MM4=MM4+1
      GO TO 300
      NCON(M,4)=NC1
      NCON(M,3)=NC1+1
      GO TO 300
185      C
      C
      C      QUADRATIC ELEMENTS
200      GC TO (205,225,245),LL
205      NCON(M,1)=NC1
      NCON(M,2)=NC1+1
      IF (L.EQ.1) GO TO 210
      NCON(MM2,7)=NCON(M,1)
      NCON(MM2,6)=NCON(M,2)
      NCON(MM2,5)=NCON(M,3)
      MM2=MM2+1

```


210	GO TO 300	DD	01620
	IF (I.EQ.1) GO TO 300	DD	01630
	IF ((MS(K,2).EQ.0).AND.(MS(K,3).EQ.0)) GO TO 300	DD	01640
	IF (M.NE.M1) GO TO 215	DD	01650
	MM3=MEL(KL,3)	DD	01660
	MM4=MEL(K,1)	DD	01670
215	IF ((MS(K,2).EQ.1).AND.(MS(K,3).EQ.1)) GO TO 220	DD	01680
	GO TO 300	DD	01690
220	IF (K.EQ.NSCON(KL,9)) GO TO 300	DD	01700
	NCON(MM3,7)=NCON(MM4,1)	DD	01710
	NCON(MM3,6)=NCON(MM4,2)	DD	01720
	NCON(MM3,5)=NCON(MM4,3)	DD	01730
	MM3=MM3+1	DD	01740
	MM4=MM4+1	DD	01750
	GO TO 300	DD	01760
225	NCON(M,8)=NC1	DD	01770
	NCON(M,4)=NC1+1	DD	01780
	GO TO 300	DD	01790
245	NCON(M,7)=NC1	DD	01800
	NCON(M,6)=NC1+1	DD	01810
	NCON(M,5)=NC1+2	DD	01820
	GO TO 300	DD	01830
C		DD	01840
C	CUBIC ELEMENTS	DD	01850
C		DD	01860
250	GO TO (255,285,290,295),LL	DD	01870
255	NCON(M,1)=NC1	DD	01880
	NCON(M,2)=NC1+1	DD	01890
	NCON(M,3)=NC1+2	DD	01900
	NCON(M,4)=NC1+3	DD	01910
	IF (L.EQ.1) GO TO 260	DD	01920
	NCON(MM2,10)=NCON(M,1)	DD	01930
	NCON(MM2,9)=NCON(M,2)	DD	01940
	NCON(MM2,8)=NCON(M,3)	DD	01950
	NCON(MM2,7)=NCON(M,4)	DD	01960
	MM2=MM2+1	DD	01970
	GO TO 300	DD	01980
260	IF (I.EQ.1) GO TO 300	DD	01990
	IF ((MS(K,2).EQ.0).AND.(MS(K,3).EQ.0)) GO TO 300	DD	02000
	IF (M.NE.M1) GO TO 265	DD	02010
	MM3=MEL(KL,3)	DD	02020
	MM4=MEL(K,1)	DD	02030
265	IF ((MS(K,2).EQ.1).AND.(MS(K,3).EQ.1)) GO TO 270	DD	02040
	GO TO 300	DD	02050
270	IF (K.EQ.NSCON(KL,9)) GO TO 300	DD	02060
	NCON(MM3,10)=NCON(MM4,1)	DD	02070
	NCON(MM3,9)=NCON(MM4,2)	DD	02080
	NCON(MM3,8)=NCON(MM4,3)	DD	02090


```

NCCN(MM3, 7)=NCON(MM4,4)
MM3=MM3+1
MM4=MM4+1
GO TO 300
285 NCON(M,12)=NC1
NCON(M,5)=NC1+1
GO TO 300
290 NCON(M,11)=NC1
NCON(M,6)=NC1+1
GO TO 300
295 NCON(M,10)=NC1
NCON(M,9)=NC1+1
NCON(M,8)=NC1+2
NCON(M,7)=NC1+3
300 NCI=NC1+NKIND1
NCON(M,13)=NKIND
NCON(M,14)=NSCON(K,7)
CONTINUE
350 IF ((I,NE.1).AND.(L3.EQ.1)) GO TO 355
GO TO 375
355 IF ((MS(K,2).EQ.0).AND.(MS(K,3).EQ.0)) GO TO 375
MM5=MEL(K,2)
MM6=MEL(KL,4)
MM7=MEL(KL1,4)
MM8=MEL(KL2,3)
MM9=MEL(KL,3)
MM10=MEL(K,1)
GO TO (360,365,370),NKIND
360 IF (MS(K,2).NE.1) GO TO 362
NCCN(MM9,4)=NCCN(MM10,1)
IF (MS(KL,8).EQ.1) NCCN(MM7,3)=NCCN(MM9,4)
362 IF (MS(K,3).NE.1) GO TO 375
NCON(MM6,3)=NCON(MM5,2)
IF (MS(KL,5).EQ.1) NCCN(MM8,4)=NCCN(MM6,3)
GO TO 375
365 IF (MS(K,2).NE.1) GO TO 367
NCCN(MM9,7)=NCCN(MM10,1)
IF (MS(KL,8).EQ.1) NCCN(MM7,5)=NCCN(MM9,7)
367 IF (MS(K,3).NE.1) GO TO 375
NCON(MM6,5)=NCON(MM5,3)
IF (MS(KL,5).EQ.1) NCCN(MM8,7)=NCCN(MM6,5)
GO TO 375
370 IF (MS(K,2).NE.1) GO TO 372
NCCN(MM9,10)=NCCN(MM10,1)
IF (MS(KL,8).EQ.1) NCCN(MM7,7)=NCCN(MM9,10)
372 IF (MS(K,3).NE.1) GO TO 375
NCON(MM6,7)=NCCN(MM5,4)
IF (MS(KL,5).EQ.1) NCCN(MM8,10)=NCCN(MM6,7)

```



```

600  CONTINUE
      NBAND=(NBAND+1)*2
      WRITE (6,650) NBAND
650  FORMAT (//, ' HALF BAND WIDTH FOR PLISOP STIFFNESS MATRIX=', I5)
      RETURN
700  NSTOP=1
      WRITE (6,725) MAXNEL
725  FORMAT (//, ' DATA REJECTED ***** GREATER THAN', I5)
      1,/, *****
      RETURN
800  NSTICP=1
      WRITE (6,825) MAXNJT
825  FORMAT (//, ' DATA REJECTED ***** GREATER THAN', I5)
      1,/, *****
      RETURN
      END
DD 03060
DD 03070
DD 03080
DD 03090
DD 03100
DD 03110
DD 03120
DD 03130
DD 03140
DD 03150
DD 03160
DD 03170
DD 03180
DD 03190
DD 03200
DD 03210

```

```

SUBROUTINE COORD
C THIS SUBROUTINE DETERMINES X,Y COORDINATES OF NODES FOR 4, 8,
C AND 12 NODE ELEMENTS. FORCE AND DISPLACEMENT BOUNDARY
C CONDITIONS ARE ALSO DETERMINED HERE.
C
IMPLICIT REAL*8 (A-H,O-Z)
DIMENSION XI(12),ETA(12)
DIMENSION NQ1(3),NC1(4)
COMMON/INT/NPT,NEL,NPUNCH,NSTOP,NJT,NPLOT,NKIND,NSEL,NGROW,NGCOL,
1 NCLDAD,NPBC
CCMCMN/SF/VAL(12)
CCMCMN/MESH1/ NSCON(20,9),MS(20,8),MEL(20,4)
COMMON/MESH2/ NCR(4),NRR(4)
CCMCMN/MESH3/ NCON(135,14)
CCMCMN/CORD1/CORD(454,4),ELCON(1,4),NBC(454,2)
CCMCMN/CORD2/BOUND(48,2)
CCMCMN/STAT/WR,DR,TH,W,X(33),Y(33),EXPX(48),EXPY(48)
DATA NQ1/1,8,7/
DATA NC1/1,10,11,12/
FORMAT(///,3,COORDINATES OF JOINTS',//,' JOINT NUMBER',8X,'X COOR
1DINATE',5X,'Y COORDINATE',//)
FORMAT(5X,I3,2X,4(G14.5,3X),I3,2I5)
FORMAT(110,2G15.8)
F1(X1,A1)=(2.D0*(DEXP(A1*(X1+1.D0))-1.D0)/
1(DEXP(A1*2.D0)-1.D0))-1.D0
PI=3.14159265359D0

```


[illegible]


```

DC 180 N=5,7
XI(N)=XIVAL+2*DELXI
DO 200 N=1,3
NI=NQ1(N)
ETA(N1)=ETAVAL
DC 210 N=2,6,4
ETA(N)=ETAVAL-DELETEA
DO 220 N=3,5
ETA(N)=ETAVAL-2*DELETEA
IF((EXPX(K).NE.0.DO).OR.(EXPY(K).NE.0.DO)) GO TO 1000
GO TO 350

      CUBIC ELEMENTS
DC 260 N=1,4
XI(N)=XIVAL
DC 270 N=5,12,7
XI(N)=XIVAL+DELXI
DO 280 N=6,11,5
XI(N)=XIVAL+2*DELXI
DC 290 N=7,10
XI(N)=XIVAL+3*DELXI
DO 300 N=1,4
NI=NC1(N)
ETA(N1)=ETAVAL
DO 310 N=2,9,7
ETA(N)=ETAVAL-DELETEA
DO 320 N=3,8,5
ETA(N)=ETAVAL-2*DELETEA
DC 330 N=4,7
ETA(N)=ETAVAL-3*DELETEA
IF((EXPX(K).NE.0.DO).OR.(EXPY(K).NE.0.DO)) GO TO 1050
DO 400 N=1,NPT
NI=NSCON(M,N)
XI=XI(N)
ETAL=ETA(N)
CALL SHAPE (X11,ETAL,NPTB)
CCORD(N1,1)=0.DO
CCORD(N1,2)=0.DO
I11=I1
DC 360 NN=1,NPTB
CCPD(N1,1)=CCPD(N1,1)+VAL(NN)*8CCUND(I11,1)
CCRD(N1,2)=CCRD(N1,2)+VAL(NN)*8CCUND(I11,2)
I11=I11+1
CCNT=INUE
ETAVAL=ETAVAL-NKIND*DELETEA
CCNT=INUE
M1=M2+NRR(I)-NSCON(K,1)+1

```



```

600 XIVAL=XIVAL+NKIND*DELXI
CONTINUE
II=II+NPTB
K=K+1
GO TO 800
790 K=K+NGROW
800 CONTINUE
C WRITE (6,10)
NPBC=0
NCLOAD=0
READ(11,2999) I1,I2,I3,I4,I5,I6
2999 FORMAT(6I10)
WRITE(6,2999) I1,I2,I3,I4,I5,I6
C CORRECT THE CIRCULAR BOUNDARY
DC 3000 N=I2,I3,I5
FORMAT (15,D25.16)
3412 CORD(N,2)=W/WR+W*DR/WR- DSQRT((W/WR)**2-CORD(N,1)**2)
3000 IF(NKIND.EQ.1) GO TO 73
P=W/WR
DC 4000 N=I1,I4,I5
IF(CORD((N+I2-I1),1).GT.(R-0.1D-5)) GO TO 58
ANGA=DARSIN(CORD((N+I2-I1),1)/R)
59 IF(CORD((N-I1+1),1).EQ.0.D0) GO TO 56
ANGB=DARSIN(CORD((N-I2+1),1)/R)
IF(NKIND.EQ.3) GO TO 74
57 ANGC=(ANGA+ANGB)/2.D0
CORD(N,1)=DSIN(ANGC)*R
4000 CORD(N,2)=W/WR+W*DR/WR-DCOS(ANGC)*R
73 DO 850 I=1,NJT
KK=0
C COMPUTE DEFLECTION B. C. CODES
IF((NPUNCH.EQ.1).AND.(CORD(I,2).EQ.0.D0))KK=1
IF((NPUNCH.EQ.2).AND.(CORD(I,2).EQ.0.D0))KK=2
IF(CORD(I,1).EQ.0.D0)KK=2
IF((CORD(I,1).EQ.0.D0).AND.(CORD(I,2).EQ.0.D0)) KK=3
IF(I.EQ.19)KK=3
IF(KK.EQ.0) GO TO 5
NPBC=NPBC+1
NPBC(NPBC,1)=I
NPBC(NPBC,2)=KK
5 W5=5.D0*W-1.D-6 W5=10.D0*W
IF(NCLOAD.NE.0) W5=10.D0*W
802 IF(CORD(I,1).GE.W5) GO TO 801
CORD(I,3)=0.D0
CORD(I,4)=0.D0
WRITE (6,20) I,(CORD(I,J),J=1,2)
C CONTINUE
850

```



```

C      COMPUTE LOAD B, C
      IF(NPUNCH.EQ.1) GO TO 860
      IF(NPUNCH.EQ.3) GO TO 860
C      FCR APPLIED MOMENT
      NCLOAD=2
      IF (NPUNCH.EQ.2) GO TO 861
      CORD(NJTUP,3)=-1.D6
      CORD((NJTUP+2),3)= 1.D6
      GO TO 765
861  CORD(NJTUP,3)=1.D6/6.D0
      CORD((NJTUP+1),3)=1.D6/3.D0
      GO TO 765
C      FCR NO MOMENT APPLIED
      CORD(NJTUP,3)=1.D6/6.D0
      CORD((NJTUP+1),3)=2.D6/3.D0
      CORD((NJTUP+2),3)=1.D6/6.D0
      RETURN
765  IF(EXPX(K).EQ.0.D0) GO TO 2000
1000  FOR EXPONENT IN XI DIRECTION
      DO 1001 N=1,7,2
      XI(N)=F1(XI(N),EXPX(K))
      DO 1002 N=2,6,2
      XI(N)=(XI(N-1)+XI(N+1))/2.D0
      XI(8)=(XI(7)+XI(1))/2.D0
C      FOR EXPONENT IN THE ETA DIRECTION
      IF(EXPY(K).EQ.0.D0) GO TO 350
      DO 2001 N=1,7,2
      ETA(N)=F1(ETA(N),EXPY(K))
      DO 2002 N=2,6,2
      ETA(N)=(ETA(N-1)+ETA(N+1))/2.D0
      ETA(8)=(ETA(7)+ETA(1))/2.D0
      GO TO 350
1050  IF(EXPX(K).EQ.0.D0) GO TO 2050
      DO 1051 N=1,10,3
      XI(N)=F1(XI(N),EXPX(K))
      DO 1052 N=2,11,3
      NM=N-1
      NP=N+2
      IF(NP.EQ.13) NP=1
      IF(XI(NM).LT.XI(NP)) GO TO 1053
      XI(N)=2.D0 * XI(NM)/3.D0 + XI(NP)/3.D0
      XI(N+1)=2.D0 * XI(NP)/3.D0 + XI(NM)/3.D0
      GO TO 1052
1053  XI(N)=2.D0 * XI(NP)/3.D0 + XI(NM)/3.D0
      XI(NP)=2.D0 * XI(NM)/3.D0 + XI(NP)/3.D0
      CCNTINUE
1052  IF(EXPY(K).EQ.0.D0) GO TO 350
2050  DO 2051 N=1,10,3

```



```

2051 ETA(N)=F1(ETA(N),EXPY(K))
DO 2052 N=2,11,3
NM=N-1
NP=N+2
IF(NP.EQ.13) NP=1
IF(ETA(NM).LT.ETA(NP)) GO TO 2053
ETA(N)=2.D0*ETA(NM)/3.D0+ETA(NP)/3.D0
ETA(N+1)=2.D0*ETA(NP)/3.D0+ETA(NM)/3.D0
GC TO 2052
2053 ETA(N)=2.D0*ETA(NP)/3.D0+ETA(NM)/3.D0
ETA(N+1)=2.D0*ETA(NM)/3.D0+ETA(NP)/3.D0
CONTINUE
GC TO 350
74 ANG=2.D0*ANGB/3.D0+ANGA/3.D0
ANGD=2.D0*ANGA/3.D0+ANGB/3.D0
CCRD(N,1)=DSIN(ANGC)*R
CCRD(N,2)=W/WR+W*DR/WR-DCOS(ANGC)*R
CCRD(N+16,1)=DSIN(ANGD)*R
CCRD(N+16,2)=W/WR+W*DR/WR-DCOS(ANGC)*R
GC TO 73
801 NLOAD=NJT-I+1
NJTUP=I
GC TO 802
56 ANG=0.D0
GC TO 57
58 ANGA=PI/2.D0
GC TO 59
END

```

```

02190
02200
02210
02220
02230
02240
02250
02260
02270
02280
02290
02300
02310
02320
02330
02340
02350
02360
02370
02380
02390
02400
02410
02420
02430
02440
02450
02460
EEEEEEEEEEEEEEEEEEEE
EEEEEEEEEEEEEEEEEEEE
EEEEEEEEEEEEEEEEEEEE
EEEEEEEEEEEEEEEEEEEE
EEEEEEEEEEEEEEEEEEEE
EEEEEEEEEEEEEEEEEEEE
EEEEEEEEEEEEEEEEEEEE
EEEEEEEEEEEEEEEEEEEE
EEEEEEEEEEEEEEEEEEEE
EEEEEEEEEEEEEEEEEEEE
EEEEEEEEEEEEEEEEEEEE
EEEEEEEEEEEEEEEEEEEE
EEEEEEEEEEEEEEEEEEEE
EEEEEEEEEEEEEEEEEEEE
EEEEEEEEEEEEEEEEEEEE
EEEEEEEEEEEEEEEEEEEE
EEEEEEEEEEEEEEEEEEEE
EEEEEEEEEEEEEEEEEEEE
EEEEEEEEEEEEEEEEEEEE
EEEEEEEEEEEEEEEEEEEE
EEEEEEEEEEEEEEEEEEEE
EEEEEEEEEEEEEEEEEEEE
EEEEEEEEEEEEEEEEEEEE
EEEEEEEEEEEEEEEEEEEE
EEEEEEEEEEEEEEEEEEEE

```

```

SUBROUTINE SHAPE(X,Y,NPEL)
IMPLICIT REAL*8 (A-H,O-Z)
DIMENSION XYL(4,2),XYQ(8,2),XYC(12,2),IPERM(4)
COMMON/SP/VAL(12)
DATA XYL/1.0D0,-1.0D0,-1.0D0,-1.0D0,1.0D0,1.0D0,-1.0D0,-1.0D0/
DATA XYQ/1.0D0,0.0D0,-1.0D0,-1.0D0,-1.0D0,-1.0D0,0.0D0,0.0D0/
1 DATA XYL/1.0D0,-1.0D0,-1.0D0,-1.0D0,-1.0D0,-1.0D0,-1.0D0,-1.0D0/
10 DATA XYC/1.0D0,-1.0D0,-1.0D0,-1.0D0,-1.0D0,-1.0D0,-1.0D0,-1.0D0/
20 DATA XYC/1.0D0,-1.0D0,-1.0D0,-1.0D0,-1.0D0,-1.0D0,-1.0D0,-1.0D0/
30 DATA XYC/1.0D0,-1.0D0,-1.0D0,-1.0D0,-1.0D0,-1.0D0,-1.0D0,-1.0D0/
40 DATA XYC/1.0D0,-1.0D0,-1.0D0,-1.0D0,-1.0D0,-1.0D0,-1.0D0,-1.0D0/
F1(X,Y,X1,Y1)=(ONE+X*X1)*(ONE+Y*Y1)/FOUR
F2(X,Y,X1,Y1)=(ONE+X*X1)*(ONE+Y*Y1)/FOUR
F3(X,Y,X1,Y1)=(ONE-X*X1)*(ONE+Y*Y1)/TWO
F4(X,Y,X1,Y1)=(ONE-X*X1)*(ONE+Y*Y1)/TWO

```

```

00010
00020
00030
00040
00050
00060
00070
00080
00090
00100
00110
00120
00130
00140
00150
FFFFFFFFFFF
FFFFFFFFFFF
FFFFFFFFFFF
FFFFFFFFFFF
FFFFFFFFFFF
FFFFFFFFFFF
FFFFFFFFFFF
FFFFFFFFFFF
FFFFFFFFFFF
FFFFFFFFFFF
FFFFFFFFFFF
FFFFFFFFFFF
FFFFFFFFFFF
FFFFFFFFFFF
FFFFFFFFFFF
FFFFFFFFFFF
FFFFFFFFFFF
FFFFFFFFFFF
FFFFFFFFFFF
FFFFFFFFFFF
FFFFFFFFFFF
FFFFFFFFFFF
FFFFFFFFFFF
FFFFFFFFFFF
FFFFFFFFFFF

```



```

FF 00640
FF 00650
FF 00660
FF 00670
FF 00680

```

```

X1=XYC(IJ,1)
Y1=XYC(IJ,2)
VAL(IJ)=FCM(Y,X,Y1,X1)
RETURN
END

```

700

```

GG 00010
GG 00020
GG 00030
GG 00040
GG 00050
GG 00060
GGW00070
GGW00080
GGW00090
GGW00100
GGW00110
GG 00120
GG 00130
GG 00140
GG 00150
GG 00160
GG 00170
GG 00180
GG 00190
GG 00200
GG 00210
GG 00220
GG 00230
GG 00240
GG 00250
GG 00260
GG 00270
GG 00280
GG 00290
GG 00300
GG 00310
GG 00320
GG 00330
GG 00340
GG 00350
GG 00360
GG 00370
GG 00380

```

```

SUBROUTINE GRID
IMPLICIT REAL*8 (A-H,O-Z)
REAL*4 X,Y,RANGE,XSCALE,YSCALE,LABEL
DATA LABEL/4H
INTEGER*4 N1,MC,I TYPE,IXUP,IYRT,MDXAX,MDYAX,IWIDE,IHIGH,IGRID,
1 LAST,N,NJT
DIMENSION X(454),Y(454),RANGE(4)
COMMON/MESH1/ NCON(20,9),MS(20,8),MEL(20,4)
COMMON/MESH2/ NCR(4),NRR(4)
COMMON/MESH3/ NCON(135,14)
COMMON/CORD1/CORD(454,4),ELCON(1,4),NBC(454,2)
COMMON/TITL/TITLE(12)
COMMON/INT/NPT,NEL,NPUNCH,NSTOP,NJT,NPLOT,NKIND,NSEL,NGROW,NGCOL,
1 NCLOAD,NPBC

```

X,Y DIMENSIONED MAXNJT

```

DATA I TYPE/0/,IXUP/15/,IYRT/0/,MDXAX/2/,MDYAX/2/,IWIDE/9/,
1 I HIGH/15/,IGRID/0/

```

```

XMAX=-1.0D+20
YMAX=-1.0D+20
YMIN=1.0D+20
DO 20 I=1,NJT
XMAX=DMAX1(XMAX,CORD(I,1))
YMAX=DMAX1(YMAX,CORD(I,2))
XMIN=DMIN1(XMIN,CORD(I,1))
YMIN=DMIN1(YMIN,CORD(I,2))
IF (XMIN-GE.0.D0) GO TO 40
XMAX=XMAX-XMIN
DO 30 I=1,NJT
CORD(I,1)=CORD(I,1)-XMIN
IF (YMIN-GE.0.D0) GO TO 60
YMAX=YMAX-YMIN
DO 50 I=1,NJT
CORD(I,2)=CORD(I,2)-YMIN
GO TO (70,110),NPLOT

```

20

30

40

50

60

C
C
C

C


```

C          PLOT ON PRINTER
C 70      RANGE(1)=XMAX
          RANGE(2)=0.0
          RANGE(3)=YMAX
          RANGE(4)=0.0
          IF (RANGE(1).LT.RANGE(3)) RANGE(1)=RANGE(3)
          IF (RANGE(1).GT.RANGE(3)) RANGE(3)=RANGE(1)
          DO 80 I=1,NNJT
            X(I)=CORD(I,1)
            Y(I)=CORD(I,2)
            WRITE (6,90)
            FORMAT (I,1)
            NNJT=NNJT
          CALL UTPLLOT (X,Y,NNJT,RANGE,1,0)
          RETURN
C          PLOT ON PLOTTER
C 110     XSCALE=1.5D0*(YMAX/9.D0)
          YSCALE=1.5D0*(XMAX/15.D0)
          IF (XSCALE.GT.YSCALE) YSCALE=XSCALE
          IF (XSCALE.LT.YSCALE) XSCALE=YSCALE
          N1=NPT+1
          MC=1
          DO 150 I=1,NEL
            IF (I.EQ.NEL) MC=3
            DO 120 J=1,NPT
              J1=NCON(I,J)
              IF (J.EQ.1) J2=J1
              X(J)=CORD(J1,2)
              Y(J)=-CORD(J1,1)
              J=J+1
            X(J)=CORD(J2,2)
            Y(J)=-CORD(J2,1)
            CALL DRAW (N1,X,Y,MC,ITYPE,LABEL,TITLE,XSCALE,YSCALE,IXUP,IYRT,
              1IMDXAX,MDYAX,IWIDE,IHIGH,IGRID,LAST)
            MC=2
          CCNTINUE
          CONTINUE
          RETURN
          END
C 120
C 150
C 200

```

```

GG 00390
GG 00400
GG 00410
GG 00420
GG 00430
GG 00440
GG 00450
GG 00460
GG 00470
GG 00480
GG 00490
GG 00500
GG 00510
GG 00520
GG 00530
GG 00540
GG 00550
GG 00560
GG 00570
GG 00580
GG 00590
GG 00600
GG 00610
GG 00620
GG 00630
GG 00640
GG 00650
GG 00660
GG 00670
GG 00680
GG 00690
GG 00700
GG 00710
GG 00720
GG 00730
GG 00740
GG 00750
GG 00760
GG 00770
GG 00780
GG 00790
GG 00800

```

```

C          SUBROUTINE PLISOP
C          THIS PROGRAM PERFORMS A PLANE STRESS OR A PLANE STRAIN ANALYSIS
C          HH 00010
C          HH 00020

```


BY THE FINITE ELEMENT METHOD. NUMERICALLY INTEGRATED ISOPARAMETRIC
 ELEMENTS ARE USED THROUGHOUT.
 PROFESSOR GILLES CANTIN AT THE NAVAL POSTGRADUATE SCHOOL 1972
 MODIFIED BY L.J.SMITH, MAY 1974

INPUT CARDS NEEDED (PASSED VIA MAIN)

TITLE (20A4) ONE CARD PER PROBLEM
 PROBLEM PARAMETERS (10I5) ONE CARD PER PROBLEM
 COL. VARIABLE
 1-5 NEL NUMBER OF ELEMENTS (MAX. IS 135, 8 NODE ELEMENTS)
 6-10 NJT NUMBER OF JOINTS (MAX. IS 454)
 11-15 NMAT NUMBER OF MATERIALS (MAX. IS 1)
 16-20 NLOAD NUMBER OF CONCENTRATED LOADS
 21-25 NPBC NUMBER OF JOINTS WITH BOUNDARY CONDITIONS
 26-30 NSTRESS ZERO FOR PLANE STRESS PROBLEMS, ONE FOR P-STRAIN
 31-35 NGP NUMBER OF GAUSS POINTS DESIRED IN THE INTEGRATION
 36-40 NTLD 1 IF A THERMAL LOAD IS PRESENT 0 OTHERWISE
 41-45 NTBY 1 IF A BODY FORCE STRETCH IS TO BE CONSIDERED
 46-50 NTIN 1 IF AN INITIAL STRETCH IS PRESENT 0 OTHERWISE
 IF INTLD, NTBY OR NTIN ARE DIFFERENT THAN 0, THEN NJT
 CARDS WILL BE NEEDED BELOW FOR THE CONSISTENT LOAD VECTOR

JCINT CARDS (I10,4G15.8,1I5) NJT CARDS PER PROBLEM

COL. VARIABLE
 1-10 JOINT NUMBER
 11-25 X COORDINATE OF THE JOINT
 26-40 Y COORDINATE OF THE JOINT
 41-55 X COMPONENT OF THE LOAD AT THE JOINT
 56-70 Y COMPONENT OF THE LOAD AT THE JOINT
 71-75 IND IF IND IS NOT 0 THE COORDINATE SYSTEM IS POLAR,
 X IS THE RADIUS VECTOR, Y IS THE POLAR ANGLE IN DEGREES
 FOR THE LOAD, X IS A RADIAL LOAD AND Y IS A TANGENT LOAD

MATERIAL PROPERTIES (CODED IN INPUT)

COL. VARIABLE
 1-10 MATERIAL NUMBER
 11-20 YOUNG'S MODULUS
 21-30 POISSON'S RATIO
 31-40 COEFFICIENT OF THERMAL EXPANSION
 41-50 THICKNESS OF THE ELEMENT

ELEMENT CARDS (15I4) NEL CARDS PER PROBLEM

COL. VARIABLE
 1-4 ELEMENT IDENTIFICATION NUMBER
 5-52 ELEMENT CONNECTIVITY (COUNTERCLOCKWISE)
 53-56 KIND 1 FOR FOUR NODAL POINT ELEMENT


```

700      I=I*2-1
1000     I=I+1
2000     WRITE(6,2000) I,ALOAD(II),ALOAD(III)
1000     CONTINUE
3000     FORMAT(2X,I3,2G15.4)
1000     FORMAT(/,/,DISPLACEMENTS',/,3X,' JOINT',1X,' U',12X,' V',/)
3000     WRITE(6,3000)
1000     FORMAT(/,/,REACTIONS',/,3X,' JOINT',1X,' RX',12X,' RY',/)
800      DO 800 I=1,NPBC
1000     WRITE(6,2000) NBC(I,1),REACT(I,1),REACT(I,2)
800     CONTINUE
4000     WRITE(6,4000)
1000     WRITE(6,4000) EQUILIBRIUM CHECK ',/'
2500     MJP=MJT+1
1000     WRITE(6,2500) REACT(MJP,1),REACT(MJP,2)
2500     FORMAT(5X,2G15.4)
6000     CALL STRESS(NPEL)
6500     RETURN
1000     WRITE(6,6500) MBD,NBAND
6500     FORMAT(5X,' MAX. BAND (',113,') EXCEEDED, NBAND = ',114)
1000     STOP
1000     END

```

```

HH 01470
HH 01480
HH 01490
HH 01500
HH 01510
HH 01520
HH 01530
HH 01540
HH 01550
HH 01560
HH 01570
HH 01580
HH 01590
HH 01600
HH 01610
HH 01620
HH 01630
HH 01640
HH 01650
HH 01660
HH 01670
HH 01680

```

```

1000     SUBROUTINE INPUT (A-H,O-Z)
1000     IMPLICIT REAL*8 (A-H,O-Z)
1000     COMMON/MDIM/MEL,MJT,MMT,MBD
1000     COMMON/TITLE/TITLE(12),NMAT,NCLCAD,NPBC,NCON(135,14),NSTRES,NGP,
1000     1LX(8),LJT(8),NTLD,LTRY,NTIN
1000     COMMON/COORD/COORD(454,2),CLOAD(454,2),ELCON(1,4),NBC(454,2)
1000     DATA CHK/,STOP/,ZRO=0.0D0
1000     PI=3.14159265359D0
1000     REWIND 10
1000     FORMAT(10A8)
1000     IF (TITLE(1).EQ.CHK) STOP
1000     DO 1050 I=1,MJT
1000     DO 1050 J=1,2
1000     NBC(I,J)=0
1000     COORD(I,J)=ZRO
1000     CLOAD(I,J)=ZRO
1000     CONTINUE
1000     DO 1060 I=1,MMT
1000     DO 1060 J=1,4
1000     ELCON(I,J)=ZRO
1000     CONTINUE

```

```

II 00010
II 00020
II 00030
II 00040
II 00050
II 00060
II 00070
II 00080
II 00090
II 00100
II 00110
II 00120
II 00130
II 00140
II 00150
II 00160
II 00170
II 00180
II 00190
II 00200
II 00210
II 00220
II 00230

```



```

1E'//)
UC 2400 I=1,NEL
2400 READ(10,2500) IJT,(NCON(IJT,J),J=1,14)
2500 FCRMAT(1514)
DC 2600 I=1,NEL
WRITE(6,2700) I,(NCON(I,J),J=1,14)
2600 CONTINUE
2700 FCRMAT(2X,I3,14I5)
C
C
WRITE BOUNDARY CONDITION CODES
2800 WRITE(6,2800)
FCRMAT(//,' BOUNDARY CONDITION CODE',//,5X,'JNT NO',6X,'CODE'//)
DO 2900 I=1,NPBC
WRITE(6,3100) (NBC(I,J),J=1,2)
2900 CONTINUE
3100 FCRMAT(5X,I5,I10)
NPBC=NPNBC-1
DO 4000 K=1,NPBC
DO 4000 I=1,NPBCM
IF(NBC(I,2).EQ.7) GO TO 3600
GC TO 4000
NI=NBC(I,1)
DO 3800 J=1,NPBCM
NBC(J,1)=NBC(J+1,1)
NBC(J,2)=NBC(J+1,2)
NBC(NPBC,1)=NI
NBC(NPBC,2)=7
4000 CONTINUE
C
C
READ LOAD VECTOR FROM SERVICE PROGRAM
IF((NTLD+NTBY+NTIN).EQ.0) RETURN
DO 4200 I=1,NJT
READ(5,4100) IJT,CLX,CLY
4100 FCRMAT(5X,I15,2G25.16)
CLCAD(IJT,1)=CLOAD(IJT,1)+CLX
CLCAD(IJT,2)=CLOAD(IJT,2)+CLY
4200 CONTINUE
RETURN
4300 WRITE(6,4350) MEL,NEL
4350 FCRMAT(5X,' MAX. NUMBER (' ,113,' ) OF ELEMENTS EXCEEDED, NEL=' ,114)
STOP
4400 WRITE(6,4450) MJT,NJT
4450 FCRMAT(5X,' MAX. NUMB. ( ' ,113,' ) OF JOINTS EXCEEDED, NJT =' ,114)
STOP
4500 WRITE(6,4550) MMT,NMAT

```



```

4550 FORMAT(5X,' MAX. NUMB. (' ,112,' ) CF MATERIAL EXCEEDED, NMAT=' ,114)
      STOP
4600 WRITE(6,4650) MJT,NCLOAD
4650 FCRMAT(5X,' MAX. NUMB. (' ,113,' ) CF C. LOADS EXC., NCLOAD =' ,114)
      STOP
4700 WRITE(6,4750) MJT,NPBC
4750 FCRMAT(5X,' MAX. N. (' ,113,' ) OF JOINTS WITH BOUND. COND. EXCEED,
      1 NPBC =' ,114)
      STOP
      END

```

```

II 01200
II 01210
II 01220
II 01230
II 01240
II 01250
II 01260
II 01270
II 01280
II 01290

```

```

SUBROUTINE MERGE(NPEL,NEQ)
IMPLICIT REAL*8 (A-H,Q-Z)
DIMENSION SOL/BGK( 908,64),STK(16,16),AK(16,16),B(3,16)
COMMON/UNT1/NEL,NJT,NMAT,ALOAD( 908),ABGN
COMMON/UNT2/NEL,NJT,NMAT,NLOAD,NPBC,NCON(135,14),NSTRES,NGP,
1 LM(8),LJT(8),NILD,LTRY,NFIN
COMMON/COORD1/COORD(454,2),CLOAD(454,2),ELCCCN(1,4),NBC(454,2)
COMMON/COORD2/ELAST(3,3),SS(24,16),SN(24,16)
COMMON/TITLE/TITLE(12)
REWIND 12
ZRC=0.0D0
DO 100 I=1,36
DC 100 J=1,24
SS(I,J)=ZRC
SN(I,J)=ZRC
DO 200 IK=1,NPEL
DC 110 NN=1,NPEL
LJT(NN)=NCON(IK,NN)-1)*2
LM(NN)=(NCON(IK,NN)-1)*2
NS=3*NPEL
DO 120 I1=1,NPEL
I2=LJT(I1)
DO 120 J1=1,2
COORD(I1,J1)=COORD(I2,J1)
MATN=NCON(IK,I1)*8
MATN=NCON(IK,I3)*8
NM=ELCON(MATN,1)
YM=ELCON(MATN,2)
PTK=ELCON(MATN,4)
IF(NSTRES.EQ.1) TK=1.0D0
CALL ELASM(ELAST,YM,PRTIO,NSTRES)
CALL ELAS5(STK,AK,B,NS,N,NGP)
WRITE(12) SS,SN
IF(TK.EQ.0.0D0) TK=1.0D0
DC 200 I=1,NPEL

```

```

JJ 00010
JJ 00020
JJW00030
JJW00040
JJW00050
JJW00060
JJW00070
JJW00080
JJ 00090
JJ 00100
JJ 00110
JJ 00120
JJ 00130
JJ 00140
JJ 00150
JJ 00160
JJ 00170
JJ 00180
JJ 00190
JJ 00200
JJ 00210
JJ 00220
JJ 00230
JJ 00240
JJ 00250
JJ 00260
JJ 00270
JJ 00280
JJ 00290
JJ 00300
JJ 00310
JJ 00320
JJ 00330
JJ 00340
JJ 00350

```



```

JJ 00360
JJ 00370
JJ 00380
JJ 00390
JJ 00400
JJ 00410
JJ 00420
JJ 00430
JJ 00440
JJ 00450
JJ 00460
JJ 00470
JJ 00480
JJ 00490
JJ 00500
JJ 00510
JJ 00520

```

```

200      J=1,NPEL
      DO 200 K=1,2
      I=LM(I)+K
      KK=2*(I-1)+K
      DO 200 L=1,2
      JJ=LM(J)+L-I+1
      IF(JJ.LE.0) GO TO 200
      LL=2*(J-1)+L
      BGK(I,J)=BGK(I,J)+STK(KK,LL)*TK
      CONTINUE
      SUM=ZRO
      DO 300 I=1,NEQ
      SUM=SUM+BGK(I,1)
      ABGN=SUM*1.0D20
      RETURN
      END
300

```

```

KK 00010
KK 00020
KK 00030
KK 00040
KK 00050
KK 00060
KK 00070
KK 00080
KK 00090
KK 00100
KK 00110
KK 00120
KK 00130
KK 00140
KK 00150
KK 00160
KK 00170
KK 00180
KK 00190
KK 00200
KK 00210
KK 00220
KK 00230
KK 00240
KK 00250
KK 00260
KK 00270
KK 00280

```

```

C      C      ELASTIC MATRIX FOR PLANE
      SUBROUTINE ELASM(D,E,PR,NN)
      IMPLICIT REAL*8 (A-H,O-Z)
      THIS SUBROUTINE ASSEMBLES THE ELASTIC MATRIX FOR PLANE
      STRESS (NN=0)
      DIMENSION D(3,3)
      TW=1.0D0
      DO 20 I=1,3
      DO 20 J=1,3
      IF(NN.EQ.0) GO TO 10
      IF(NN.EQ.0) C MATRIX FOR PLANE STRAIN
      ER=E/((CN+PR)*(CN-TW*PR))
      D(1,1)=ER*(CN-PR)
      D(1,2)=ER*PR
      D(2,1)=D(1,2)
      D(2,2)=D(1,1)
      D(3,3)=ER*(.5D0-PR)
      RETURN
      C      C      ELASTIC MATRIX FOR PLANE STRESS
      ER=E/(CN-PR**2)
      D(1,1)=ER**PR
      D(1,2)=D(1,2)
      D(2,1)=D(1,2)
      D(2,2)=ER*(1.-PR)/TW
      RETURN
      END
10

```



```

SLBRROUTINE QUAD5(STK,AK,B,NS,N,NGP)
QUAD5 IS A NUMERICAL INTEGRATION SUBROUTINE THAT FORMS THE STIFFNESS
MATRIX X FOR ANY OF THE THREE QUADRILATERAL ELEMENTS IN THIS FAMILY.
GAUSSIAN QUADRATURE WITH A MAXIMUM OF FIVE ORDINATES IS USED.
CODED BY PROFESSOR GILLES CANTIN AT THE NAVAL POSTGRADUATE SCHOOL

THE SUBROUTINE IS CALLED WITH THE FOLLOWING STATEMENT:
CALL QUAD5(STK,AK,SS,SN,NS,N,NGP)
THE CALLING PROGRAM MUST OBTAIN THE FOLLOWING COMMON STATEMENT:
COMMON COORD(12,2),ELAST(3,3)
STK IS AN ARRAY DIMENSIONED NXN THAT WILL CONTAIN THE STIFFNESS
MATRIX UPON RETURN TO THE CALLING PROGRAM
SS AND SN ARE THE STRESS AND STRAIN VECTORS NODAL POINT DISPLACEMENTS
TRANSFORMATION MATRIX, BOTH ARE DIMENSIONED NSXN WHERE
NS IS 3*NPT AND N IS 2*NPT
AK IS AN ARRAY DIMENSIONED NXN REQUIRED IN FORMK
B IS AN ARRAY DIMENSIONED 2XN REQUIRED IN FORMK

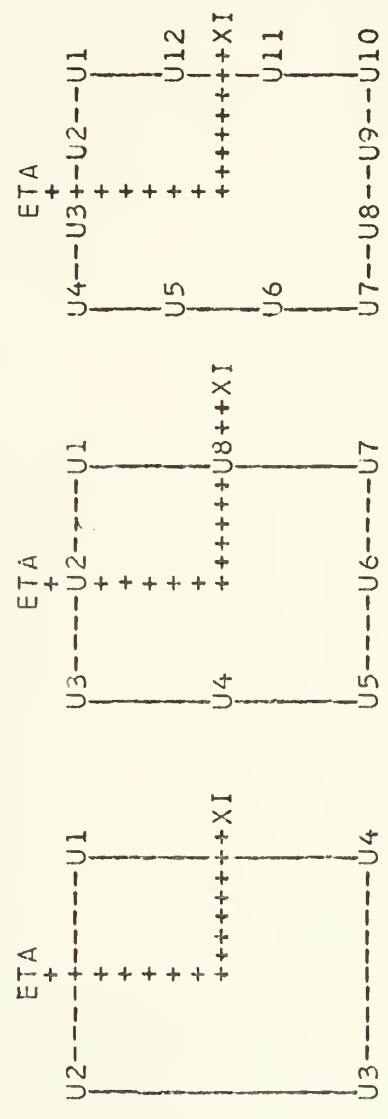
NGP IS THE NUMBER OF GAUSS POINTS USED IN THE INTEGRATION
COORD(12,2) IS AN ARRAY CONTAINING THE COORDINATES OF ALL
THE NODAL POINTS OF THE ELEMENT TO BE CONSTRUCTED
ELAST(3,3) IS AN ARRAY CONTAINING ALL THE ELASTIC CONSTANTS
OF THE ELEMENT, THE ORDER OF THE STRESS COMPONENTS
IS: SIGMAX,SIGMAY,TAUXY

```

```

00010
00020
00030
00040
00050
00060
00070
00080
00090
00100
00110
00120
00130
00140
00150
00160
00170
00180
00190
00200
00210
00220
00230
00240
00250
00260
00270
00280
00290
00300
00310
00320
00330
00340
00350
00360
00370
00380
00390
00400
00410
00420
00430
00440
00450

```



```

IMPLICIT REAL*8 (A-H,O-Z)
DIMENSION X2(2),X3(3),X4(4),X5(5),A2(2),A3(3),A4(4),A5(5)

```

CC


```

Y=XI(J)
CALL FORMK(AK,X,Y,B,N)
AIAIJ=AIA(I,J)
DO 200 K=1,N
  DO 200 L=1,N
    STK(K,L)=STK(K,L)+AIAIJ*AK(K,L)
  200 STK(K,L)=STK(K,L)+AIAIJ*AK(K,L)
DO 300 I=1,N
  DO 300 J=1,N
    STK(I,J)=(STK(I,J)+STK(J,I))*0.5D0
  300 STK(J,I)=STK(I,J)
NPT=N/2
IGC=NPT/4
DO 400 I=1,NPT
  GO TO (400,500,600),IGC
  400 X=XYL(I,1)
  Y=XYL(I,2)
  GO TO 700
  500 X=XYQ(I,1)
  Y=XYQ(I,2)
  GO TO 700
  600 X=XYC(I,1)
  Y=XYC(I,2)
  700 CALL FORMK(AK,X,Y,B,N)
DO 800 L=1,3
  DO 800 M=1,3
    AK(L,M)=0.0D0
  DO 800 N=1,3
    AK(L,M)=AK(L,M)+ELAST(L,NN)*B(NN,M)
  800 II=3*(I-1)
  DO 900 J=1,3
    IJ=II+J
  DO 900 K=1,N
    SS(IJ,K)=AK(J,K)
  900 SN(IJ,K)=B(J,K)
1000 CONTINUE
RETURN
END

```

```

00940
00950
00960
00970
00980
00990
01000
01010
01020
01030
01040
01050
01060
01070
01080
01090
01100
01110
01120
01130
01140
01150
01160
01170
01180
01190
01200
01210
01220
01230
01240
01250
01260
01270
01280
01290
01300

```

```

J
J
J
J
J
J
J
J
J
J
J
J
J
J
J
J
J
J
J
J
J
J
J
J
J
J
J
J
J
J
J
J
J
J
J

```

```

C SUBROUTINE FORMK(AK,X,Y,B,N)
C THIS SUBROUTINE FORMS THE STIFFNESS AND THE B MATRIX AS FUNCTIONS OF
C XI AND ETA FOR THE THREE DIFFERENT QUADRILATERAL ELEM. IN THIS FAMILY
C
C IMPLICIT REAL*8 (A-H,C-Z)
C DIMENSION AJ(2,2),AJN(2,2),DNX(2,8),W1(2,12),B(3,16)

```

```

MM 00010
MM 00020
MM 00030
MM 00040
MM 00050
MMW00060

```



```

1,B1(16,3),AK(16,16)
COMMON COORD(12,2),ELAST(3,3),SS(24,16),SN(24,16)
C INITIALISE
ZERO=0.0DO
DO 10 I=1,3
DO 10 J=1,N
10 B(I,J)=ZERO
CNE=1.0DO
TWC=2.0DO
FOUR=4.0DO
NPT=N/2
CFCRM (2XNPT) MATRIX OF DERIV. OF THE INTERP. FUNCT. WRT XI AND ETA
C
C IGC=N/8
GO TO (20,30,40),IGC
C
C LINEAR FUNCTIONS
20 W1(1,3)=- (CNE-Y)/FOUR
W1(1,4)=-W1(1,3)
W1(1,1)= (CNE+Y)/FOUR
W1(1,2)=-W1(1,1)
W1(2,3)=- (CNE-X)/FOUR
W1(2,4)=- (CNE+X)/FOUR
W1(2,1)=-W1(2,4)
W1(2,2)=-W1(2,3)
GO TO 50
30 CONTINUE
C
C QUADRATIC FUNCTIONS
TXPY=TWC*X+Y
TXMY=TWC*X-Y
TYPX=TWC*Y+X
TYMX=TWC*Y-X
CPY=CNE+Y
CPX=CNE+X
CMX=CNE-X
W1(1,5)=CMY*TXPY/FOUR
W1(1,6)=-CMY*X
W1(1,7)=CMY*TXMY/FOUR
W1(1,8)=CMY*OMY/TWO
W1(1,1)=OPY*TXPY/FOUR
W1(1,2)=-OPY*X
W1(1,3)=OPY*TXMY/FOUR
W1(1,4)=-OPY*OMY/TWO
MMW000070
MMW000080
MMW000090
MMW000100
MMW000110
MMW000120
MMW000130
MMW000140
MMW000150
MMW000160
MMW000170
MMW000180
MMW000190
MMW002000
MMW002010
MMW002020
MMW002030
MMW002040
MMW002050
MMW002060
MMW002070
MMW002080
MMW002090
MMW002100
MMW002110
MMW002120
MMW002130
MMW002140
MMW002150
MMW002160
MMW002170
MMW002180
MMW002190
MMW002200
MMW002210
MMW002220
MMW002230
MMW002240
MMW002250
MMW002260
MMW002270
MMW002280
MMW002290
MMW002300
MMW002310
MMW002320
MMW002330
MMW002340
MMW002350
MMW002360
MMW002370
MMW002380
MMW002390
MMW002400
MMW002410
MMW002420
MMW002430
MMW002440
MMW002450
MMW002460
MMW002470
MMW002480
MMW002490
MMW002500
MMW002510
MMW002520
MMW002530
MMW002540

```



```

      W1(2,5)=OMX*TPPX/FOUR
      W1(2,6)=-OPX*CMX/TWO
      W1(2,7)=OPX*TYMX/FOUR
      W1(2,8)=-Y*OPX
      W1(2,1)=OPX*TPPX/FOUR
      W1(2,2)=OPX*CMX/TWO
      W1(2,3)=OMX*TYMX/FOUR
      W1(2,4)=-Y*CMX
      GO TO 50
40 CC CONTINUE

      CUBIC FUNCTIONS
      OPX=ONE+X
      OPY=ONE+Y
      CMX=ONE-X
      CMY=ONE-Y
      TPTMNX=3.0D0+2.0D0*X-9.0D0*X*X
      TPTMNX=3.0D0-2.0D0*X-9.0D0*X*X
      TPTMNY=3.0D0+2.0D0*Y-9.0D0*Y*Y
      TPTMNY=3.0D0-2.0D0*Y-9.0D0*Y*Y
      TYPO=3.0D0*Y+ONE
      TYMO=3.0D0*Y-ONE
      TXPC=3.0D0*X+ONE
      TXMC=3.0D0*X-ONE
      TPTMEX=10.0D0-27.0D0*X*X+18.0D0*X*X*X
      TPTMEX=10.0D0-27.0D0*X*X+18.0D0*X*X*X
      TMNPEY=10.0D0-9.0D0*X*X+13.0D0*X*X*Y
      TMNPEY=10.0D0-9.0D0*X*X+13.0D0*X*X*Y
      TIT=32.0D0/9.0D0
      TITN=32.0D0/9.0D0
      W1(1,7)=CMY*TMTPPX/TIT
      W1(1,8)=-TPTMNX*CMY/TITN
      W1(1,9)=TPTMNX*CMY/TITN
      W1(1,10)=-CMY*TMTPMX/TIT
      W1(1,11)=-OPY*CMY*TYMO/TITN
      W1(1,12)=-OPY*CMY*TYPO/TIT
      W1(1,1)=OPY*TMTPMX/TIT
      W1(1,2)=TPTMNX*OPY/TITN
      W1(1,5)=-TPTMNX*OPY/TIT
      W1(1,4)=-OPY*TMTPMX/TIT
      W1(1,5)=-OPY*CMY*TYPO/TITN
      W1(1,6)=CMY*CMY*TYMO/TIT
      W1(1,7)=CMX*TMNPEY/TIT
      W1(2,8)=OPX*CMX*TXPC/TITN
      W1(2,9)=-OPX*CMX*TXMC/TITN
      W1(2,10)=OPX*CMX*TMNPEY/TIT
      W1(2,11)=-TPTMNY*CMX/TITN

```

```

MM 00550
MM 00560
MM 00570
MM 00580
MM 00590
MM 00600
MM 00610
MM 00620
MM 00630
MM 00640
MM 00650
MM 00660
MM 00670
MM 00680
MM 00690
MM 00700
MM 00710
MM 00720
MM 00730
MM 00740
MM 00750
MM 00760
MM 00770
MM 00780
MM 00790
MM 00800
MM 00810
MM 00820
MM 00830
MM 00840
MM 00850
MM 00860
MM 00870
MM 00880
MM 00890
MM 00900
MM 00910
MM 00920
MM 00930
MM 00940
MM 00950
MM 00960
MM 00970
MM 00980
MM 00990
MM 01000
MM 01010
MM 01020

```

CC


```

1(2,12)= TMTMNY*OPX/TTN
W1(2,1) =-OPX*TMNMEY/TTT
W1(2,2) =OPX*OMX*TXPG/TTN
W1(2,3) =-OPX*OMX*TXMO/TTT
W1(2,4) =-OPX*TMNMEY/TTT
W1(2,5) =OMX*TMNMEY/TTN
W1(2,6) =-OMX*TPTMNY/TTN
50 CONTINUE
CC
CC FORM JACOBIAN OF THE TRANSFORMATION IN AJ(I,J)
CC
      DC 100 I=1,2
      DC 100 J=1,2
      AJ(I,J)=ZERO
      DO 100 K=1,NPT
100 AJ(I,J)=AJ(I,J)+W1(I,K)*COORD(K,J)
CC
CC CALCULATE DETERMINANT OF THE JACOBIAN
CC
      DTJ=AJ(1,1)*AJ(2,2)-AJ(1,2)*AJ(2,1)
CC
CC INVERT JACOBIAN IN AJIN
CC
      AJIN(1,1)=AJ(2,2)/DTJ
      AJIN(1,2)=-AJ(1,2)/DTJ
      AJIN(2,1)=-AJ(2,1)/DTJ
      AJIN(2,2)=AJ(1,1)/DTJ
CC
CC FORM (2XNPT) MATRIX OF DERIVATIVES OF INTERP. FUNCT WRT X AND Y
CC
      DO 200 I=1,2
      DO 200 J=1,NPT
      DNX(I,J)=ZERO
      DO 200 K=1,2
200 DNX(I,J)=DNX(I,J)+AJIN(I,K)*W1(K,J)
CC
CC FORM B(I,J) MATRIX
CC
      DO 300 I=1,NPT
      IOD=2*I-1
      IEV=2*I
      B(1,IOD)=DNX(1,I)
      B(2,IEV)=DNX(2,I)
      B(3,IEV)=DNX(1,I)
      B(3,IOD)=DNX(2,I)
300
CC
CC FORM STIFFNESS BY THE CONGRUENT TRANSFORMATION BT*D*B
CC

```



```

500 DO 500 I=1,N
      DC 500 J=1,3
      B1(I,J)=ZERO
500 DO 500 K=1,3
      B1(I,J)=B1(I,J)+B (K,I)*ELAST(K,J)
      DC 600 I=1,N
      DC 600 J=1,N
      AK(I,J)=ZERO
600 DO 600 K=1,3
      AK(I,J)=AK(I,J)+B1(I,K)*B(K,J)
      DC 700 I=1,N
      DC 700 J=1,N
      AK(I,J)={(AK(I,J)+AK(J,I))/2.0D0)*DTJ
700 AK(J,I)=AK(I,J)
      RETURN
      END

```

```

MM 01510
MM 01520
MM 01530
MM 01540
MM 01550
MM 01560
MM 01570
MM 01580
MM 01590
MM 01600
MM 01610
MM 01620
MM 01630
MM 01640
MM 01650
MM 01660

```

```

SUBROUTINE LDT(N,M)
THIS SUBROUTINE DECOMPOSES THE COEFFICIENT MATRIX A* OF THE LINEAR
BANDED SYMMETRICALLY USED, AND IT MUST BE STORED IN A RECTANGULAR
THE UPPER BAND ONLY IS ITS DIAGONAL ELEMENTS AND THE FIRST COLUMN
ARRAY (A) WITH ALL DESTROYED IN THE PROCESS AND THE RESULTS RETURNED IN
MATRIX (A) IS DESTROYED IN THE FIRST COLUMN AND THE REST (L
THE SAME ARRAY CONTAINS THE ELEMENTS OF THE UNIT TRIANGULAR MATRIX (L
OF THE MATRIX WITHOUT ITS IMPLIED UNIT DIAGONAL ELEMENTS.
IN BANDED FORM WITHOUT ITS IMPLIED UNIT DIAGONAL ELEMENTS.

```

```

NN 00010
NN 00020
NN 00030
NN 00040
NN 00050
NN 00060
NN 00070
NN 00080
NN 00090
NN 00100
NN 00110
NN 00120
NN 00130
NN 00140
NN 00150
NN 00160
NN 00170
NN 00180
NN 00190
NN 00200
NN 00210
NN 00220
NN 00230
NN 00240
NN 00250
NN 00260
NN 00270

```

```

A IS THE NAME OF THE COEFFICIENT MATRIX
N IS THE NUMBER OF EQUATIONS IN THE SYSTEM
M IS THE HALF BAND WIDTH OF THE SYSTEM
CODED BY GILLES CANTIN, NAVAL POSTGRADUATE SCHOOL, MAY 1972

```

```

IMPLICIT REAL*8 (A-H,O-Z)
COMMON/SOL/A( 908,64),B( 908),ABGN
AN=N
APZRO=ABGN*1.0D-30/AN
AVSN=APZRO/ABGN
ZRO=0.0D0
NM=N-1
DC 300 I=1,NM
      DIAG=A(I,I)
      IF(DIAG.EQ.ZRO) GO TO 400
      IF(DIAG.LE.APZRO) WRITE(6,2000) I
DC 100 J=2,M

```

```

CCCCCCCCCCCCCCCC

```



```

100 IF( . DABS(A(I,J)).LE.AVSN) A(I,J)=0.000
DC 300 J=2,M
L=I+J-1
IF(L.GT.N) GO TO 300
AA=A(I,J)*DIAG
IF(AA.EQ.ZRO) GO TO 300
DC 200 K=J,M
ML=I+K-J
200 A(L,ML)=A(L,ML)-AA*A(I,K)
300 CONTINUE
400 WRITE(6,1000) I
STOP
1000 FORMAT(//,5X,' MATRIX IS SINGULAR ',115)
2000 FORMAT(//,5X,' WARNING MATRIX IS NEARLY SINGULAR EXECUTION CONTINUES ',115//,5X,' RESIDUAL ITERATION MAY YIELD ERRONEOUS RESULTS
2 //)
END
SUBROUTINE SOLV(N,M)
THIS SUBROUTINE PERFORMS A FORWARD SUBSTITUTION, FOLLOWED BY A
BACKWARD SUBSTITUTION FOR THE SYSTEM (A*) X=(B), AFTER THE
MATRIX (A) HAS BEEN DECOMPOSED BY THE SUBROUTINE LDLOT
A IS THE NAME OF THE DECOMPOSED MATRIX OF COEFFICIENT MEMBER
B IS THE NAME OF THE COLUMN LOAD VECTOR OR RIGHT HAND
N M IS THE ANSWERS ARE RETURNED IN THIS VECTOR UPON EXIT
IS THE NUMBER OF EQUATIONS IN THE SYSTEM
IS THE HALF BAND WIDTH OF THE SYTEM
AFTER ONE CALL TO LDLT, ONE CALL OF SLV PER LOAD VECTOR IS REQUIRED
CODED BY GILLES CANTIN, NAVAL POSTGRADUATE SCHOOL, MAY 1972
IMPLICIT REAL*8 (A-H,O-Z)
COMMON/SOL/A( 908,64),B( 908),ABGN
NM=N-1
I=1,NM
BI=B(I)
DC 100 J=2,M
L=I+J-1
IF(L.GT.N) GO TO 100
B(L)=B(L)-A(I,J)*BI
CONTINUE
DC 200 I=1,N
B(I)=B(I)/A(I,1)
DC 300 L=2,N
IR=N-L+1
BIRP=B(IR+1)
DC 300 J=2,M

```



```

ILO=0
IUP=0
DC 210 J=1,NPEL
IJT=NCON(I,J)
ILO=IUP+1
IUP=ILO+2
WRITE(6,5000) IJT, (SSEL(K), K=ILO, IUP), (SNEL(L), L=ILC, IUP)
210 CONTINUE
220 FFORMAT(5X, I5, 6G12.4)
5000 FFORMAT(//, 2X, ' S-T-R-E-S-S-E-S / S-T-R-A-I-N-S FOR ELEMENT', I3PP
4000 FFORMAT(//, 5X, ' JOINT', I1X, 'SIG X ', 6X, 'SIG Y ', 7X, 'TAU ', 7X, 'EPS X
1, 7X, 'EPS Y ', 7X, 'GAMMA ', //)
1CT=0
DC 300 I2=1, NPEL
I2A=NCON(I, I2)
DC 250 J2=1, 3
1CT=1CT+1
SSJNT(I2A, J2)=SSEL(1CT)+SSJNT(I2A, J2)
SNJNT(I2A, J2)=SNJNT(I2A, J2)
DC 500 I3=1, NJT
SCNT=SNJNT(I3, 7)
DO 400 J3=1, 3
SSJNT(I3, J3)=SSJNT(I3, J3)/SCNT
SNJNT(I3, J3)=SNJNT(I3, J3)/SCNT
GAU=SSJNT(I3, 3)
XPSY=((SSJNT(I3, 1))+SSJNT(I3, 2))/2.0D0
XMSY=((SSJNT(I3, 1))-SSJNT(I3, 2))/2.0D0
AINT=DSQRT(XMSY*XMSY+GAU*GAU)
SSJNT(I3, 4)=XPSY+AINT
SSJNT(I3, 5)=XPSY-AINT
SSJNT(I3, 6)=(SSJNT(I3, 4)-SSJNT(I3, 5))/2.0D0
IF (DABS(XMSY).LE.0.00001D0) GO TO 420
RAN=-GAU/XMSY
IF (DABS(RAN).LE.0.01D0) GO TO 450
RGC=DATAN(RAN)
RAN=DSIGN(PI, GAU)/2.0D0
SSJNT(I3, 7)=RAN*180.0D0/(2.0D0*PI)
GAU=SNJNT(I3, 3)
XPSY=((SNJNT(I3, 1))+SNJNT(I3, 2))/2.0D0
XMSY=((SNJNT(I3, 1))-SNJNT(I3, 2))/2.0D0
AINT=DSQRT(XMSY*XMSY+GAU*GAU)
SNJNT(I3, 4)=XPSY+AINT
SNJNT(I3, 5)=XPSY-AINT
SNJNT(I3, 6)=(SNJNT(I3, 4)-SNJNT(I3, 5))/2.0D0
SNJNT(I3, 7)=SSJNT(I3, 7)
WRITE(6, 1000)

```



```

DC 600 I=1,NJT
WRITE(6,2000) I,(SSJNT(I,J),J=1,7)
CONTINUE
600
DC 800 I=1,25
Y(I)=SSJNT(I,1)
CONTINUE
800
FORMAT(2D25.16)
6218 Y(14)=SSJNT(1,1)
2000 FORMAT(5X,I5,G12.4,5X,I6I2.4)
WRITE(6,3000)
DC 700 I=1,NJT
CONTINUE
700
WRITE(6,2000) I,(SNJNT(I,J),J=1,6),SSJNT(I,7)
1000 FORMAT(//,1X, A-V-E-R-A-G-E S-T-R-E-S-E-S AT THE JOINTS',
1,7X, JOINT',1X, SIG X',6X, SIG Y',7X, TAU',7X, S.MAXPP
2,7X, S.MIN',7X, T.MAX',12X, TET(DEG.)'//)
3000 FORMAT(//,1X, A-V-E-R-A-G-E S-T-R-A-I-N-S AT THE JOINTS',
1,7X, JOINT',1X, EPS X',6X, EPS Y',7X, GAMMA',7X, E.MAXPP
2,7X, E.MIN',7X, G.MAX',12X, TET(DEG.)'//)
RETURN
END

```

```

SUBROUTINE BCOND(NBAND)
IMPLICIT REAL*8 (A-H,O-Z)
COMMON/SOL/BGK( 903:64),ALOAD( 908),ABGN
COMMON/UNT1/NEL,NJT,NMAT,NPBC,NCON(135,14),NSTRES,NGP,
1LM(6),LJT(8),NTLD,LIBY,NTIN
COMMON/N/COORD1/COORD(454,2),CLOAD(454,2),ELCON(1,4),NBC(454,2)
COMMON/I/IFL/ITILE(12)
PI=3.14159265359D0
NEQ=NJT*2
DO 200 I=1,NPBC
IJT=NBK(I,1)
IEQ=IJT*2-1
KODE=NBC(I,2)
IDIA=0
GC TO (110,120,130,140,150,160,170),KODE
110 IEQ=IEQ+1
112 BGK(IEQ,1)=ABGN
IF(IDIA.EQ.1) GO TO 132
GC TO 200
GC TO 112
130 IDIA=1
GO TO 112

```



```

132 IDIA=0
133 GO TO 110
134 DXY=CLoad(IJT,2)
135 IEQ=IEQ+1
136 ALOAD(IEQ)=ALCAD(IEQ)-BGK(IEQ,1)*DXY
137 BGK(IEQ,1)=ABGN
138 DC 146 J=2,NBAND
139 IRCW=IEQ-J+1
140 ICCW=IEQ-1+J
141 IF(IRCW.LT.1) GO TO 144
142 ALUAD(IRCW)=ALCAD(IRCW)-BGK(IRCW,J)*DXY
143 IF(ICOL.GT.NEQ) GO TO 146
144 ALOAD(ICOL)=ALCAD(ICOL)-BGK(IEQ,J)*DXY
145 CONTINUE
146 IF(IDIA.EQ.1) GO TO 162
147 GO TO 200
148 DXY=CLoad(IJT,1)
149 GO TO 143
150 IDIA=1
151 DXY=CLoad(IJT,1)
152 GO TO 143
153 IDIA=0
154 GO TO 140
155 ALPHA=CLoad(IJT,2)*PI/180.000
156 CAL=DCOS(ALPHA)
157 SAL=DSIN(ALPHA)
158 IEQ=IEQ+1
159 DC 180 J=3,NBAND
160 IRCW=IEQ-J+2
161 JN=J-1
162 IF(IRCW.LT.1) GO TO 175
163 A1=BGK(IRCW,JM)*CAL+BGK(IRCW,J)*SAL
164 A2=BGK(IRCW,J)*CAL-BGK(IRCW,JM)*SAL
165 BGK(IRCW,JM)=A1
166 BGK(IRCW,J)=A2
167 IF((IEQ+J-1).GT.NEQ) GO TO 180
168 A3=BGK(IEQ,J)*CAL+BGK(IEQ,JM)*SAL
169 A4=BGK(IEQ,JM)*CAL-BGK(IEQ,J)*SAL
170 BGK(IEQ,J)=A3
171 BGK(IEQ,JM)=A4
172 CONTINUE
173 A1=BGK(IEQ,1)*CAL+BGK(IEQ,2)*CAL*SAL*2.0 +BGK(IEQ,1)*SAL*SAL
174 A2=BGK(IEQ,2)*CAL*CAL-SAL*SAL)+(BGK(IEQ,1)-BGK(IEQ,1))*SAL*CAL
175 BGK(IEQ,1)=A1
176 BGK(IEQ,2)=A2
177 ABGN=BGK(IEQ,1)
178 CONTINUE
179 RETURN

```


END

QQ 00710

```

SUBROUTINE DISPL (A-H,C-Z)
IMPLICIT REAL*8 (A-H,C-Z)
COMMON/MDIM/MEL,MJT,MMT,MBD
COMMON/TITL/TITLE(12)
COMMON/SQL/PGK( 908,64), DISP( 908),ABGN
COMMON/UNIT1/NEL,NJT,NMAT,NCLCAD,NPBC,NCON(125,14),NSTRES,NGP,
1LM(8),LJT(8),NTLD,LTBV,NFIN
COMMON/CORD1/COORD(454,2),CLOAD(454,2),NBC(454,2)
COMMON/REACT(455,2)
DIMENSION REACT(455,2)
EQUIVALENCE (BGK(1,1),REACT(1,1))
PI=3.14159265359D0
DO 200 I=1,NPBC
  IJT=NBC(I,I)
  IEQ=IJT*2-1
  KCDE=NBC(I,2)
  IDIA=0
  DPBC=0.GD0
  GC TC (110,120,130,140,150,160,170),KODE
  IEQ=IEQ+1
  JR=2
110 REACT(I,JR)=-DISP(IEQ)*ABGN
112 DISP(IEQ)=DPBC
  IF(IDIA.EQ.1) GO TO 132
  IF(IDIA.EQ.2) GO TO 162
  GO TO 200
  JR=1
120 GC TC 112
130 IDIA=1
  JR=1
132 IDIA=0
  GC TC 110
140 DPBC=CLCAD(IJT,2)
  GC TC 110
150 JR=1
  DPBC=CLCAD(IJT,1)
  GC TC 112
160 IDIA=2
  JR=1
  DPBC=CLCAD(IJT,1)
  GC TC 112
162 IDIA=0

```

RRR 00010
RRR 00020
RRR 00030
RRR 00040
RRW 00050
RRW 00060
RRW 00070
RRW 00080
RRW 00090
RRR 00100
RRR 00110
RRR 00120
RRR 00130
RRR 00140
RRR 00150
RRR 00160
RRR 00170
RRR 00180
RRR 00190
RRR 00200
RRR 00210
RRR 00220
RRR 00230
RRR 00240
RRR 00250
RRR 00260
RRR 00270
RRR 00280
RRR 00290
RRR 00300
RRR 00310
RRR 00320
RRR 00330
RRR 00340
RRR 00350
RRR 00360
RRR 00370
RRR 00380
RRR 00390
RRR 00400
RRR 00410
RRR 00420

BIBLIOGRAPHY

1. Adamek, J.R., An Automatic Mesh Generator Using Two and Three-Dimensional Isoparametric Finite Elements, Master's Thesis, Naval Postgraduate School, Monterey, 1973.
2. Appl, F.J. and Koerner, D.R. "Stress Concentration Factors for U-Shaped, Hyperbolic and Rounded V-Shaped Notches," ASME Paper G9-DE-2, 1969.
3. Bakhshandehpour, M., Finite Element Solution for Axisymmetric Transient Thermal Stresses, Master's Thesis, Naval Postgraduate School, Monterey, 1972.
4. Cantin, J.G., PLISOP, an internally documented FORTRAN deck, Naval Postgraduate School, Monterey, March 1972.
5. Cole, A.G., and Brown, A.F.C., "Photoelastic Determination of Stress Concentration Factors Caused by a Single U-Notch on One Side of a Plate in Tension," Journal of the Royal Aeronautical Society, v. 62, p. 597, August 1958.
6. Faires, V.M., Design of Machine Elements, 4th ed., MacMillan, 1965.
7. Flynn, P.D., and Roll, A.A., "A Comparison of Stress-Concentration Factors in Hyperbolic and U-Shaped Grooves," Experimental Mechanics, v. 7, p. 272, June 1967.
8. Howland, R.C.J., "On the Stresses in the Neighbourhood of a Circular Hole in a Strip Under Tension," Phil. Trans. Royal Society, v. 229, p. 49, 1930.
9. Kikukawa, M., "A Note on the Stress Concentration Factor of a Notched Strip," Proceedings 10th International Congress of Applied Mechanics, Elsevier, N.Y., p. 337, 1962.
10. Leonidas, E., A General Purpose Three Dimensional Stress Analysis Program, Master's Thesis, Naval Postgraduate School, Monterey, 1971.
11. Neuber, H., Kerbspannungslehre, 2nd ed., Springer, Berlin, 1958; translation, Theory of Notch Stresses, Office of Technical Services, Dept. of Commerce, Washington, D.C., 1961.
12. Peterson, R.E., Stress Concentration Factors, Wiley, 1974.

13. Pfeifer, C.G., Evaluation of a Three-Dimensional Stress Analysis Program, Master's Thesis, Naval Postgraduate School, Monterey, 1972.
14. Shanks, D., "Non-Linear Transformations of Divergent and Slowly Convergent Sequences," Journal of Mathematics and Physics, v. 34, p. 1, April 1955.
15. Timoshenko, S. and Goodier, J.N., Theory of Elasticity, 2nd ed., McGraw-Hill, 1951.
16. Zienkiewicz, O.C., The Finite Element Method in Engineering Science, McGraw-Hill, 1971.

INITIAL DISTRIBUTION LIST

	No. Copies
1. Defense Documentation Center Cameron Station Alexandria, Virginia 22314	2
2. Library, Code 0212 Naval Postgraduate School Monterey, California 93940	2
3. Chairman, Department of Mechanical Engineering Naval Postgraduate School Monterey, California 93940	2
4. Prof. John E. Brock, Code 59Bc Naval Postgraduate School Monterey, California 93940	2
5. Lt. Howard L. Crego SMC 1195 Naval Postgraduate School Monterey, California 93940	1
6. R.E. Peterson Westinghouse Research Labs Pittsburgh, Pennsylvania 15235	1
7. LCDR Lawrence J. Smith 21022 Hagerstown Huntington Beach, California 92646	2

Thesis
S5963
c.1

Smith

Stress concentration
factors for circular
notches.

152695

Thesis
S5963
c.1

Smith

Stress concentration
factors for circular
notches.

152695

thesS5963

Stress concentration factors for circula



3 2768 002 00950 8

DUDLEY KNOX LIBRARY